Neurotransmitter receptors in three rodent models of Parkinson's disease – A quantitative multireceptor study

Von der Fakultät für Mathematik, Informatik und Naturwissenschaften der RWTH Aachen University zur Erlangung des akademischen Grades einer Doktorin der Naturwissenschaften genehmigte Dissertation

vorgelegt von

Diplom-Biologin

Jennifer Nadine Cremer, geb. Lopez Escobar

aus Aachen

Berichter: Prof. Dr. Hermann Wagner
Prof. Dr. med. Dr. med. h.c. Karl Zilles

Tag der mündlichen Prüfung: 26. Juli 2013

Diese Dissertation ist auf den Internetseiten der Hochschulbibliothek online verfügbar.

Entstanden in Kooperation der Institute:

Institut für Neurowissenschaften und Medizin (INM-1 und INM-2)
des Forschungszentrums Jülich

Institut für Biologie II (Zoologie)
der RWTH Aachen University

Berichter:

Prof. Dr. Hermann Wagner, RWTH Aachen University

Prof. Dr. med. Dr. med. h.c. Karl Zilles, RWTH Aachen University

Erklärung

Hiermit versichere ich, Jennifer Nadine Cremer, an Eides statt, dass ich die vorliegende Arbeit selbstständig angefertigt und keine anderen als die angegebenen Hilfsmittel und Quellen verwendet habe. Textstellen oder Abbildungen, die wörtlich oder abgewandelt aus anderen Arbeiten stammen, habe ich mit einer Quellenangabe versehen. Diese Arbeit wurde weder vollständig noch in Teilen einem anderen Prüfungsamt zur Erlangung eines akademischen Grades vorgelegt. Frühere Promotionsanträge wurden von mir nicht gestellt.

Jennifer Nadine Cremer Jülich, September 2013

Neurotransmitter receptors in three rodent models of Parkinson's disease – A quantitative multireceptor study

Abbreviations

AMPA	α-amino-3-hydroxy-5-methyl-4-isoxazolepropionic acid
ANOVA	ANalysis Of VAriance
AK	aphakia
BZ	benzodiazepine
CA	cornu ammonis
cAMP	cyclic adenosine monophosphate
CB	cerebellum
CCD	charge-coupled device
CPu	caudate-putamen (striatum)
dATP	deoxyadenosine triphosphate
DG	dentate gyrus
DJ-1	= PARK7
GABA	γ-amino butyric acid
IP	imaging plate
ISH	in situ hybridization
L-DOPA	L-3,4-dihydroxyphenylalanine
LRRK2	Leucine-Rich Repeat Kinase 2 = PARK 8
LTP	long-term potentiation
M	motor cortex
mRNA	messenger ribonucleic acid
NMDA	N-methyl-D-aspartate
OB	olfactory bulb
PD	parkinson's disease
PINK-1	PTEN-Induced Putative Kinase 1 = PARK6
Pir	piriform cortex
Pitx3	pituitary homeobox 3
PSL	photo stimulated luminescence
RD	retinal degeneration
RING	Really Interesting New Gene
ROI	region of interest

Abbreviations

RT	room temperature
S	somatosensory cortex
SA	specific activity
SD	standard deviation
SN	substantia nigra
TdT	terminal deoxynucleotidyl transferase
TH	tyrosine hydroxylase
UPP	ubiquitin-proteasome pathway
UPSIT	University of Pennsylvania Smell Identification Test
V	visual cortex
WT	wild type
5-HT	serotonin

Introduction

"There appears to be sufficient reason for hoping that some remedial process may ere long be discovered, by which, at least, the progress of the disease may be stopped" (James Parkinson, 1817, An Essay on the Shaking Palsy)

1. Parkinson's disease

Parkinson's disease (PD) is the second most common neurodegenerative disorder in man. The clinical syndrome of PD is mainly characterized by its cardinal symptoms rigidity, resting tremor, bradykinesia and postural instability (Fahn, 2003), while the histopathological hallmark is a severe degeneration of dopamine producing neurons in the substantia nigra of the mesencephalon (Greenfield and Bosanquet, 1953). Besides movement-related symptoms, non-motor symptoms affecting cognition, sensory systems, sleep and psyche are frequent comorbidities of the disease (Fahn, 2003). Although major ongoing effort was put into PD research, today the cause and the detailed pathogenesis of the neurodegenerative processes in PD remain elusive. Thus, the quotation stated above still expresses a major source of motivation for recent studies on the issue as it did nearly two hundred years ago, when it was stated by James Parkinson in his first description of the "Shaking Palsy".

While the pathophysiology and clinical features of PD are well-known, the etiology leading to dopaminergic cell loss remains unclear, being most likely influenced by a combination of genetic susceptibilities, environmental factors and general aging processes (Klein and Schlossmacher, 2007; Thomas and Beal, 2007). Current medications manage to provide symptomatic relief that enables patients to cope with the disease for a considerably long time, however, they fail to cure the disease by stopping the dopaminergic cell loss (Fahn, 2003; Thomas and Beal, 2007). Thus, the molecular mechanisms decisive for the pathogenesis have to be understood to develop new promising targets for therapeutic intervention.

Neurotransmitter receptors are targets for pharmaceutical intervention in numerous neurological and psychiatric diseases, since differential alterations of transmitter systems

are often found in such disorders of humans as well as in respective animal models (Zilles et al., 1999; Palomero-Gallagher et al., 2009, 2012; Cremer, 2011). In case of PD, the degeneration of dopamine producing neurons in the substantia nigra results in a lack of dopaminergic neurotransmission, which can be pharmaceutically compensated for a considerably long, however, limited time by the application of the dopamine precursor L-Dopa (Bauer et al., 1982). Additionally, differential changes of the adrenergic, the cholinergic and the dopaminergic system have been described for PD (reviewed by Xu et al., 2012), indicating a complex interdependency between different transmitter systems. Thus, a comprehensive study of neurotransmitter receptor expression in PD could improve our understanding of the underlying molecular mechanisms.

To date, little is known about neurotransmitter receptor expression in rodent models of PD. Although there is evidence of neurotransmitter receptors being affected in mouse models of hereditary Parkinsonism (i.e. *Parkin* and *DJ-1*, see 2.2), to our knowledge, no comprehensive characterization of multiple receptor systems has been performed.

Therefore, the aim of this study was a systematic, comparative analysis of the density and regional distribution of numerous receptor types of different transmitter systems within the brain of three well established mouse models of PD.

2. Rodent models of Parkinson's disease

2.1. *Pitx3 aphakia* mice

The *aphakia* mutation was first described in 1968 as a "mutation in the mouse characterized by abnormal lens formation, folding of the eyecup, and eventual ocular disorganization" (Varnum and Stevens, 1968). The correspondent homeobox gene *Pitx3* was isolated almost thirty years later (Semina et al., 1997). For some time, *Pitx3 aphakia* mice were studied exclusively as a model for abnormal lens development (Grimm et al., 1998; Graw, 1999; Rieger et al., 2001). This changed in 2003, when a decisive histopathological feature of *Pitx3 aphakia* mice attracted scientific interest, i.e. the fact that these mice exhibit a selective and severe loss of dopaminergic neurons in the substantia nigra (Hwang et al., 2003; Nunes et al., 2003; van den Munckhof et al., 2003; Smidt et al., 2004). For this reason, the *Pitx3 aphakia* mouse was established as a model for Parkinson's disease. Smidt et al. (2004) assumed that "molecular analysis of the underlying mechanisms might provide new insights for understanding the selective degeneration observed in Parkinson patients". The described cell loss in the substantia nigra of *Pitx3 aphakia* mice entails a reduction of dopaminergic innervation in the striatum (van den Munckhof et al., 2003).

At the motor level, *Pitx3 aphakia* mice exhibit both impairments of locomotor activity in general and deficits in striatum-dependent cognitive and nigrostriatal pathway-sensitive behavioral tests (Hwang et al., 2005; van den Munckhof et al., 2006; Ardayfio et al., 2008). The former is indicated by reduced spontaneous locomotor activity (van den Munckhof et al., 2006), the latter two are reflected by impairments concerning rotarod learning, t-maze performance, inhibitory avoidance tasks, challenging beam and pole test (Hwang et al., 2005; Ardayfio et al., 2008).

Recently, it was shown that the *aphakia* mouse is not only a model for PD on a pathological and behavioral level. Moreover, it was demonstrated that mutations of the *Pitx3* gene in humans are indeed associated with an increased risk for Parkinson's disease (Fuchs et al., 2009; Haubenberger et al., 2011; Le et al., 2011; Tang et al., 2012). Furthermore, the above mentioned motor deficits of *Pitx3 aphakia* mice were reversed by L-DOPA treatment (Hwang et al., 2005; van den Munckhof et al., 2006), which in case of chronic administration lead to L-DOPA-induced dyskinesia, that also occurs after long term L-DOPA use in PD patients (Ding et al., 2007).

Taken together, *Pitx3 aphakia* mice represent a promising animal model of PD exhibiting its crucial hallmarks at the neuropathological, symptomatic and pharmacological level.

2.2. Mouse models of hereditary Parkinsonism

In most cases the etiology of PD is unknown, but there is "a well-established genetic component in a considerable subset of patients" (Klein and Schlossmacher, 2006). The first described heritable form of PD was linked to alpha-synuclein in 1997 (Polymeropoulos et al., 1997). In the following fifteen years numerous genes linked to familial forms of PD have been identified, such as *Parkin* (Kitada et al., 1998), *DJ-1* (Abou-Sleiman et al., 2003; Bonifati et al., 2003; Hague et al., 2003), *PINK-1* (Valente et al., 2001; Valente et al., 2002) or *LRRK2* (Paisan-Ruiz et al., 2004; Zimprich et al., 2004). Transgenic animal models in which the correspondent genes were inhibited by conditional knock out have provided important insights into the function of the PD-linked genes and for the pathogenesis of PD. Molecular mechanisms such as mitochondrial dysfunction, oxidative stress and abnormal protein accumulation were identified as key elements of PDs' pathogenesis (Abou-Sleiman et al., 2006; Nunomura et al., 2007; Henchcliffe and Beal, 2008). Within the framework of the present study two knockout models of hereditary Parkinsonism were analyzed, i.e. the *Parkin* and the *DJ-1* knockout mouse.

2.2.1. *Parkin* knockout mice

The *Parkin* gene codes for a RING (really interesting new gene) finger protein that functions as an E3 ubiquitin ligase in the ubiquitin-proteasome pathway (UPP) (Imai et al., 2000; Shimura et al., 2000; Tanaka et al., 2001) (cf. fig. 1). The UPP plays a crucial role for protein homeostasis within the cell by regulating the level of short-lived proteins and promoting the removal of damaged and misfolded proteins. The two major steps of the pathway are the tagging of the target protein by covalent attachment of multiple ubiquitin molecules and the subsequent degradation of the substrate by the 26S proteasome complex (Glickman and Ciechanover, 2002). Its dysfunction has been linked to the pathogenesis of neurodegenerative disorders like Alzheimer's and Parkinson's disease (Ciechanover and Brundin, 2003; Giasson and Lee, 2003).

Homozygous *Parkin* gene mutations account for almost half of all early-onset PD cases (Lucking et al., 2000). *Parkin*-related PD is mainly characterized by an early average age of disease onset (~30 years), nigral degeneration, the absence of Lewy bodies and PD specific motor deficits that respond to L-DOPA treatment (Hayashi et al., 2000; Kitada et al., 2000; Lucking et al., 2000).

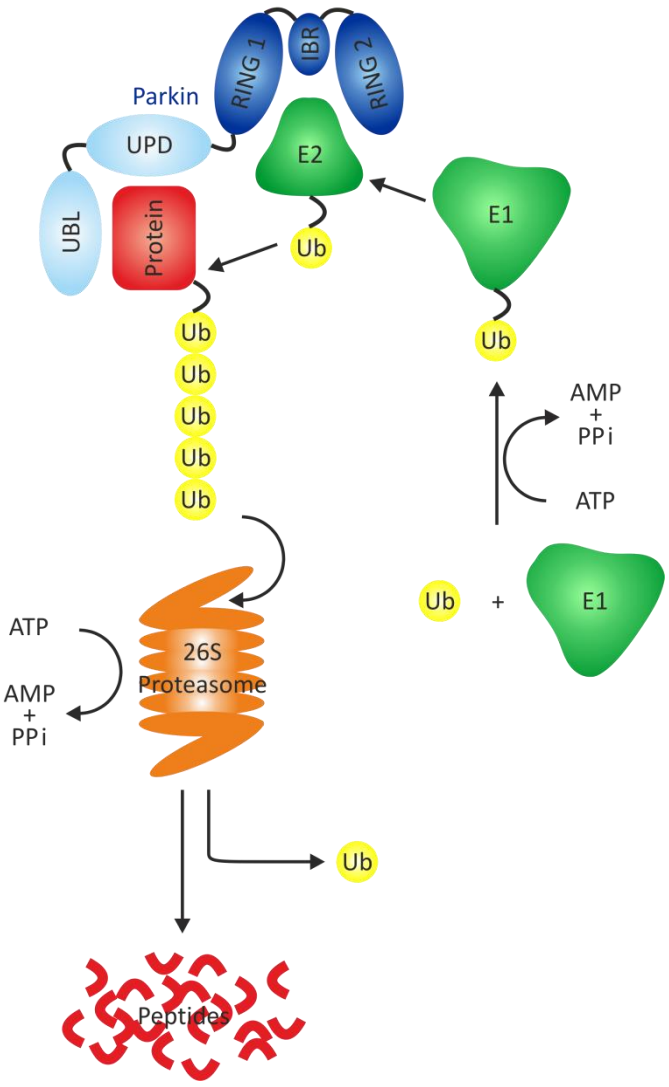

Fig.1 Simplified scheme of the Parkin-directed ubiquitin-proteasome pathway (UPP)
Ubiquitin (Ub) is activated ATP-dependently by an Ub-activating enzyme (E1) and then transferred to an Ub-conjugating enzyme (E2). The Ub-ligating enzyme (E3), in this case Parkin, covalently attaches the ubiquitin to the target protein. A poly-Ub chain is formed by repetition of the procedure and becomes a signal for proteolytic cleavage by the 26S proteasome complex.
(UPD: unique parkin domain, UBL: Ub-like domain, RING: really interesting new gene, IBR: in-between RING)
Based on a report by Tanaka et al. (2001).

In contrast to *Parkin*-associated PD in humans, the knockout of the *Parkin* gene in mice does not result in dopaminergic cell loss in the substantia nigra (Goldberg et al., 2003). Nevertheless, *Parkin* knockout mice exhibit physiological and behavioral differences compared to control animals that make these mice a promising model to contribute to the exploration of PD pathogenesis. The dopamine concentration in the striatum of *Parkin* knockout mice is increased, for instance, while the synaptic excitability is decreased. Of particularly interest is the fact that deficits in behavioral paradigms sensitive to nigrostriatal dysfunction have been described, despite the unaltered number of dopaminergic neurons (Goldberg et al., 2003).

Impairments of long-term depression and long-term potentiation have been described for striatal medium spiny neurons of *Parkin* knockout mice (Kitada et al., 2009). In their set of experiments Kitada and colleagues were able to restore long-term depression by co-application of either D_1- or D_2-like receptor agonists, indicating changes of receptor-dependent dopaminergic transmission in these mice. This hypothesis corresponds to previous results, demonstrating an upregulation of dopamine receptor densities (D_1 and D_2) in the striatum of *Parkin* knockout mice (Sato et al., 2006).

2.2.2. *DJ-1* knockout mice

The DJ-1 protein is a molecular chaperone which is induced during oxidative stress and primarily localized to mitochondria (Shendelman et al., 2004; Zhang et al., 2005). So far, the function of DJ-1 is not fully understood. Xiong et al. (2009) demonstrated that PINK1, Parkin and DJ-1 form a cytoplasm-located complex that promotes the described E3 ubiquitin ligase activity of Parkin. In contrast, Thomas et al. (2011) did not find complexes of the three proteins and suggested that DJ-1 works in parallel to the PINK1/parkin pathway to assure mitochondrial function in case of oxidative stress.

Mutations of the *DJ-1* gene are comparatively rare and account for approximately 1% of the PD cases with early onset (Abou-Sleiman et al., 2003). *DJ-1* related Parkinson's disease is also characterized by a young average age at disease onset (~30 years) and PD-specific motor

symptoms like bradykinesia and rigidity that show a good response to L-DOPA therapy (Hague et al., 2003).

Similar to *Parkin* knockout mice, *DJ-1* knockout mice do not exhibit a reduced number of dopaminergic neurons in the substantia nigra but numerous physiological and behavioral differences compared to control animals, such as a reduction of evoked dopamine overflow in the striatum as well as motor impairments, e.g. hypoactivity and gait abnormalities (Chen et al., 2005; Goldberg et al., 2005; Chandran et al., 2008). Long-term depression has been shown to be abolished at hippocampal CA1 synapses of *DJ-1* knockout mice, but could be rescued by application of the dopamine receptor agonist quinpirole (Wang et al., 2008), thus, implying dopamine-receptor dependent changes of synaptic transmission in these mice.

3. Aims of the study

In this work, quantitative receptor autoradiography was used to investigate the density and distribution of neurotransmitter receptors in unfixed frozen brain tissue (Zilles et al., 2002b; Zilles et al., 2004) of three well established mouse models of PD.

Changes of a respective receptor system most often coincide with differential alterations of other receptor systems. Thus, in order to obtain a comprehensive perspective, 19 to 21 different receptor types, covering seven neurotransmitter systems were systematically investigated in eleven brain regions along the rostro-caudal axis of the brain.

The aims of the present study can be summarized as follows.

- Characterization of neurotransmitter receptor density and distribution in the brain of *Pitx3 aphakia* mice, which exhibit the crucial hallmarks of PD on a neuropathological, symptomatic and pharmacological level
- Analysis of neurotransmitter receptor expression in the brain of *Parkin* and *DJ-1* knockout mice, two models of hereditary parkinsonism
- Investigation of mRNA transcription levels of selected neurotransmitter receptors in the brain of *Parkin* and *DJ-1* knockout mice
- Analysis and discussion of possible correlations between the receptor alterations and pathological or functional aspects
- Novel data concerning the role of non-dopamine neurotransmitter receptors in PD

Materials and methods

1. Animals

All experiments were performed according to the German animal welfare act and approved by the responsible governmental agency, LANUV NRW (Landesamt für Natur, Umwelt und Verbraucherschutz NRW). All animals were kept under standard laboratory conditions with access to food and water ad libitum.

Male, 12 weeks old *Parkin* and *DJ-1* knockout mice (B6.129S4-Park2^{tm1Shn}/J; B6.Cg-Park7^{tm1Shn}/J, The Jackson Laboratory, USA) and corresponding control animals (C57BL/6J, The Jackson Laboratory, USA) were used for autoradiographic analysis. Male animals of 6-8 months of age were used for in situ hybridization experiments. The mice (29 +/- 4 g bodyweight) were anesthetized using CO_2 and subsequently decapitated. The brains were immediately removed, frozen in isopentane at -50°C and stored at -80°C.

Male *Pitx3 aphakia* mice of 4-6 months of age and corresponding control animals (C57Bl/6J) were generously provided for autoradiographic analysis by Prof. Dr. Jochen Graw (Institute of Developmental Genetics, Helmholtz Zentrum München, Germany). The mice (28 +/- 3 g bodyweight) were anesthetized using CO_2 and subsequently decapitated. After immediate preparation, the brains were frozen in isopentane at -70°C, stored on dry ice and delivered to Forschungszentrum Jülich. Subsequently, the brains were stored at -80°C.

2. Tissue processing

The unfixed, deep-frozen brains were serially sectioned in the coronal plane with a cryostat (Leica Instruments GmbH, Germany) at -15°C. Slices for receptor autoradiography were 10 µm thick whereas the thickness of the slices for in situ hybridization was 20 µm. The slices were mounted on pre-cooled, silan-coated slides and dried on a heating plate at 35°C for 15 minutes. Alternating sections were either processed for quantitative in vitro receptor

autoradiography according to standard protocols (Zilles et al., 2002a, 2002b, 2004; Palomero-Gallagher et al, 2003) or histological staining (cresyl violet staining), respectively. The slices were stored in plastic boxes, vacuum-sealed and stored at -80°C.

The sections designated for in situ hybridization (Cremer et al., 2010) were fixed in 4 % paraformaldehyde dissolved in 0.1 M phosphate buffered saline (PBS) (pH 7.4) for 30 min (RT). The sections were subsequently washed in PBS (3 x 10 min; RT), dehydrated in 70 %, 95 % and 100 % ethanol (10 min each; RT) and stored in ethanol at 4°C until hybridization experiments.

3. [^{3}H]-receptor autoradiography

3.1. Binding procedure

In short, the autoradiographic labeling method used in the present work consisted of three steps: a preincubation, a main incubation, and a rinsing step (Zilles et al., 2002a).

During preincubation the sections were rehydrated, the pH value was adapted and endogenous receptor binding substances were washed out.

In the main incubation sections were incubated either in a buffer solution containing the respective [^{3}H]-ligand or the [^{3}H]-ligand and a specific, non-radioactive displacer (about a thousand times higher concentrated). The former approach demonstrates the total binding of the ligand whereas the latter represents the nonspecific, and therefore nondisplaceable binding. Nonspecific binding is generally less than 10 % of the total binding and thus does not receive further consideration. The final concentration of tritiated ligand dissolved in the buffer solution was measured by triplicated liquid scintillation measurement.

The rinsing step stopped the binding procedure and surplus [^{3}H]-ligand and buffer salts were washed out.

Detailed incubation protocols of all used [^{3}H]-ligands are summarized in table 1, including receptor subtypes, non-radioactive displacers, buffer compositions, incubation and washing times.

Finally, the incubated sections were dried under a flow of cold air and stored at room temperature until exposition against ß$^-$-sensitive films. Brains of knockout and control animals were randomized and processed simultaneously.

Table 1: Summary of [^{3}H]-ligands, receptor subtypes, displacers and incubation conditions

Receptor	[^{3}H]-ligand	Displacer	Incubation buffer	Preincubation	Main incubation	Rinsing
AMPA	AMPA [10nM]	Quisqualate [10µm]	50mM Tris-acetate (pH 7.2) +100mM KSCN*	3 x 10min at 4°C	45min at 4°C	4 x 4s at 4°C 2 x 2s in 2,5% Glutaraldehyde in acetone
Kainate	Kainate [9.4nM]	SYM 2081 [100µM]	50mM Tris-citrate (pH 7.1) +10mM Calcium acetate*	3 x 10min at 4°C	45min at 4°C	3 x 4s at 4°C 2 x 2s in 2,5% Glutaraldehyde in acetone
NMDA	MK 801 [3.3nM]	MK 801 [100µM]	50mM Tris-HCl (pH 7.2) +50µM Glutamate +30µM Glycine* +50µM Spermidine*	15min at 4°C	60min at 22°C	2 x 5min at 4°C 1s in distilled water
mGlu2/3	LY 341,495 [1nM]	L-Glutamate [1mM]	Phosphate buffer (pH 7.6) (137mM NaCl; 2.7mM KCl; 4.3mM $Na_2HPO_4x2H_2O$; 1.4mM KH_2PO_4) +100mM KBr*	2 x 5min at 22°C	60min at 4°C	2 x 5min at 4°C 1s in distilled water
$GABA_A$	Muscimol [7.7nM]	GABA [10µM]	50mM Tris-citrate (pH 7.0)	3 x 5min at 4°C	40min at 4°C	3 x 3s at 4°C 1s in distilled water
$GABA_A$	SR 95531 [3nM]	GABA [1mM]	50mM Tris-citrate (pH 7.0)	3 x 5min at 4°C	40min at 4°C	3 x 3s at 4°C 1s in distilled water
$GABA_B$	CGP 54626 [2nM]	CGP 55845 [100µM]	50mM Tris-HCl (pH 7.2) +2.5mM $CaCl_2$	3 x 5min at 4°C	60min at 4°C	3 x 2s at 4°C 1s in distilled water
BZ	Flumazenil [1nM]	Clonazepam [2µM]	170mM Tris-HCl (pH 7.4)	15min at 4°C	60min at 4°C	2 x 1min at 4°C 1s in distilled water

M_1	Pirenzepine [10nM]	Pirenzepine dihydrate [2µM]	Modified Krebsbuffer (pH 7.4) (5.6mM KCl; 30.6mM NaCl; 1.2mM $MgSO_4$; 1.4mM KH_2PO_4; 5.6mM D-Glucose; 5.2mM $NaHCO_3$; 2.5mM $CaCl_2$)	15min at 4°C	60min at 4°C	2 x 1min at 4° C 1s in distilled water
M_2	Oxotremorine-M [1.7nM]	Carbachol [10µM]	20mM Hepes-Tris (pH 7.5) +10mM $MgCl_2$	20min at 22°C	60min at 22°C	2 x 2min at 4°C 1s in distilled water
M_2	AF-DX 384 [5nM]	Atropine sulphate [100µM]	Modified Krebsbuffer (pH 7.4) (4.7mM KCl; 120mM NaCl; 1.2mM $MgSO_4$; 1.2mM KH_2PO_4; 5.6mM D-Glucose; 25mM $NaHCO_3$; 2.5mM $CaCl_2$)	15min at 22°C	60min at 22°C	3 x 4min at 4°C 1s in distilled water
M_3	4-DAMP [1nM]	Atropine sulphate [10 µM]	50 mM Tris-HCl (pH 7.4) + 0.1 mM PMSF + 1 mM EDTA	15min at 22°C	45min at 22°C	2 x 5min at 4°C 1s in distilled water
Nicotinic	Epibatidine [0.11nM]	Nicotine [100µM]	15mM Hepes (pH 7.5) +120mM NaCl +5.4mM KCl +0.8mM $MgCl_2$ +1.8mM $CaCl_2$	20min at 22°C	90min at 4°C	5min at 4°C 1s in distilled water
α_1	Prazosin [0.09nM]	Phentolamine mesylate [10µM]	50mM Na/K-phosphatebuffer (pH 7.4)	15min at 22°C	60min at 22°C	2 x 5min at 4°C 1s in distilled water
α_2	UK14,304 [0.64nM]	Phentolamine mesylate [10µM]	50mM Tris-HCl (pH 7.7) +100µM $MnCl_2$	15min at 22°C	90min at 22°C	5min at 4°C 1s in distilled water
5-HT_{1A}	8-OH-DPAT [0.3nM]	5-HT [1µM]	170mM Tris-HCl (pH 7.7) +0.01% Ascorbate* +4mM $CaCl_2$*	30min at 22°C	60min at 22°C	5min at 4°C 3 x 1s in distilled water

5-HT_2 (only for *aphakia*)	Ketanserin [1.14nM]	Mianserin [10µM]	170mM Tris-HCl (pH 7.7)	30min at 22°C	120min at 22°C	2 x 10min at 4°C 3 x 1s in distilled water
D_1 (only for *aphakia*)	SCH 23390 [1.67nM]	SKF 83566 [1µM]	50mM Tris-HCl (pH 7.4) +120mM NaCl +5mM KCl +2mM $CaCl_2$ +1mM $MgCl_2$ +1µM Mianserin*	20min at 22°C	90min at 22°C	2 x 10min at 4°C 1s in distilled water
D_2	Raclopride [0.55mM]	Butaclamol [1µM]	50mM Tris-HCl (pH 7.4) +150mM NaCl +0.1% Ascorbate	20min at 22°C	45min at 22°C	6 x 1min at 4°C 1s in distilled water
D_2/D_3	Fallyprid [4nM]	Haloperidol [10µM]	50mM Tris-HCl (pH 7.4) +5mM KCl +120mM NaCl	30min at 22°C	60min at 37°C	2 x 2min at 4°C 1s in distilled water
A_{2A}	ZM 241 385 [0.42nM]	2-Chloroadenosine [20µM]	170mM Tris-HCl (pH 7.4) +1mM EDTA (only preincubation) +2U/L adenosine deaminase (only pre- and main incubation) +10mM $MgCl_2$ (only prerinsing and main incubation)	30min at 37°C Prerinsing: 2 x 10min at 22°C	120min at 22°C	2 x 5min at 4°C 1s in distilled water

* = only added in main incubation
BZ = $GABA_A$ associated benzodiazepine binding sites

3.2. Film exposition and development

The sections were fixed on sheets of paper with double-sided adhesive tape and exposed to β^--sensitive films (Kodak, PerkinElmer LAS GmbH, Germany) between plastic plates tightly shut with metal clips and in the presence of standards of known radioactivity concentrations (GE Helthcare, Germany; laboratory-intern standards) for 9-15 weeks. Table 2 demonstrates the exposure times for all used ligands.

Afterwards, the films were developed in a photographic laboratory using a Hyperprocessor (Amersham Biosciences, Europe).

Table 2: Exposure times for the [^{3}H]-ligands

[^{3}H]-ligand	Exposure time [weeks]
AF-DX 384	10
AMPA	15
CGP 54626	10
4-DAMP	9
Epibatidine	15
Fallyprid	15
Flumazenil	9
Kainate	12
Ketanserin	15
LY 341,495	10
MK 801	12
Muscimol	12
8-OH-DPAT	15
Oxotremorine-M	15
Pirenzepine	12
Prazosin	15
Raclopride	15
SCH 23390	15
SR 95531	12
UK 14,304	15
ZM 241 385	15

4. Digital processing of autoradiographic films

4.1. Digitalization

The autoradiographic films were analyzed by means of densitometric procedures (Zilles and Schleicher, 1991, 1995; Zilles et al., 2002a).

First, the developed films were digitized using a CCD-camera (Zeiss, Carl Zeiss MikroImaging GmbH, Germany). Homogeneous illumination of the images was ensured by darkening of the room, the use of a homogeneously illuminated light table and a shading correction that was performed for each autoradiographic film. Images were saved 8-bit-coded in 256 gray values (0=black, 255=white) with a resolution of 4164 x 3120 pixels. The image analyzing software AxioVision (Zeiss, Carl Zeiss MikroImaging GmbH, Germany) was used both for digitizing the autoradiographs and for the following densitometric measurements.

4.2. Calibration and densitometric analysis

Coexposed plastic and homogenate microscales of known radioactivity concentrations were used to compute specific non-linear transformation curves for each autoradiographic film. A transformation curve represents the relationship between gray value in the autoradiograph and concentration of radioactivity in the tissue (Zilles et al., 2004). Using these transformation curves, the gray value of each pixel in an autoradiographic image was converted into corresponding concentrations of radioactivity and subsequently into receptor densities (fmol/mg protein) (Zilles et al., 2002a). The resulting linearized images, in which gray values correlate to receptor densities as a linear function, were contrast enhanced and color coded to optimally visualize the regional distribution of the analyzed neurotransmitter receptors within the brain. For this purpose, a color scale with eleven colors representing equally spaced gray value ranges was assigned to the 256 gray values of the linearized autoradiograph. The described proceeding is schematically shown in figure 2.

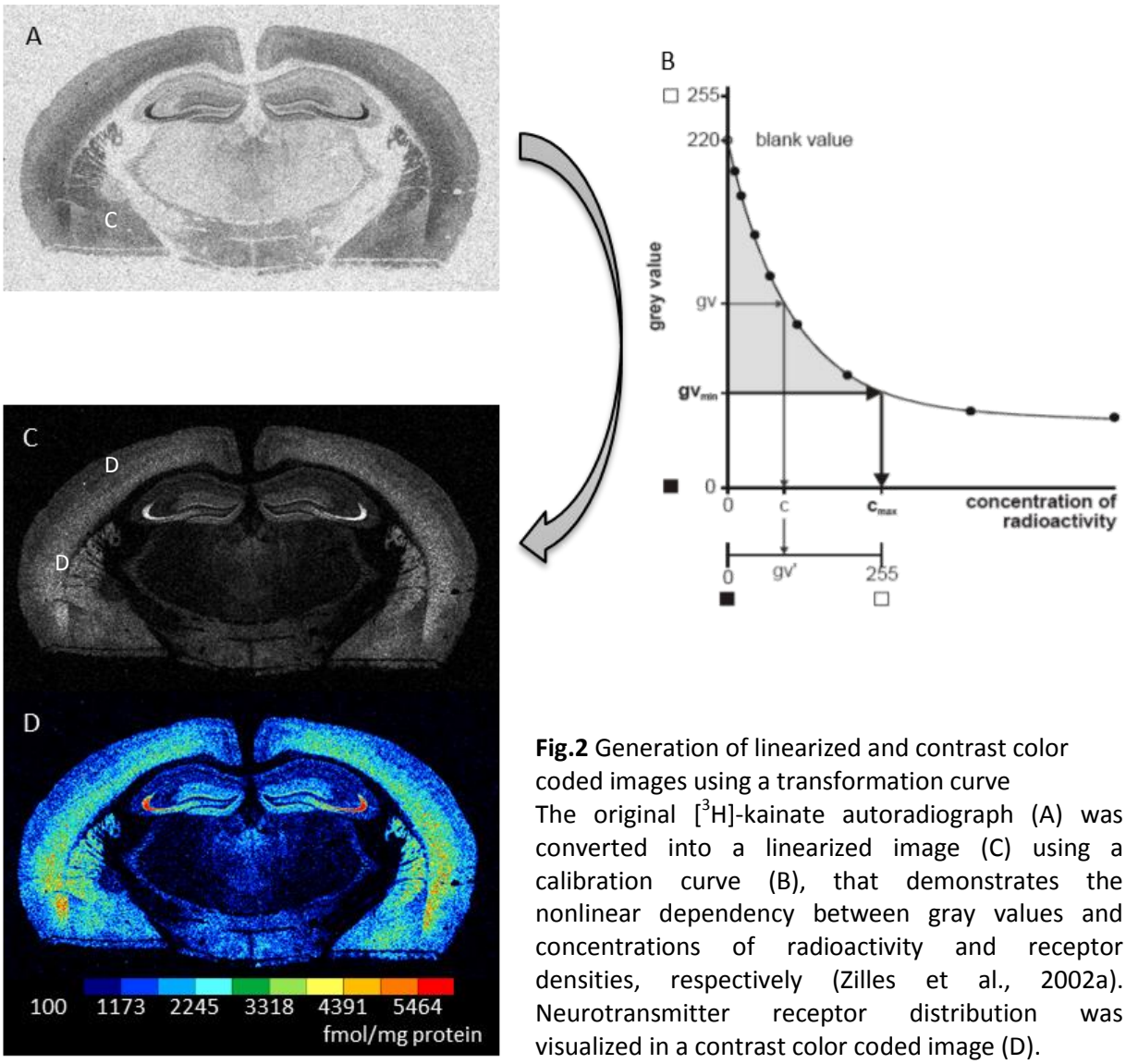

Fig.2 Generation of linearized and contrast color coded images using a transformation curve
The original [^{3}H]-kainate autoradiograph (A) was converted into a linearized image (C) using a calibration curve (B), that demonstrates the nonlinear dependency between gray values and concentrations of radioactivity and receptor densities, respectively (Zilles et al., 2002a). Neurotransmitter receptor distribution was visualized in a contrast color coded image (D).

Receptor densities (fmol/mg protein) were measured densitometrically in eleven different brain regions of interest (ROI) by interactively plotting onto the digitized autoradiographic images. The following brain regions were designated as ROI: olfactory bulb, the motor, somatosensory, piriform and visual cortices, the caudate putamen (striatum), the CA1-3 fields of the hippocampus, the dentate gyrus, the substantia nigra as well as the cerebellum. Figure 3 shows a schematic overview of the regions' locations within the mouse brain. Receptor densities were measured and averaged for three sections per animal and ROI, respectively.

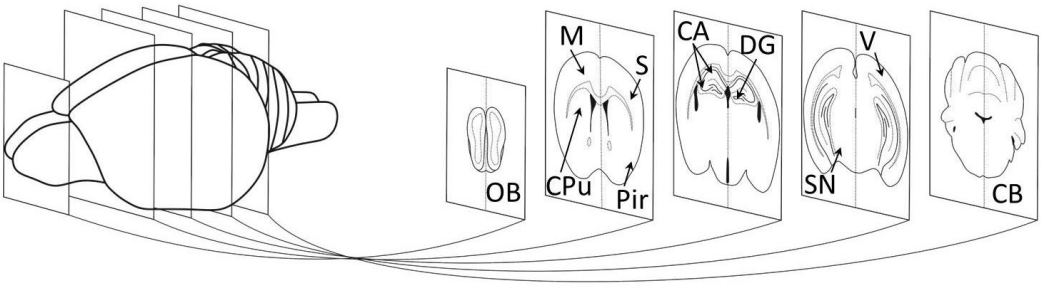

Fig.3 Overview of the analyzed brain regions
OB: olfactory bulb, **M**: motor cortex, **S**: somatosensory cortex, **Pir**: piriform cortex, **CPu**: caudate putamen (striatum), **CA**: field CA1-3 of hippocampus, **DG**: dentate gyrus, **SN**: substantia nigra, **V**: visual cortex, **CB**: cerebellum

5. In situ hybridization (ISH)

5.1. Oligonucleotides

Oligodeoxyribonucleotides (Sigma-Aldrich, Europe) complementary to mouse $GABA_B$ receptor mRNA and KA2 kainate receptor subunit mRNA were used for hybridization experiments. The $GABA_B$ probe was complementary to bases 591 - 630 (TTC AGT CCC TTT GCA TTG TCA CAC TCG GTG TCG TAG AGT C) of the $GABA_B$ receptor mRNA (GenBank no. NM_001081141). The KA2 probe was complementary to the bases 772 – 811 (TCT TCA TTA CTG GGG TAC AGG CTG ACA GAT GCG AAG CGA A) of the KA2 kainate receptor subunit mRNA (GenBank no. NM_008168.2). All probes were designed from the respective coding sequence using VectorNTI Suite 8.

5.2. Radiolabelling

The oligodeoxyribonucleotides were 3'-labelled using ^{33}P-dATP and terminal deoxynucleotidyl transferase (TdT) as previously described (Cremer et al., 2009). 0.5 pmol of the particular probe, 3 µl ^{33}P-dATP (111 TBq/mmol, 9.25 MBq in 25 µl), 30 Units of recombinant TdT and 2 µl reaction buffer were mixed. After adjusting the volume to 10 µl with bi-distilled water, the assay was incubated at 37°C for 90 min. Subsequent to the labeling reaction unincorporated nucleotides were removed using sephadex columns (ProbeQuant G-50, GE Healthcare) according to the manufacturers' protocol. The assay

volume was adjusted to 100 µl by bi-distilled water and specific activity (SA) was measured by triplicated liquid scintillation measurement.

5.3. Hybridization experiments

The hybridization procedure includes a pretreatment step using proteinase K to permeabilize the tissue, followed by the actual hybridization and a washing step. The detailed procedure is summarized in table 3. Unspecific binding was determined in selected sections by addition of 100-fold access of unlabeled oligonucleotide.

Table 3: In situ hybridization procedure

Step of the procedure	Solution	Conditions
Pretreatment	1 x SSC (pH 7.0) 2mM $CaCl_2$ 0.067mg/ml Proteinase K	15min at 22°C
Rinsing	1 x SSC (pH 7.0)	2 x 5min at 22°C
Rinsing	Distilled water	30s at 22°C
Dehydration	Ethanol (70%)	5min at 22°C
Dehydration	Ethanol (90%)	5min at 22°C
Dehydration	Ethanol (100%)	5min at 22°C
Drying		15min (cold air flow)
Hybridization	Hybridization buffer (50 % Formamide; 4 x SSC (pH 7.0); 1mM Sodium pyrophosphate; 0.25mg/ml Salmon sperm DNA; 0.1mg/ml Polyadenylic acid; 100mg/ml Dextran sulfate) + 1µl/100µl labeled probe (spin column eluate) + 1µl/100µl unlabeled probe [0.5pmol/µl]*	50µl probe buffer per section, covered with Parafilm™, incubated in a humid chamber.
Rinsing	1 x SSC (pH 7.0)	5min at 22°C
Rinsing	1 x SSC (pH 7.0)	2 x 15min at 40°C
Rinsing	1 x SSC (pH 7.0)	5min at 22°C
Rinsing	0.1 x SSC (pH 7.0)	5min at 22°C
Rinsing	Distilled water	5min at 22°C
Dehydration	Ethanol (70%)	5min at 22°C

Dehydration	Ethanol (90%)	5min at 22°C
Dehydration	Ethanol (100%)	5min at 22°C
Drying		15min (cold air flow)

* = only added to slices designated to monitor unspecific binding

5.4. Exposition

The sections were fixed on sheets of paper with double-sided adhesive tape and exposed to phosphorous imaging plates (IP) (Fujifilm Europe GmbH, Europe) for 48 hours together with ^{14}C-microscales of known radioactivity concentrations (Amersham Biosciences, Europe) calibrated for quantification of ^{33}P (see 6.2).

6. Digital processing of imaging plates

6.1. Digitalization

The IPs were digitally scanned using a BAS 5000 BioImage Analyzer (Fujifilm Europe GmbH, Europe) and photo stimulated luminescence (PSL) was measured in ROIs as described above. The image analyzing software Aida Image Analyzer v.4.13 was used both for scanning the IPs and for the following densitometric measurements.

6.2. Calibration and densitometric analysis

^{14}C-microscales of known radioactivity concentrations were used to compute specific calibration curves for each IP to convert the optical density (PSL/mm^2) within ROIs into Bq/mg tissue (Cremer et al., 2009). Estimation of specific activity of the labeled probe and the protein content of tissue standards were used to calculate mRNA copy numbers per mg protein (fmol x 10^{-3}/mg protein). The ROIs analyzed were identical as designated for autoradiography experiments except for the visual cortex, the substantia nigra and the cerebellum, which were not considered here. The mRNA levels were measured as described above and averaged for five slices per animal and ROI.

7. Statistical analysis

All data are expressed as mean ± standard deviation (SD) unless otherwise indicated. Receptorautoradiographic as well as ISH data were statistically analyzed for significant differences between control and experimental groups using analysis of variance (omnibus ANOVA, Systat® Version 13) with the following design: blocking factor: animal, between factor: experimental status, within factor: brain region, repeated measurements: neurotransmitter. A p-value <0.05 was considered statistically significant. For those receptors that revealed significant receptor density or mRNA level changes, differentiating tests for each analyzed brain region were carried out by post hoc ANOVA.

The cerebellum as well as the dopamine and adenosine receptor ligands (i.e. SCH 23390, Raclopride, Fallyprid and ZM 241 385) were not considered in the omnibus ANOVA, since receptor densities in this region and of these ligands were partially below the method-inherent detection limit. In these cases ANOVA was performed for each brain region using post hoc tests with Bonferroni correction.

8. Histological staining

Nissl staining (cresyl violet) of sections interleaved between the sections used for receptor autoradiography was performed according to established protocols. This staining enables the cytoarchitectonic identification of the regions. The staining procedure is summarized in table 4.

Table 4: Nissl staining using cresyl violet

Step of the procedure	Solution	Conditions
Fixation	Formalin (pH 7.0) (900ml distilled water; 4g NaH_2PO_4 x $1H_2O$; 6.5g Na_2HPO_4;	30min at 22°C

	100ml formaldehyde (37%))	
Rinsing	Distilled water	2 x 5min at 22°C
Staining	Cresyl violet (1000ml distilled water; 5.33g CH_3COONa; 9.33ml acetic acid 100%); 0.33g cresyl violet)	30min at 40°C
Rinsing	Distilled water	5s at 22°C
Differentiation	Propanol (70%)	1 – 10min at 22°C
Dehydration	Propanol (70%)	5min at 22°C
Dehydration	Propanol (90%)	2 x 5min at 22°C
Dehydration	Propanol (100%)	2 x 5min at 22°C
Dehydration / Intermedium	XEM	2 x 10min at 22°C
Mounting	DPX	

9. Chemicals, solutions and technical equipment

9.1. Tissue processing

- Cryostat Leica CM3050 (Leica Mikrosysteme Vertrieb GmbH, Wetzlar, Germany)
- Ethanol (Merck KGaA, Darmstadt, Germany)
- Paraformaldehyde (Sigma-Aldrich Chemie GmbH, Steinheim, Germany)
- Phosphate buffered saline (PBS) (Invitrogen, Life Technologies GmbH, Darmstadt, Germany)
- Silan-coated slides (Paul Marienfeld GmbH & Co. KG, Lauda-Königshofen, Germany)

9.2. [^{3}H]-receptor autoradiography – Binding procedure

- [^{3}H]-ligands:
    - AF-DX 384 (Perkin Elmer, Rodgau, Germany)
    - AMPA (Perkin Elmer, Rodgau, Germany)
    - CGP 54626 (Biotrend Chemikalien GmbH, Köln, Germany)
    - 4-DAMP (Perkin Elmer, Rodgau, Germany)
    - Epibatidine (Perkin Elmer, Rodgau, Germany)

- Fallyprid (Institute for Nuclear Chemistry, Johannes Gutenberg Universität Mainz, Mainz, Germany)
- Flumazenil (Perkin Elmer, Rodgau, Germany)
- Kainate (Perkin Elmer, Rodgau, Germany)
- Ketanserin (Perkin Elmer, Rodgau, Germany)
- LY 341,495 (Biotrend Chemikalien GmbH, Köln, Germany)
- MK 801 (Perkin Elmer, Rodgau, Germany)
- Muscimol (Perkin Elmer, Rodgau, Germany)
- 8-OH-DPAT (Perkin Elmer, Rodgau, Germany)
- Oxotremorine-M (Perkin Elmer, Rodgau, Germany)
- Pirenzepine (Perkin Elmer, Rodgau, Germany)
- Prazosin (Perkin Elmer, Rodgau, Germany)
- Raclopride (Perkin Elmer, Rodgau, Germany)
- SCH 23390 (Perkin Elmer, Rodgau, Germany)
- SR 95531 (Perkin Elmer, Rodgau, Germany)
- UK14,304 (Perkin Elmer, Rodgau, Germany)
- ZM 241 385 (Biotrend Chemikalien GmbH, Köln, Germany)

- Displacer:
  - Atropine sulphate (Sigma-Aldrich Chemie GmbH, Steinheim, Germany)
  - Butaclamol hydrochloride (Sigma-Aldrich Chemie GmbH, Steinheim, Germany)
  - Carbachol (Sigma-Aldrich Chemie GmbH, Steinheim, Germany)
  - CGP 55845 (Biotrend Chemikalien GmbH, Köln, Germany)
  - 2-Chloroadenosine (Sigma-Aldrich Chemie GmbH, Steinheim, Germany)
  - Clonazapam (Sigma-Aldrich Chemie GmbH, Steinheim, Germany)
  - GABA (Biotrend Chemikalien GmbH, Köln, Germany)
  - Haloperidol (Sigma-Aldrich Chemie GmbH, Steinheim, Germany)
  - L-Glutamate (Sigma-Aldrich Chemie GmbH, Steinheim, Germany)
  - Mianserin (Sigma-Aldrich Chemie GmbH, Steinheim, Germany)
  - MK 801 (Biotrend Chemikalien GmbH, Köln, Germany)
  - Nicotine-di-d-tartrate (Sigma-Aldrich Chemie GmbH, Steinheim, Germany)

- Phentolamine mesylate (Biotrend Chemikalien GmbH, Köln, Germany)
- Pirenzepine dehydrate (Sigma-Aldrich Chemie GmbH, Steinheim, Germany)
- Serotonin (Sigma-Aldrich Chemie GmbH, Steinheim, Germany)
- SKF 83566 (Sigma-Aldrich Chemie GmbH, Steinheim, Germany)
- SYM 2081 (Sigma-Aldrich Chemie GmbH, Steinheim, Germany)
- Quisqualate (Biotrend Chemikalien GmbH, Köln, Germany)

- Buffers and solutions:
  - Adenosine deaminase (Sigma-Aldrich Chemie GmbH, Steinheim, Germany)
  - Ascorbate (Sigma-Aldrich Chemie GmbH, Steinheim, Germany)
  - Acetone (VWR International, Langenfeld, Germany)
  - Calcium acetate (Sigma-Aldrich Chemie GmbH, Steinheim, Germany)
  - Calcium chloride ($CaCl_2$) (Merck KGaA, Darmstadt, Germany)
  - D-Glucose (Merck KGaA, Darmstadt, Germany)
  - Ethylenediaminetetraacetic acid (EDTA) dihydrat (Sigma-Aldrich Chemie GmbH, Steinheim, Germany)
  - Glutamate (Sigma-Aldrich Chemie GmbH, Steinheim, Germany)
  - Glutaraldehyde (Sigma-Aldrich Chemie GmbH, Steinheim, Germany)
  - Glycine (Sigma-Aldrich Chemie GmbH, Steinheim, Germany)
  - HEPES (Sigma-Aldrich Chemie GmbH, Steinheim, Germany)
  - Magnesium chloride ($MgCl_2$) (Merck KGaA, Darmstadt, Germany)
  - Magnesium sulfate ($MgSO_4$) (Sigma-Aldrich Chemie GmbH, Steinheim, Germany)
  - Manganese(II) chloride ($MnCl_2$) (Sigma-Aldrich Chemie GmbH, Steinheim, Germany)
  - Mianserin (Sigma-Aldrich Chemie GmbH, Steinheim, Germany)
  - Phenylmethanesulfonyl fluoride (PMSF) (Sigma-Aldrich Chemie GmbH, Steinheim, Germany)
  - Potassium bromide (KBr) (Sigma-Aldrich Chemie GmbH, Steinheim, Germany)
  - Potassium chloride (KCl) (Sigma-Aldrich Chemie GmbH, Steinheim, Germany)
  - Potassium phosphate monobasic (KH_2PO_4) (Merck KGaA, Darmstadt, Germany)

- Potassium thiocyanate (KSCN) (Sigma-Aldrich Chemie GmbH, Steinheim, Germany)
- Sodium bicarbonate ($NaHCO_3$) (Merck KGaA, Darmstadt, Germany)
- Sodium chloride (NaCl) (Merck KGaA, Darmstadt, Germany)
- Sodium phosphate dibasic dihydrate (Na_2HPO_4 x $2H_2O$) (Merck KGaA, Darmstadt, Germany)
- Spermidine (Sigma-Aldrich Chemie GmbH, Steinheim, Germany)
- Tris-acetate (Sigma-Aldrich Chemie GmbH, Steinheim, Germany)
- Tris-citrate (Sigma-Aldrich Chemie GmbH, Steinheim, Germany)
- Tris-HCl (Sigma-Aldrich Chemie GmbH, Steinheim, Germany)

- Liquid Scintillation Analyzer Tri-Carb 2100 TR (Packard BioScience, PerkinElmer, Rodgau, Germany)
- Liquid Scintillation Cocktail Ultima Gold XR (PerkinElmer, Rodgau, Germany)

9.3. Film exposition and development

- BioMax MR β^--sensitive films (Kodak, Sigma-Aldrich Chemie GmbH, Steinheim, Germany)
- GBX-Developer (Kodak, Sigma-Aldrich Chemie GmbH, Steinheim, Germany)
- GBX-Fixer (Kodak, Sigma-Aldrich Chemie GmbH, Steinheim, Germany)
- Hyperprocessor SRX-101A (Amersham Biosciences, GE Healthcare Europe GmbH, Europe)
- Radioactive standards (GE Healthcare GmbH, München, Germany)

9.4. Digital processing of autoradiographic films

- AxioVision image analyzing software Rel. 4.8.2 (Zeiss, Carl Zeiss MikroImaging GmbH, Göttingen, Germany)
- Digital camera AxioCam HRm (Zeiss, Carl Zeiss MikroImaging GmbH, Göttingen, Germany)

9.5. In situ hybridization (ISH)

- Oligodeoxyribonucleotides:

- $GABA_B$: -TTC AGT CCC TTT GCA TTG TCA CAC TCG GTG TCG TAG AGT C- (Sigma-Aldrich Chemie GmbH, Steinheim, Germany)
- KA2: -TCT TCA TTA CTG GGG TAC AGG CTG ACA GAT GCG AAG CGA A- (Sigma-Aldrich Chemie GmbH, Steinheim, Germany)

- ^{33}P-dATP: 111 TBq / mmol, 9,25 MBq (Perkin Elmer, Rodgau, Germany)
- Saline-sodium citrate buffer (SSC) 20 x concentrate (VWR International GmbH, Darmstadt, Germany)
- Calcium chloride ($CaCl_2$) (Sigma-Aldrich Chemie GmbH, Steinheim, Germany)
- Proteinase K from Tritirachium album (Sigma-Aldrich Chemie GmbH, Steinheim, Germany)
- Ethanol (Merck KGaA, Darmstadt, Germany)
- Formamide (Sigma-Aldrich Chemie GmbH, Steinheim, Germany)
- Sodium pyrophosphate decahydrate (Sigma-Aldrich Chemie GmbH, Steinheim, Germany)
- Deoxyribonucleic acid, single stranded from salmon testes (Sigma-Aldrich Chemie GmbH, Steinheim, Germany)
- Polyadenylic acid potassium salt (Sigma-Aldrich Chemie GmbH, Steinheim, Germany)
- Dextran sulfate sodium salt from Leuconostoc spp. (Sigma-Aldrich Chemie GmbH, Steinheim, Germany)
- Terminal Deoxynucleotidyl Transferase, recombinant (Promega GmbH, Mannheim, Germany)
- Illustra ProbeQuant G-50 micro columns (GE Healthcare GmbH, München, Germany)
- Phosphorus imaging plates (IP) (Fujifilm, Japan)
- ^{14}C-microscales (GE Healthcare UK Limited, Buckinghamshire, UK)
- BAS 5000 BioImage Analyzer (Fujifilm, Japan)
- Aida Image Analyzer v.4.13 (raytest Isotopenmessgeräte GmbH, Straubenhardt, Germany)

9.6. Histological staining

- Acetic acid (Merck KGaA, Darmstadt, Germany)
- Cresyl violet (Merck KGaA, Darmstadt, Germany)

- DPX mountant for histology (Fluka, Sigma-Aldrich Chemie GmbH, Steinheim, Germany)
- Formaldehyde solution (Merck KGaA, Darmstadt, Germany)
- 2-Propanol (Merck KGaA, Darmstadt, Germany)
- Sodium acetate (CH_3COONa) (Merck KGaA, Darmstadt, Germany)
- Sodium phosphate dibasic (Na_2HPO_4) (Merck KGaA, Darmstadt, Germany)
- Sodium phosphate monobasic monohydrate (NaH_2PO_4 x $1H_2O$) (Merck KGaA, Darmstadt, Germany)
- XEM 200 (DiaTec, Diagostische System-Technik, Bamberg, Germany)

Results

1. Regional distribution of neurotransmitter receptors

The different neurotransmitter receptors are present throughout the brain in the three PD mouse models and control mice. The principal regional distribution is also similar between the knockout and control animals with the same regions showing high, intermediate or low receptor densities, respectively. Not only the rank order of mean receptor densities (average over all cortical layers) is comparable between the strains, but also their layer-specific patterns in different cortical areas. Thus, the following description of regional receptor distribution refers to all groups, unless otherwise indicated.

1.1. Glutamate receptors

AMPA receptor densities were low in the olfactory bulb, the primary motor, somatosensory and visual areas, the striatum, the substantia nigra and the cerebellum. Higher densities were found in the piriform cortex as well as in the hippocampal regions (CA1, CA2/3 and dentate gyrus). Figure 4 shows color coded images of AMPA receptor densities to visualize the regional distribution and to show the similarity between the different strains. Mean densities of **kainate** receptors were similar between most analyzed brain regions, except for the CA1 region of the hippocampus, the substantia nigra and the cerebellum, were receptor densities were relatively low (cf. fig. 5). The **NMDA** receptor densities were heterogeneously distributed between ROIs with high receptor densities in the hippocampus (CA1 > dentate gyrus > CA2/3), intermediate densities in the motor, somatosensory, piriform and visual cortex and low densities in the olfactory bulb, the striatum and the substantia nigra. NMDA receptor densities in the cerebellum were found to be below detection limit (cf. fig. 6).

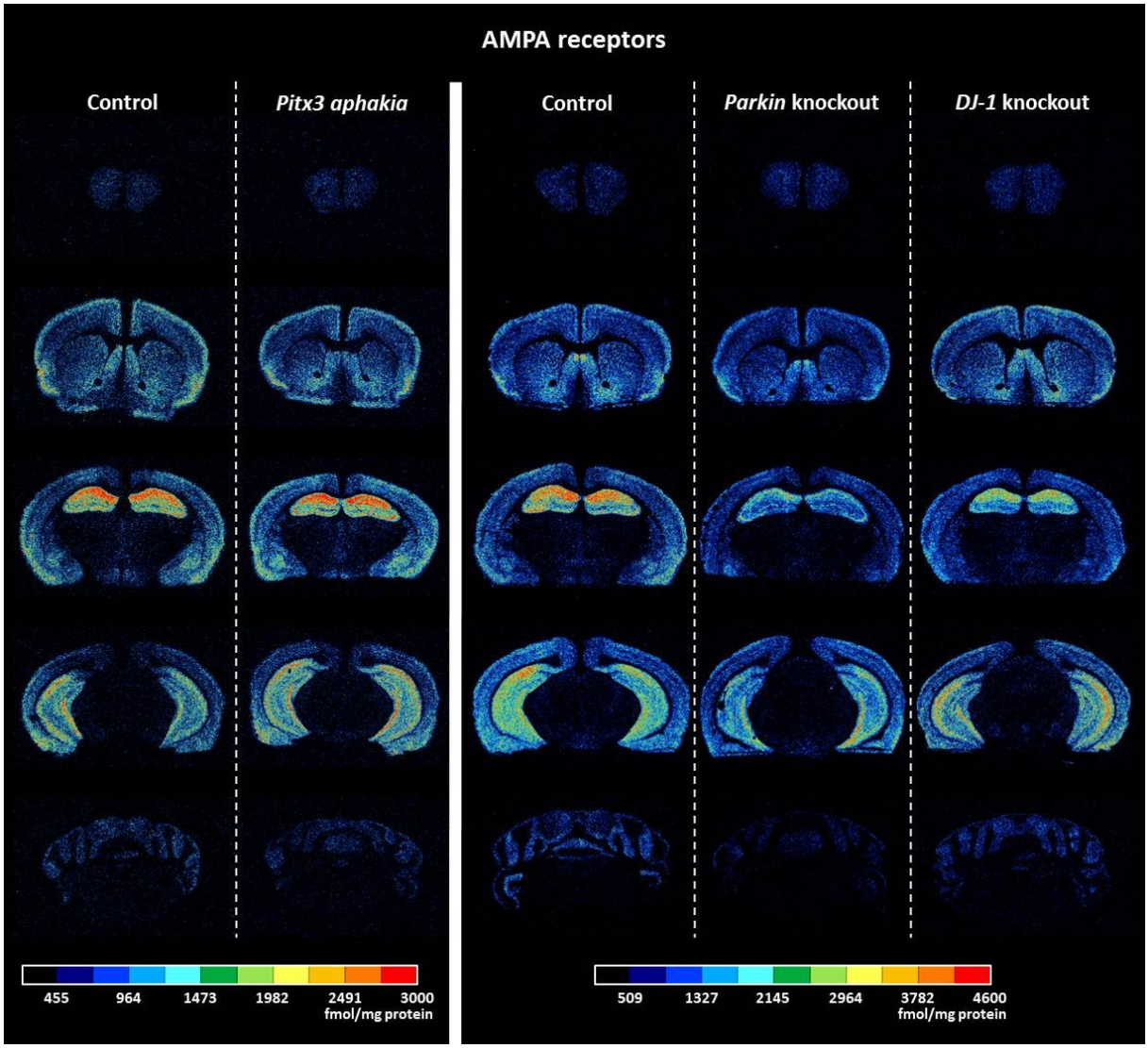

Fig.4 Color coded images of AMPA receptor densities (fmol/mg protein) in the brains of *Pitx3 aphakia, Parkin* and *DJ-1* knockout mice and corresponding control animals showing the distribution similarity between the different strains.

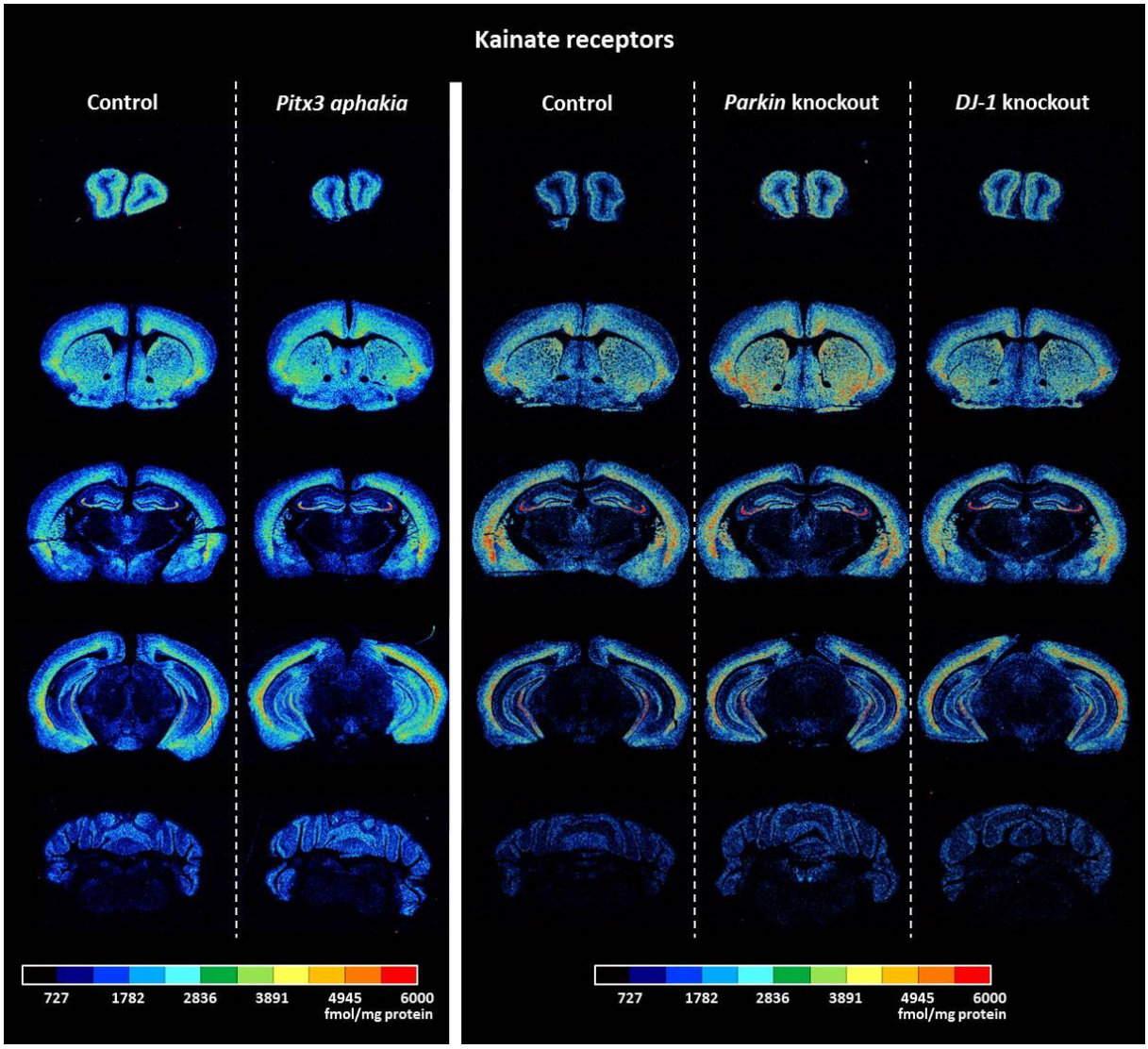

Fig.5 Color coded images of kainate receptor densities (fmol/mg protein) in the brains of *Pitx3 aphakia, Parkin* and *DJ-1* knockout mice and corresponding control animals showing the distribution similarity between the different strains.

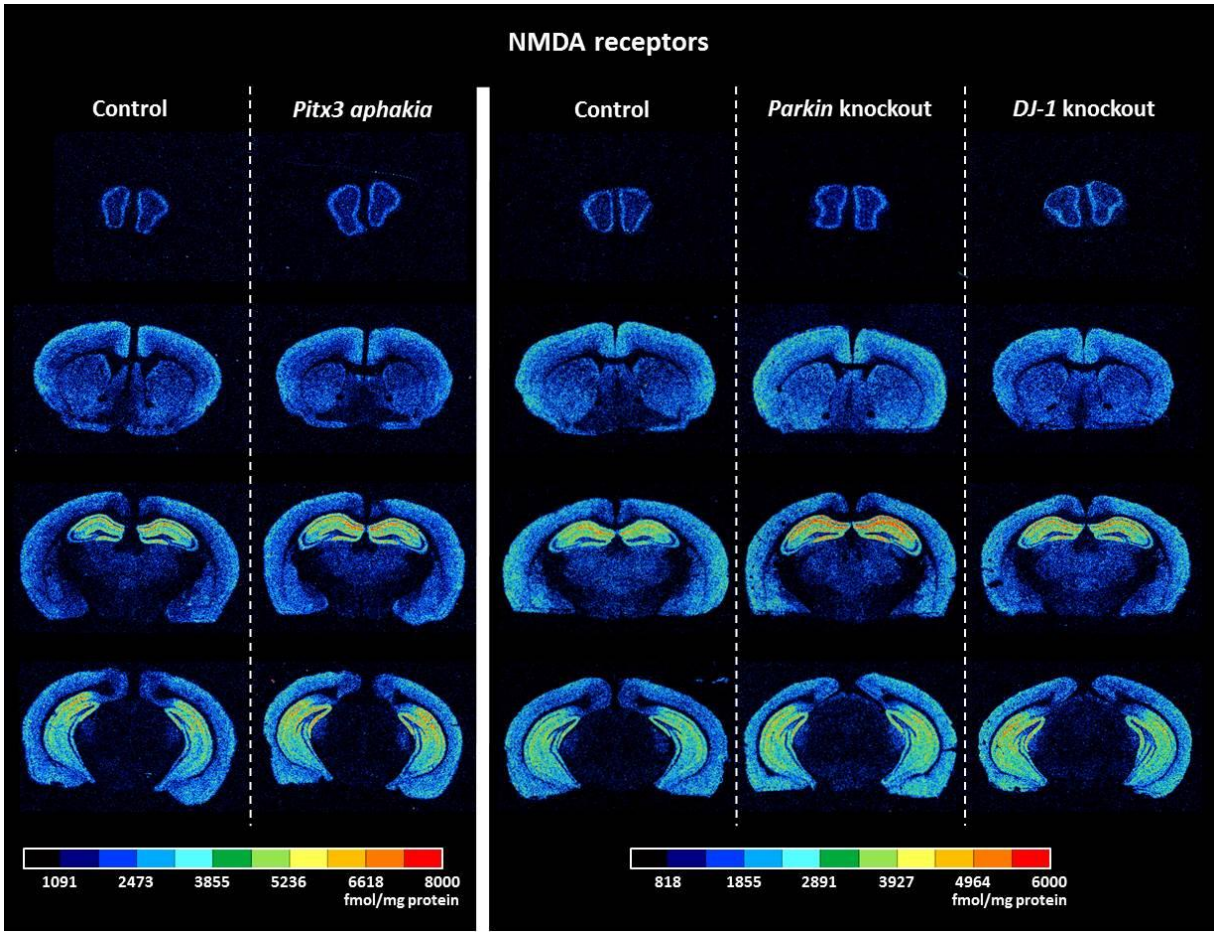

Fig.6 Color coded images of NMDA receptor densities (fmol/mg protein) in the brains of *Pitx3 aphakia, Parkin* and *DJ-1* knockout mice and corresponding control animals showing the distribution similarity between the different strains.

In general, the brains of all investigated groups showed high densities of metabotropic glutamate receptors (**$mGlu_{2/3}$**). These receptors were heterogeneously distributed, revealing high receptor densities in the motor, somatosensory, piriform and visual cortex, intermediate densities in the striatum and the dentate gyrus, and low densities in the olfactory bulb, CA1 and CA2/3, substantia nigra and cerebellum (cf. fig. 7).

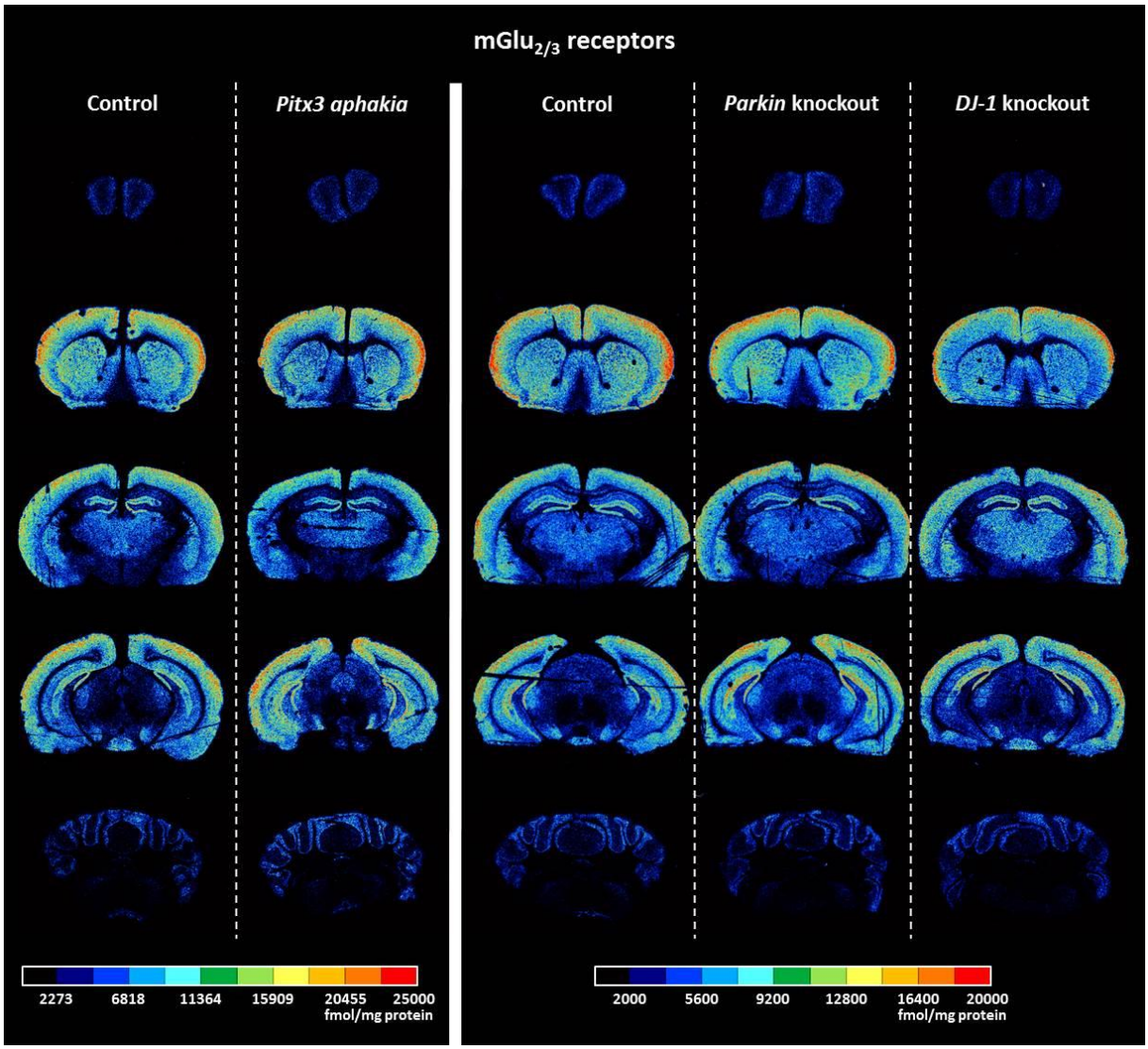

Fig.7 Color coded images of $mGlu_{2/3}$ receptor densities (fmol/mg protein) in the brains of *Pitx3 aphakia, Parkin* and *DJ-1* knockout mice and corresponding control animals showing the distribution similarity between the different strains.

1.2. GABA receptors

$GABA_A$ receptor densities revealed by *agonist* binding were homogenously distributed throughout the brain regions with the exception of a maximum in the cerebellum (cf. fig. 8). *Antagonist* binding exhibited slightly higher values in the hippocampus (CA1, CA2/3 and dentate gyrus), low values in the striatum and intermediate densities in the other ROIs (cf. fig. 9).

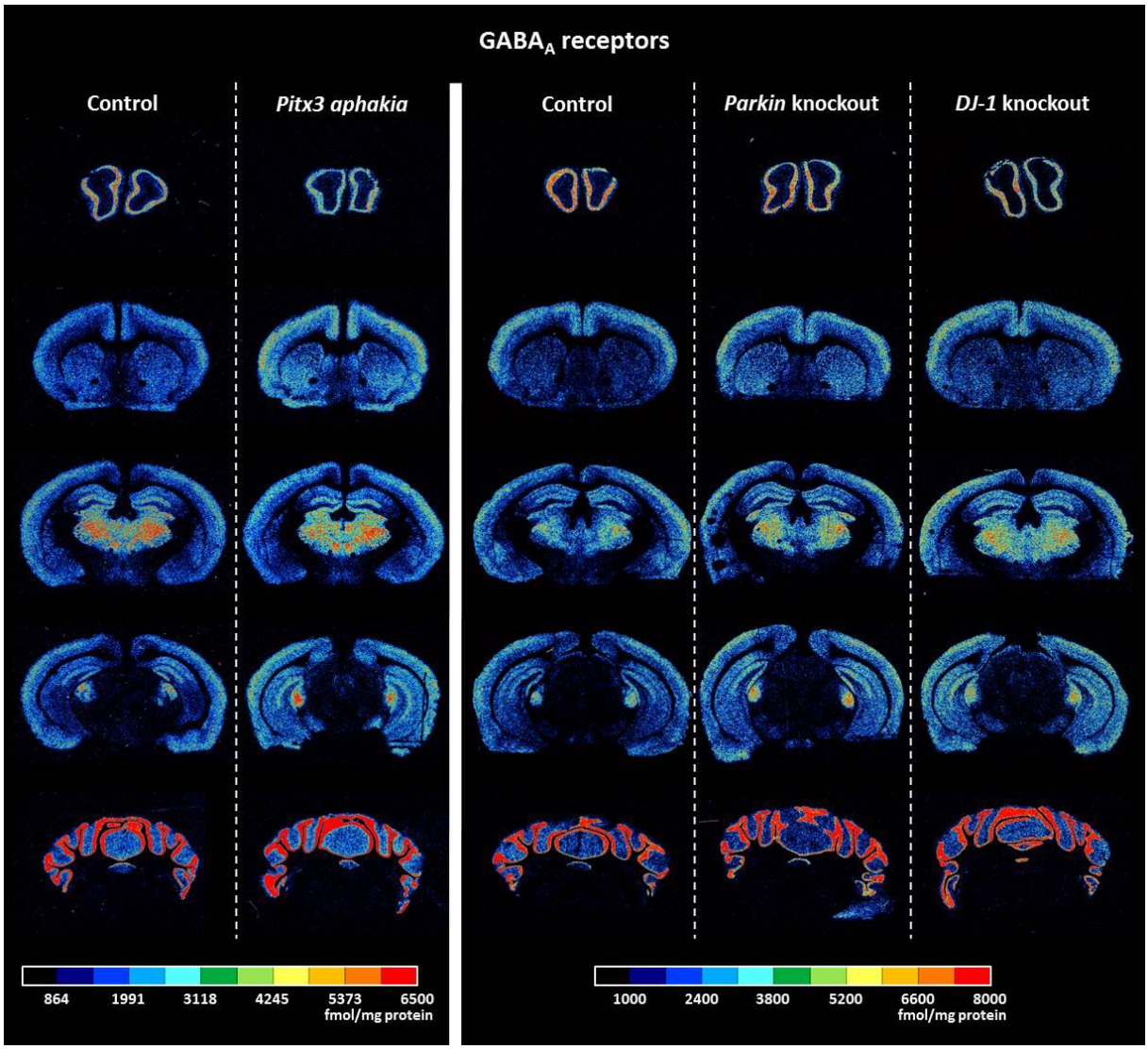

Fig.8 Color coded images of $GABA_A$ receptor densities (fmol/mg protein), revealed by agonist binding, in the brains of *Pitx3 aphakia, Parkin* and *DJ-1* knockout mice and corresponding control animals showing the distribution similarity between the different strains.

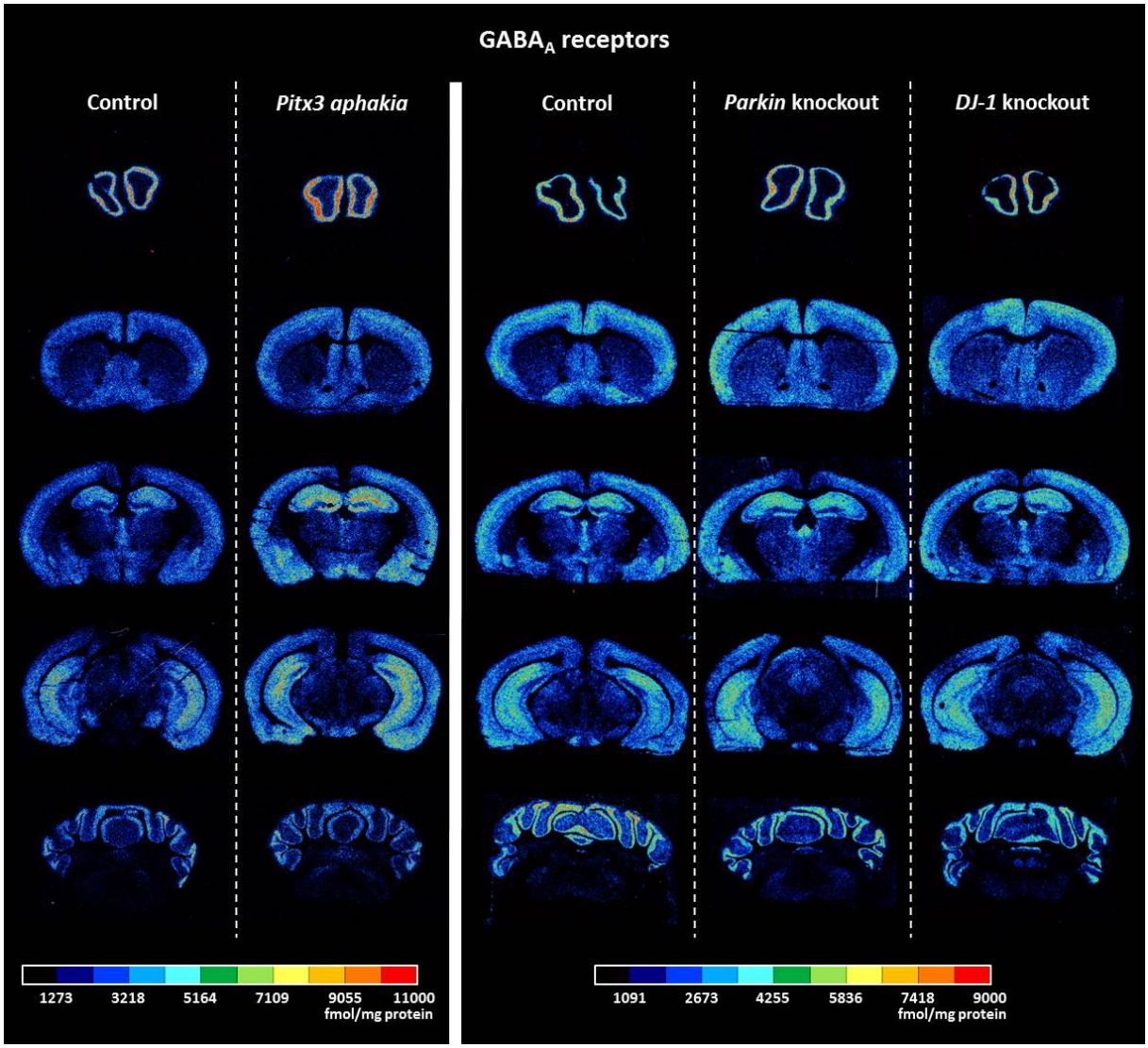

Fig.9 Color coded images of $GABA_A$ receptor densities (fmol/mg protein), revealed by antagonist binding, in the brains of *Pitx3 aphakia, Parkin* and *DJ-1* knockout mice and corresponding control animals showing the distribution similarity between the different strains.

The mean densities of $GABA_A$ associated benzodiazepine (**BZ**) binding sites were homogeneously distributed between ROIs with the exception of low densities in striatum and cerebellum and intermediate values in CA2/3. *Pitx3 aphakia* mice showed a maximum density in the substantia nigra (cf. fig. 10).

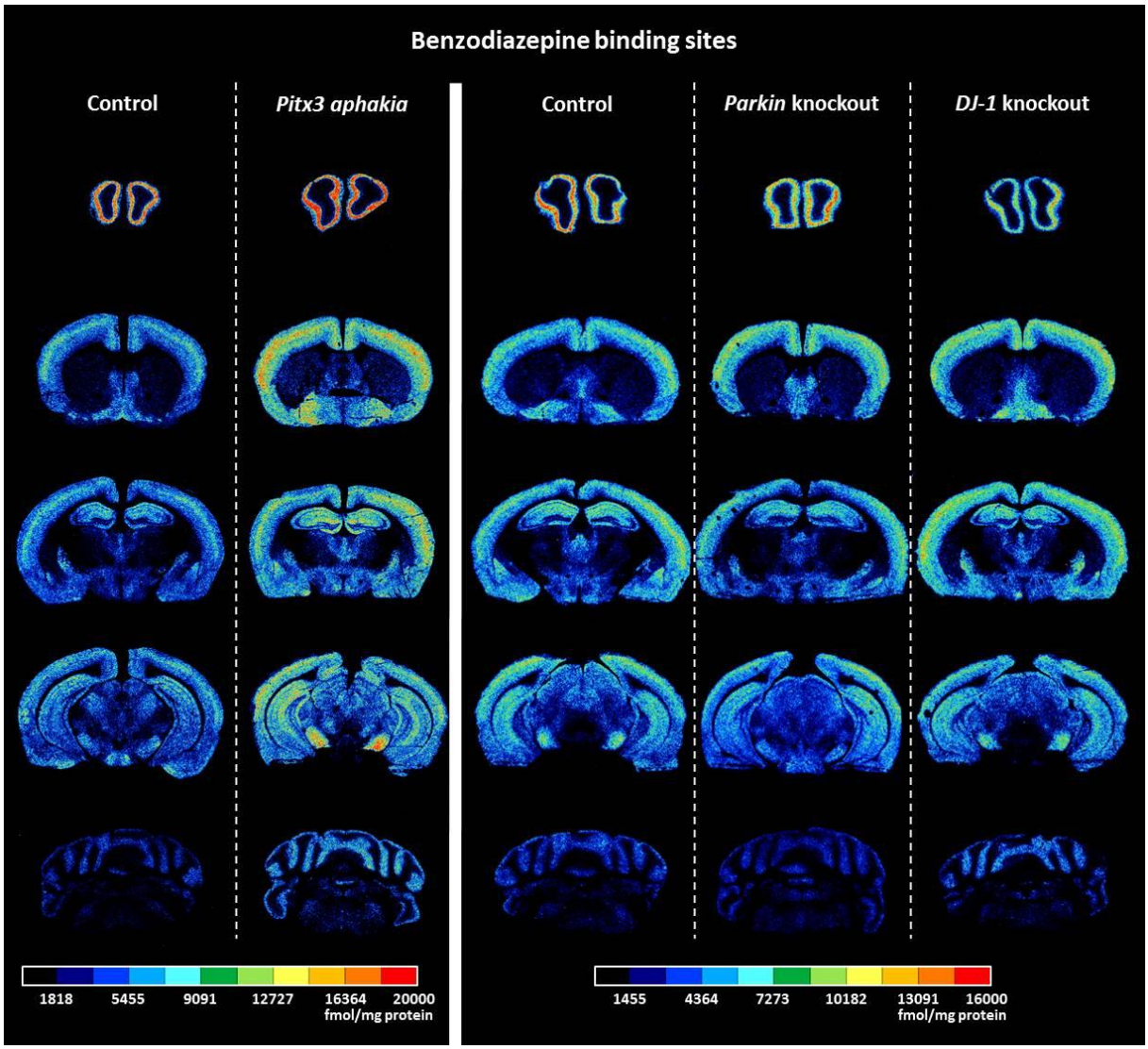

Fig.10 Color coded images of Benzodiazepine binding site densities (fmol/mg protein) in the brains of *Pitx3 aphakia, Parkin* and *DJ-1* knockout mice and corresponding control animals showing the distribution similarity between the different strains and the maximum density in the substantia nigra of *Pitx3 aphakia* mice.

In general, **$GABA_B$** receptor densities were high in motor, somatosensory, piriform and visual cortex, hippocampal regions (CA1, CA2/3 and dentate gyrus) and the cerebellum of all investigated groups. $GABA_B$ receptor densities in the olfactory bulb, striatum and substantia nigra were low (cf. fig. 11).

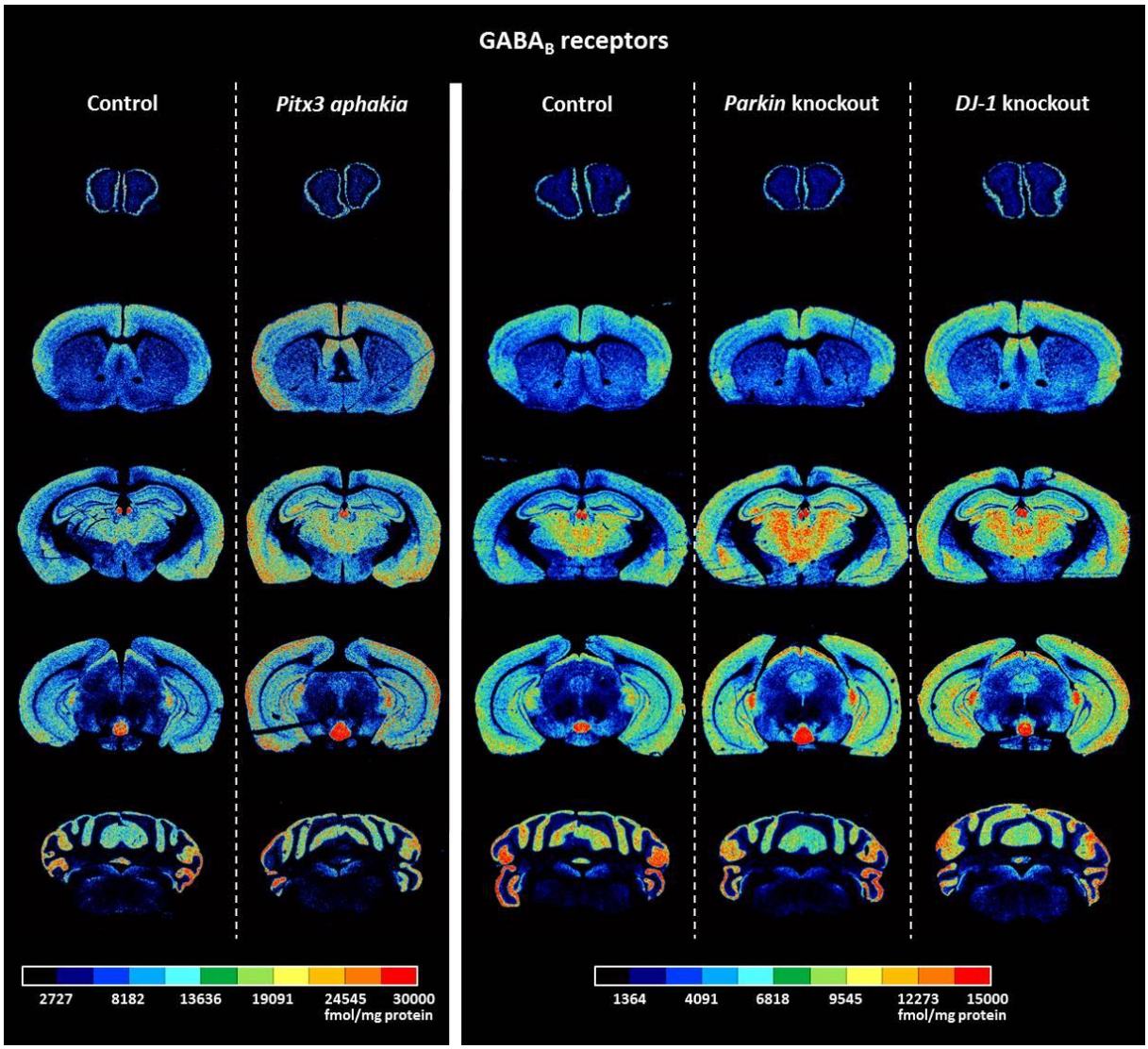

Fig.11 Color coded images of $GABA_B$ receptor densities (fmol/mg protein) in the brains of *Pitx3 aphakia, Parkin* and *DJ-1* knockout mice and corresponding control animals showing the distribution similarity between the different strains.

1.3. Acetylcholine receptors

In the cerebellum, all analyzed acetylcholine receptor subtypes with the exception of the muscarinic M_2 (and partly M_3) receptor exhibited very low densities below detection limit. Muscarinic **M_1** receptor densities showed high values in the striatum and the hippocampal regions CA1 and dentate gyrus, low values in the olfactory bulb and in particular in the substantia nigra, and intermediate densities in the other ROIs (cf. fig. 12).

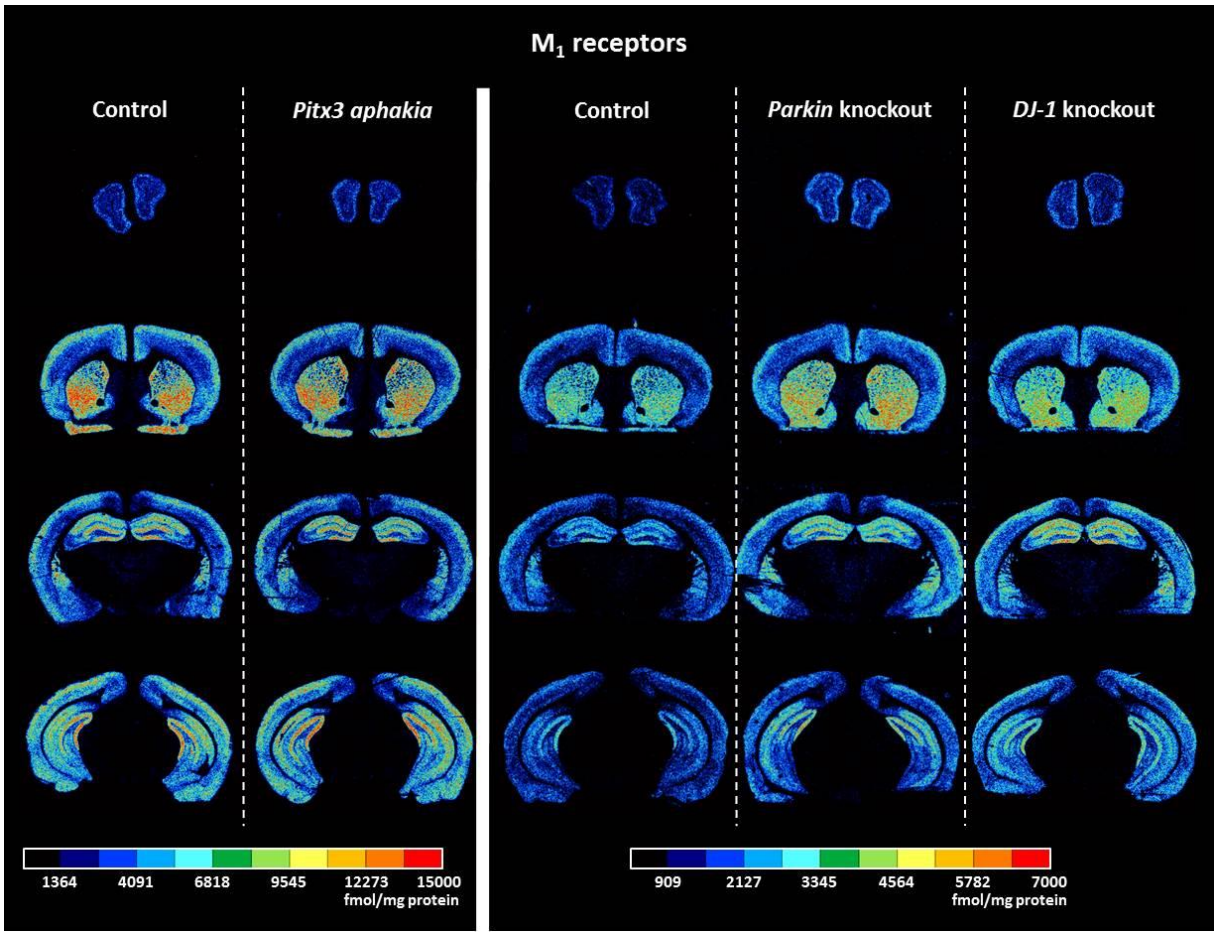

Fig.12 Color coded images of muscarinic M_1 receptor densities (fmol/mg protein) in the brains of *Pitx3 aphakia, Parkin* and *DJ-1* knockout mice and corresponding control animals showing the distribution similarity between the different strains.

M_2 receptor densities revealed by either *agonist* or *antagonist* binding were high in the olfactory bulb and the striatum, intermediate in the motor, somatosensory and visual cortex, and low in all other investigated brain regions. In the striatum, the *antagonist* binding exhibited by far higher densities in the striatum than the *agonist* (cf. fig. 13 and fig. 14).

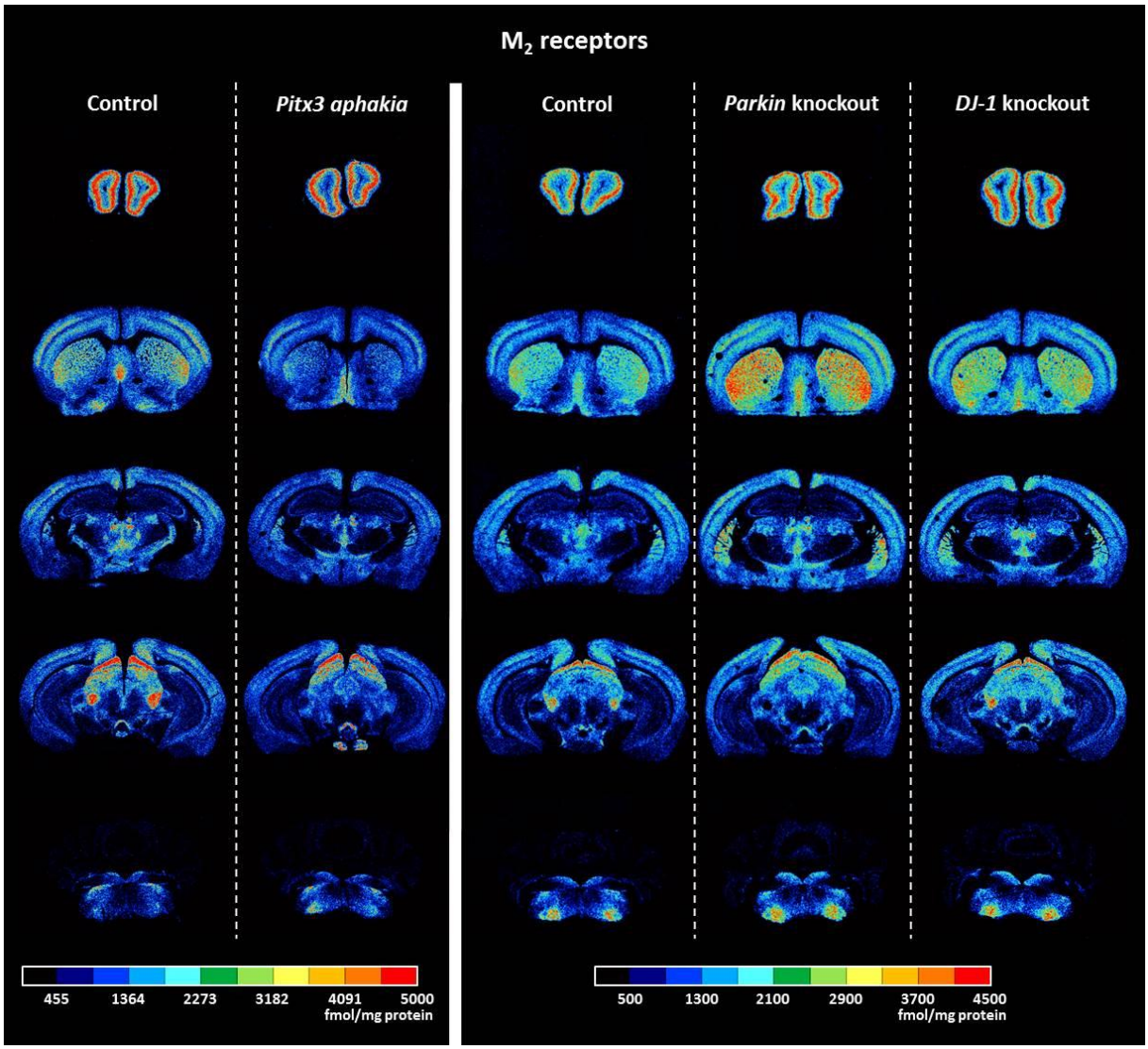

Fig.13 Color coded images of M_2 receptor densities (fmol/mg protein), revealed by agonist binding, in the brains of *Pitx3 aphakia, Parkin* and *DJ-1* knockout mice and corresponding control animals showing the distribution similarity between the different strains.

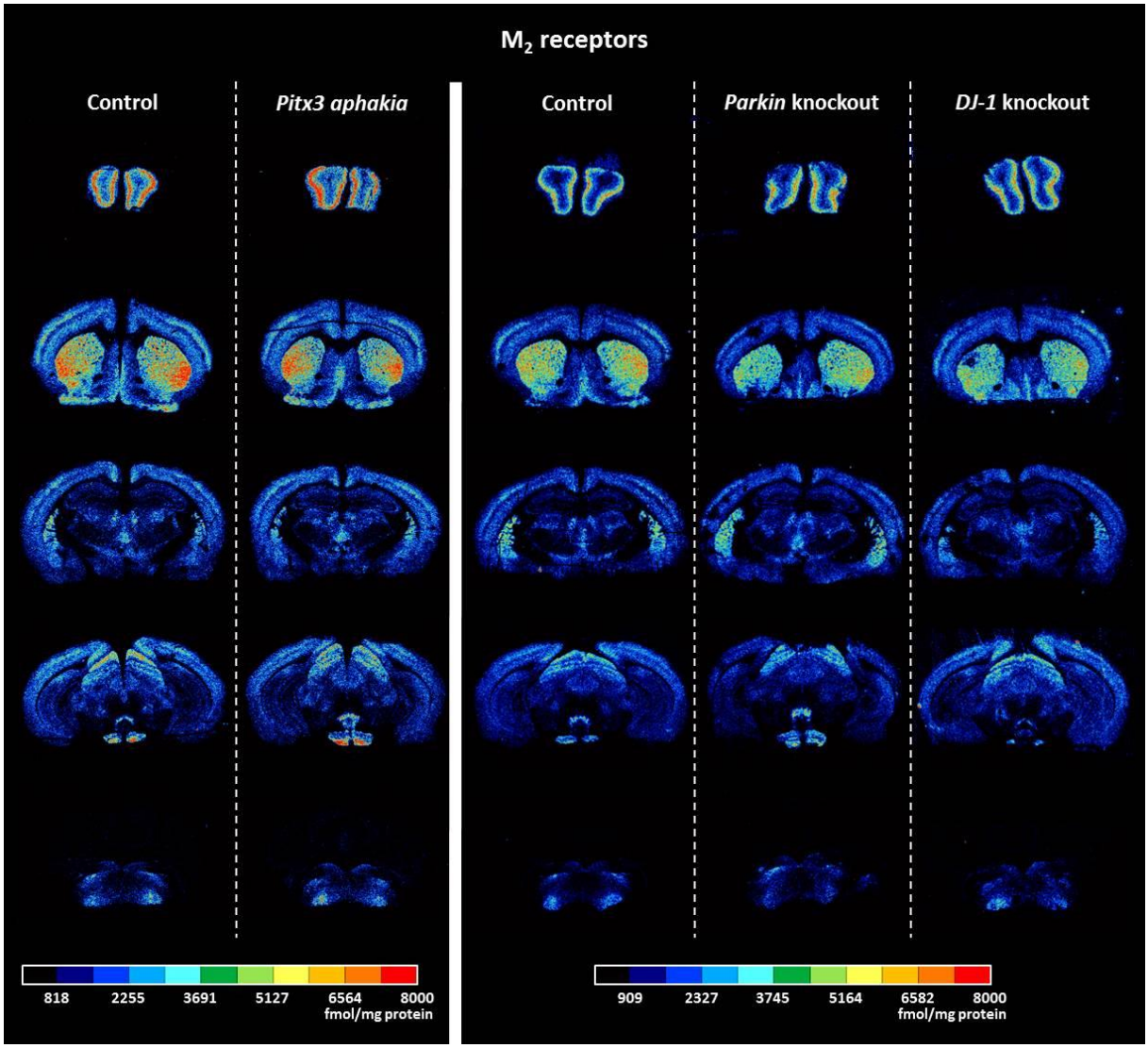

Fig.14 Color coded images of M_2 receptor densities (fmol/mg protein), revealed by antagonist binding, in the brains of *Pitx3 aphakia, Parkin* and *DJ-1* knockout mice and corresponding control animals showing the distribution similarity between the different strains.

The spatial distribution of **M_3** receptors was comparable to that described for M_1 receptors, with high densities in the striatum and CA1 region of the hippocampus, low densities in the olfactory bulb and in particular in the substantia nigra and cerebellum, while intermediate densities were measured in all other ROIs (cf. fig. 15).

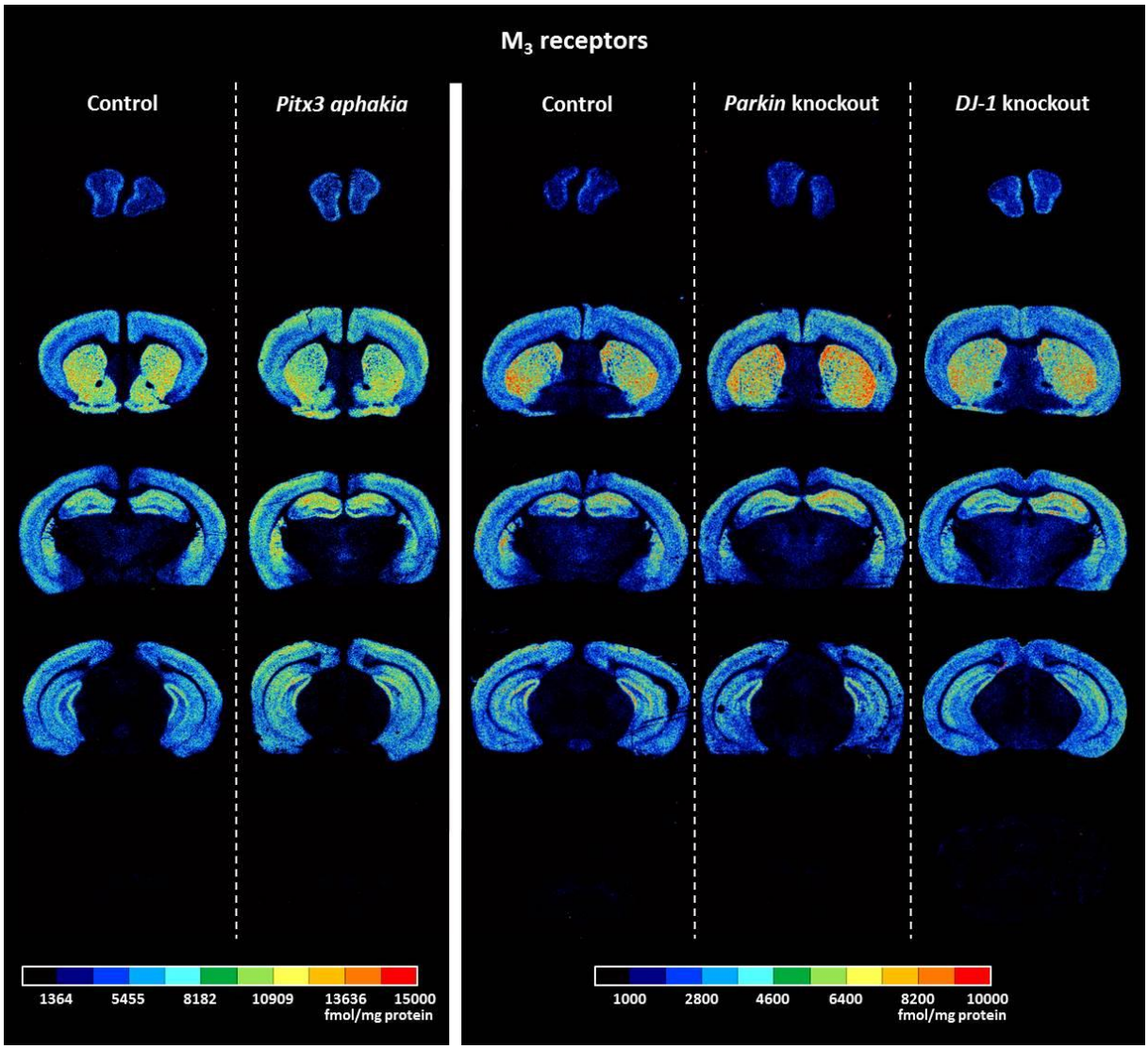

Fig.15 Color coded images of M_3 receptor densities (fmol/mg protein) in the brains of *Pitx3 aphakia, Parkin* and *DJ-1* knockout mice and corresponding control animals showing the distribution similarity between the different strains. (In case of DJ-1 knockout: background removed)

The **nicotinic** acetylcholine receptor densities were similar in all brain regions investigated here, with slightly higher densities in the motor, somatosensory and visual cortex. All groups exhibited a maximum density in the striatum, except for *Pitx3 aphakia* mice (cf. fig. 16).

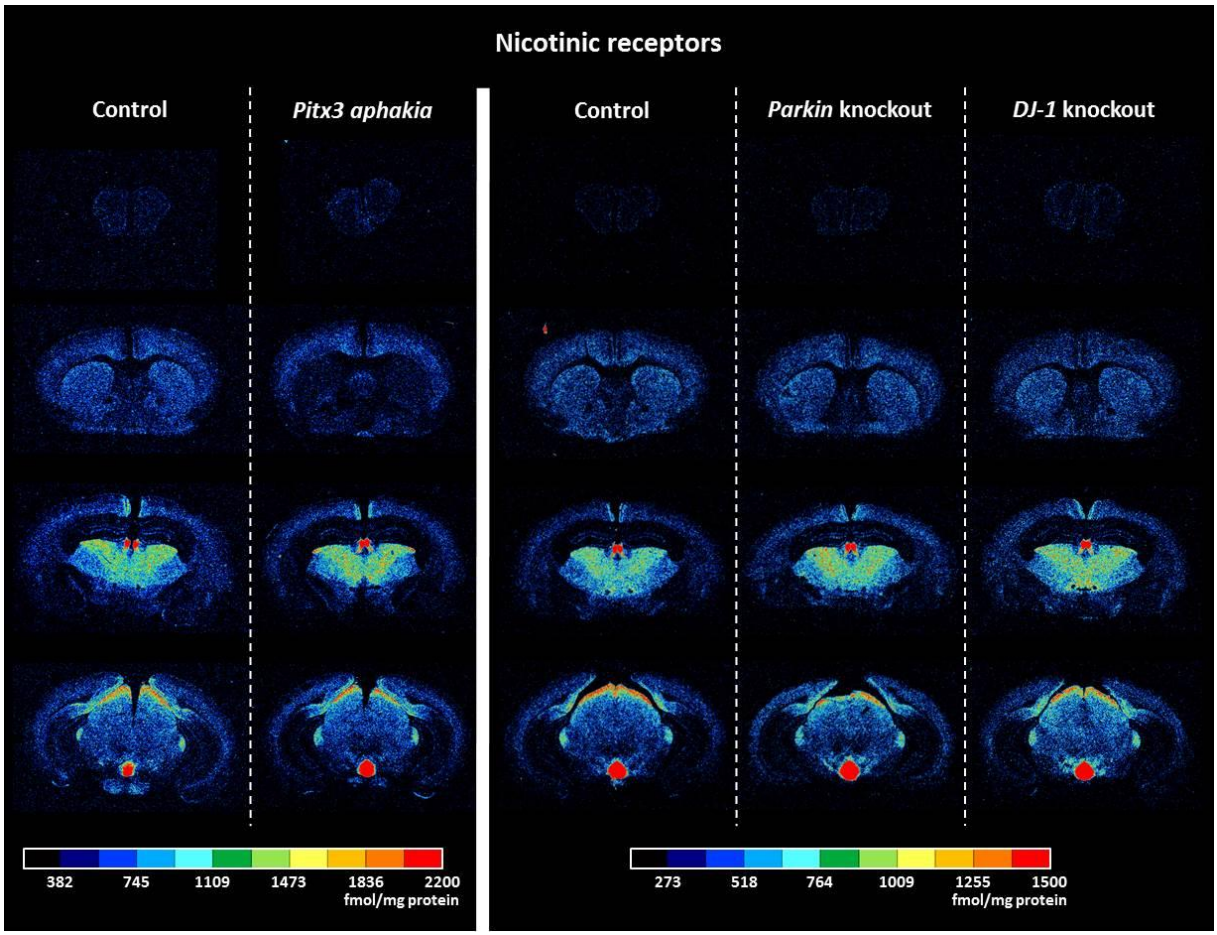

Fig.16 Color coded images of nicotinic acetylcholine receptor densities (fmol/mg protein) in the brains of *Pitx3 aphakia, Parkin* and *DJ-1* knockout mice and corresponding control animals showing the distribution similarity between the different strains and the maximum density in the striatum of all groups, except for *Pitx3 aphakia* mice.

1.4. Noradrenaline receptors

The olfactory bulb as well as motor, somatosensory, piriform and visual cortex exhibited comparatively high α_1 adrenergic receptor densities, whereas the densities in striatum, hippocampus (CA1, CA2/3 and dentate gyrus), substantia nigra and cerebellum were low (cf. fig. 17).

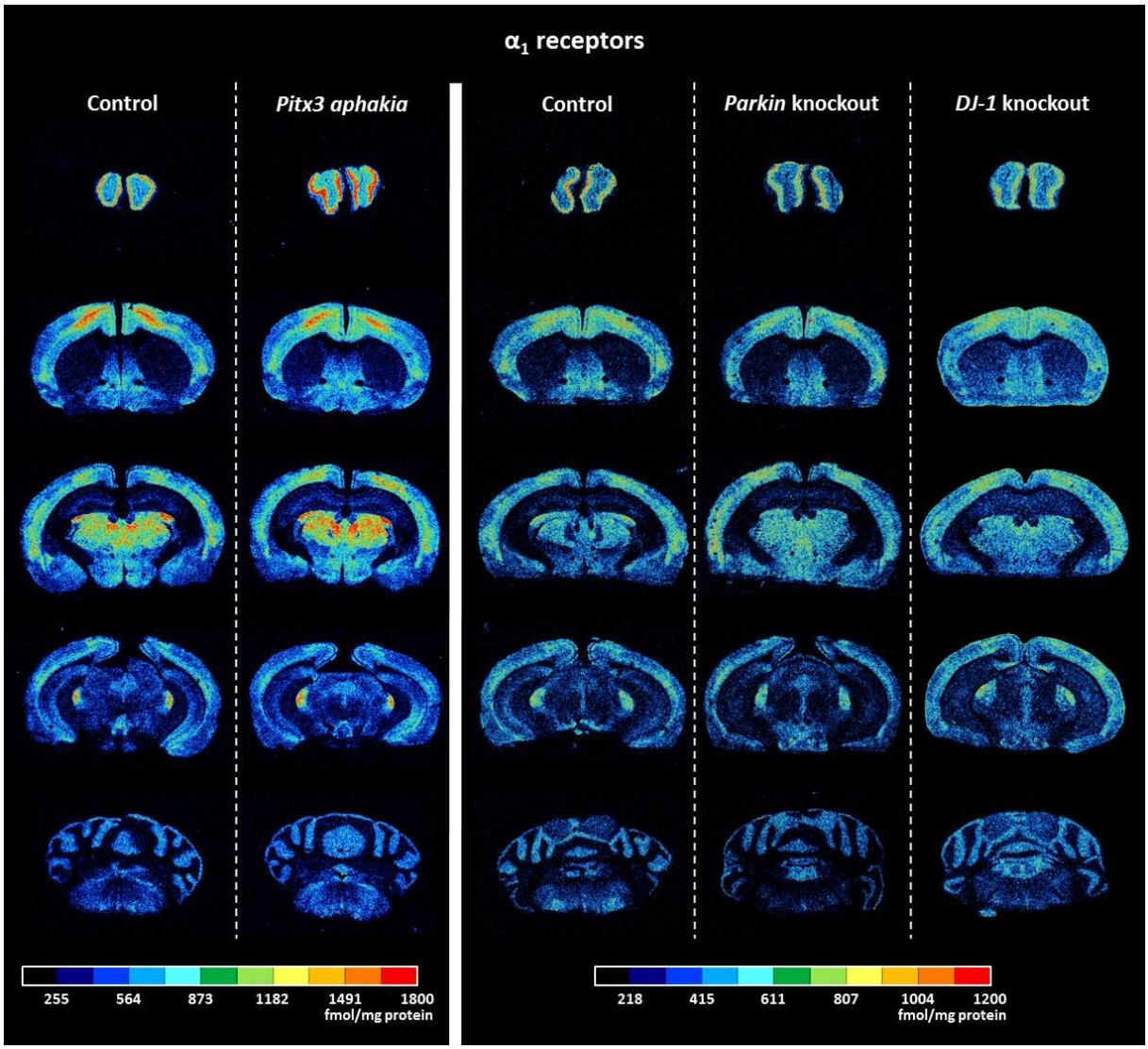

Fig.17 Color coded images of α_1 adrenergic receptor densities (fmol/mg protein) in the brains of *Pitx3 aphakia, Parkin* and *DJ-1* knockout mice and corresponding control animals showing the distribution similarity between the different strains. (In case of DJ-1 knockout: background removed)

In general, adrenergic α_2 receptor densities were low in the brains of all investigated groups and homogeneously distributed between ROIs, with the exception of high densities in the piriform cortex (cf. fig. 18).

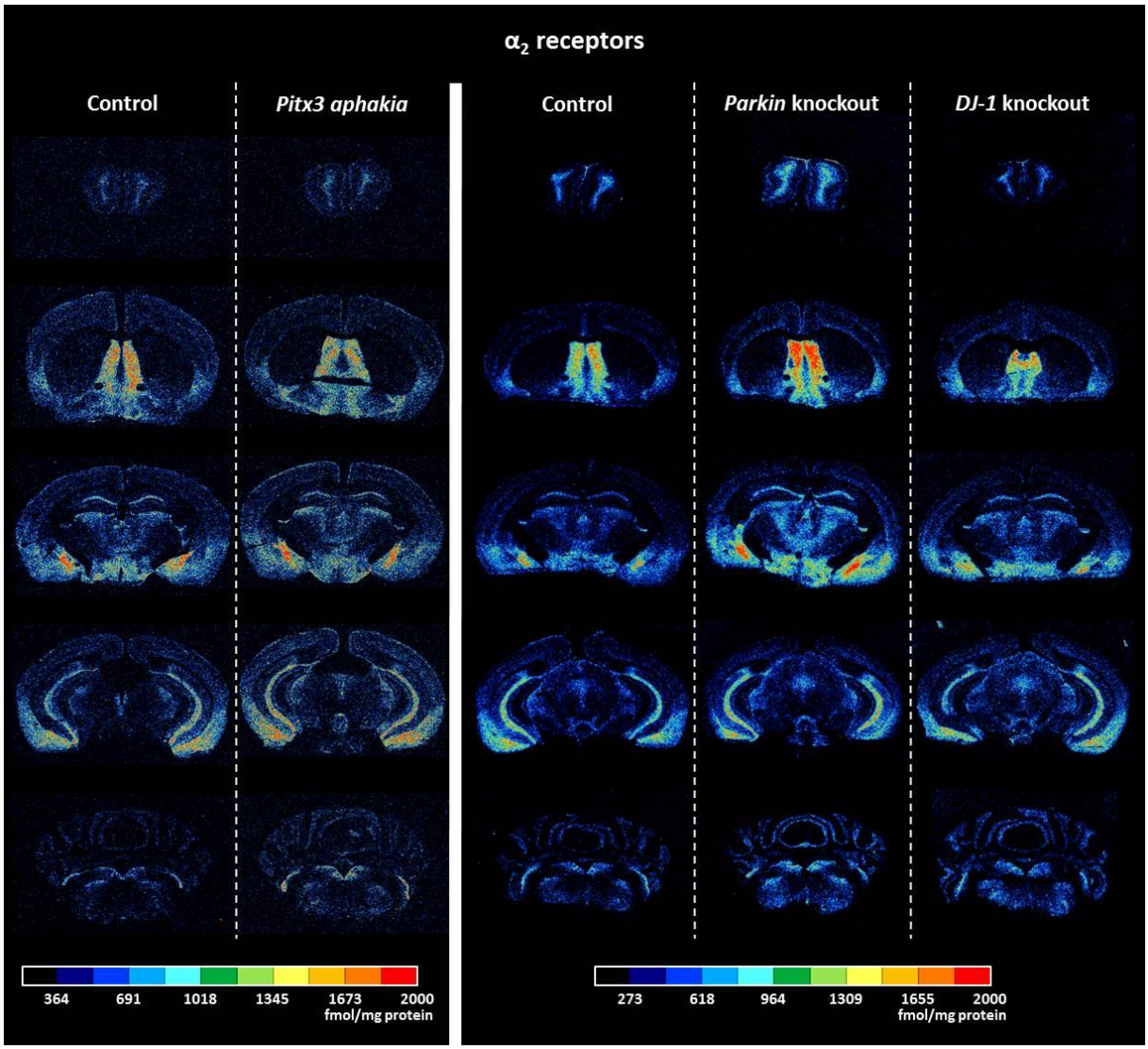

Fig.18 Color coded images of adrenergic α_2 receptor densities (fmol/mg protein) in the brains of *Pitx3 aphakia, Parkin* and *DJ-1* knockout mice and corresponding control animals showing the distribution similarity between the different strains.

1.5. Serotonin receptors

5-HT$_{1A}$ receptor densities were low in all brain regions studied, except for the CA1 region of the hippocampus, where densities were approximately three times higher than in the other ROIs (cf. fig. 19).

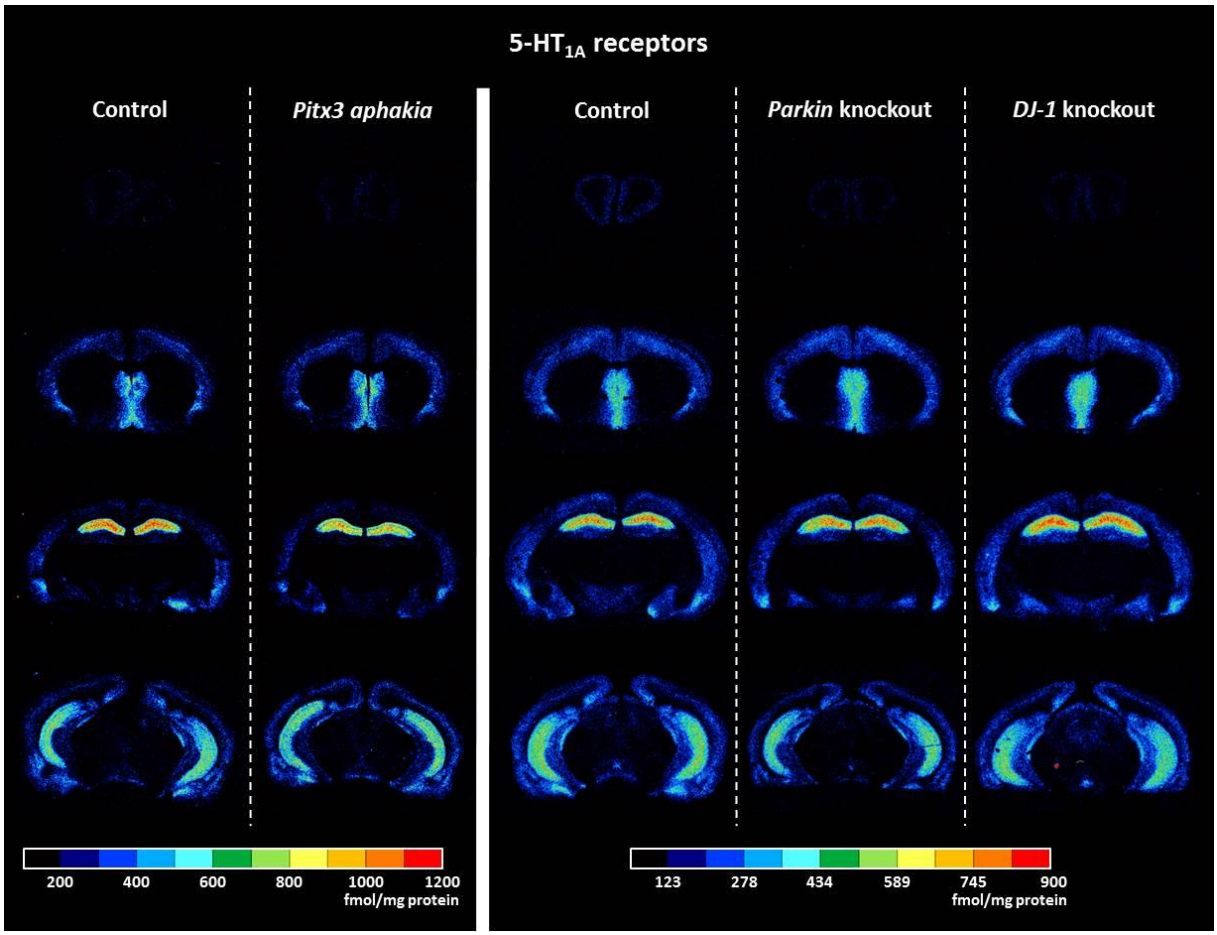

Fig.19 Color coded images of 5-HT$_{1A}$ receptor densities (fmol/mg protein) in the brains of *Pitx3 aphakia, Parkin* and *DJ-1* knockout mice and corresponding control animals showing the distribution similarity between the different strains.

5-HT$_2$ receptor densities were slightly higher in some cortical regions (i.e. motor, somatosensory, piriform and visual cortex) than in the olfactory bulb, hippocampal regions (CA1, CA2/3 and dentate gyrus), substantia nigra and cerebellum. Control animals exhibited a maximum density in the striatum, but *Pitx3 aphakia* mice did not (cf. fig. 20).

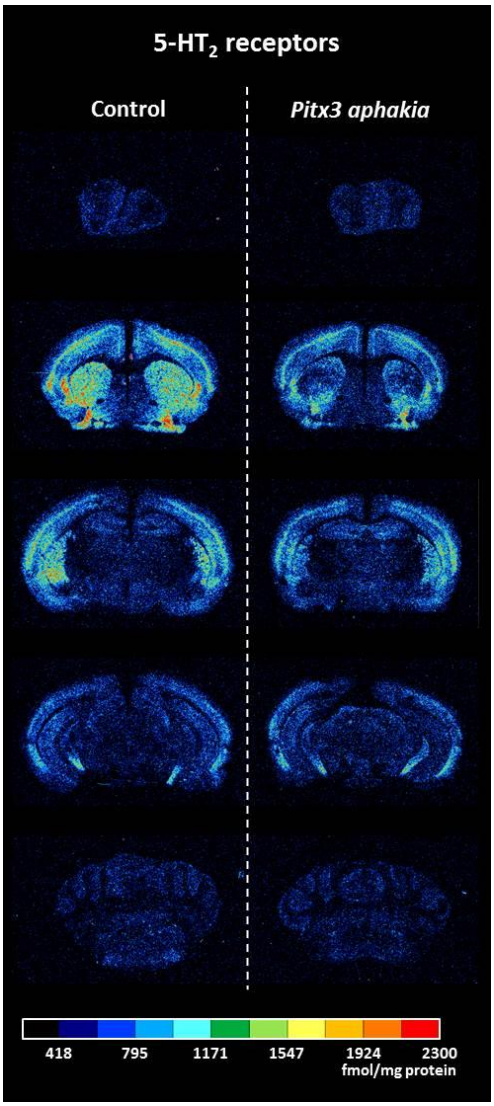

Fig.20 Color coded images of 5-HT$_2$ receptor densities (fmol/mg protein) in the brains of *Pitx3 aphakia* mice and corresponding control animals showing the distribution similarity between the different strains and the maximum density in the striatum of control mice.

1.6. Dopamine receptors

Dopamine receptor densities were below detection limit in most of the analyzed brain regions except for the striatum (**D_1, D_2** and **$D_{2/3}$** receptors) and substantia nigra (**D_1** receptors), respectively (cf. fig. 21 – 23). D_1 receptor densities in the striatum were approximately four times higher than in the substantia nigra (cf. fig. 21).

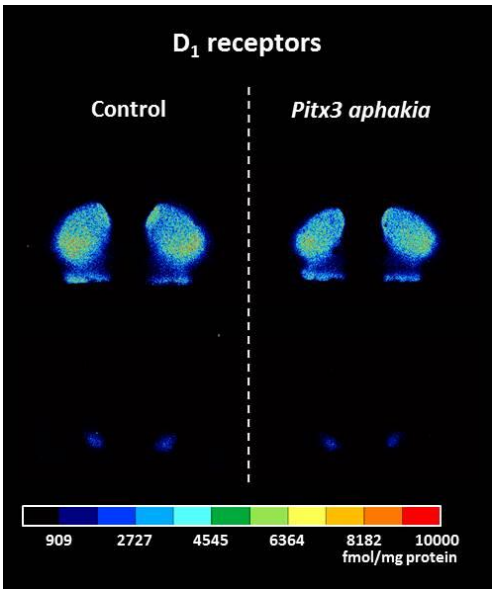

Fig.21 Color coded images of D_1 receptor densities (fmol/mg protein) in the brains of *Pitx3 aphakia* mice and corresponding control animals showing the distribution similarity between the different strains.

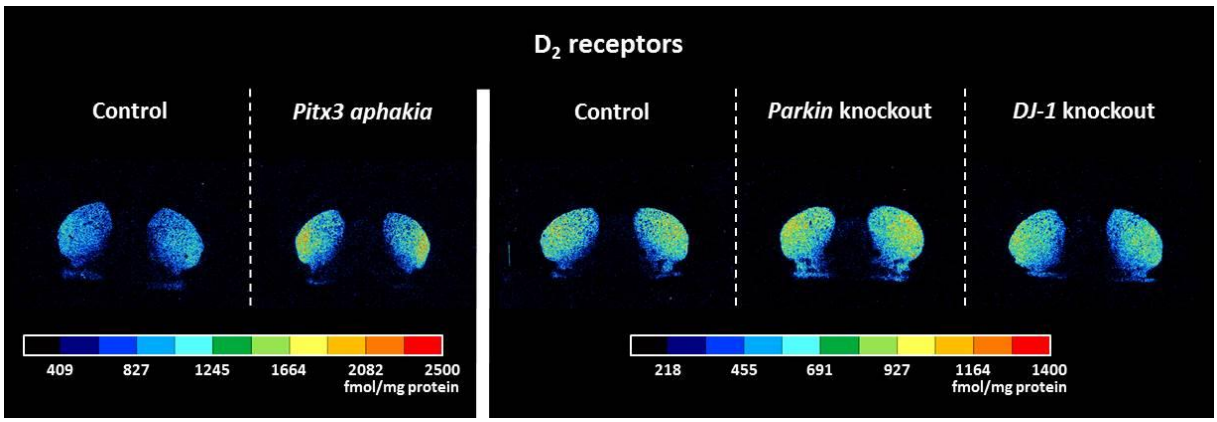

Fig.22 Color coded images of D_2 receptor densities (fmol/mg protein) in the brains of *Pitx3 aphakia, Parkin* and *DJ-1* knockout mice and corresponding control animals showing the distribution similarity between the different strains.

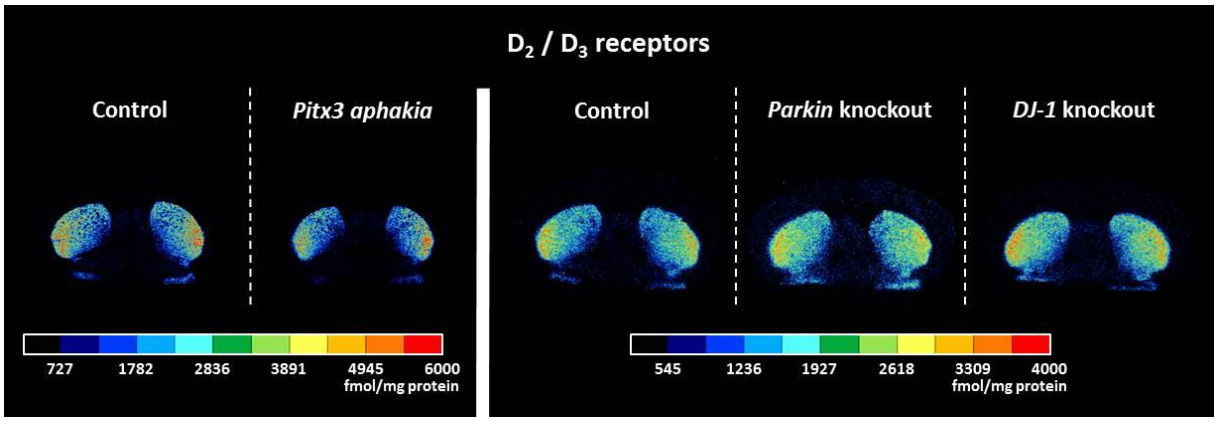

Fig.23 Color coded images of D_2 / D_3 receptor densities (fmol/mg protein) in the brains of *Pitx3 aphakia, Parkin* and *DJ-1* knockout mice and corresponding control animals showing the distribution similarity between the different strains.

1.7. Adenosine receptors

Comparable to the situation described for dopaminergic receptors, adenosine **A_{2A}** receptors were detectable in the striatum only (cf. fig. 24).

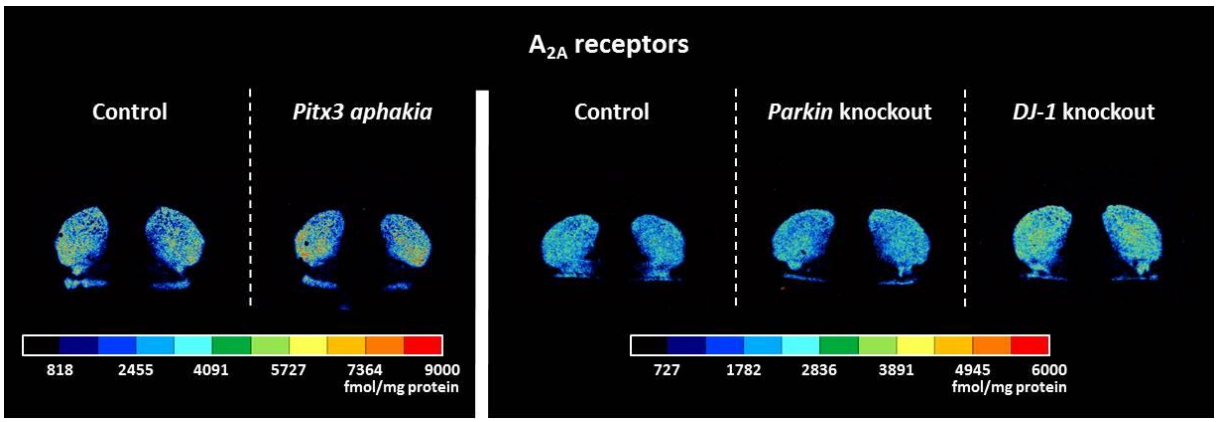

Fig.24 Color coded images of AMPA receptor densities (fmol/mg protein) in the brains of *Pitx3 aphakia, Parkin* and *DJ-1* knockout mice and corresponding control animals showing the distribution similarity between the different strains.

2. Neurotransmitter receptor densities in *Pitx3 aphakia* mouse brains

2.1. Glutamate receptors

No significant differences could be shown between the **AMPA** receptor densities of *Pitx3 aphakia* and control mice in the investigated brain regions (cf. fig. 25).

Statistical tests revealed significant alterations of **kainate** receptor densities between control and *Pitx3 aphakia* mice in the olfactory bulb ($p<0.05$), where the density was decreased by 12 % in *aphakia* mice, while the densities in the striatum ($p<0.05$) and the visual cortex ($p<0.01$) were increased by 11 and 21 %, respectively in the *Pitx3 aphakia* mice (cf. fig. 25).

The **NMDA** receptor densities were below the detection limit in the cerebellum. No significant differences could be designated in any area between control and *Pitx3 aphakia* animals (cf. fig. 25).

No significant differences were found between the densities of metabotropic glutamate receptors (**$mGlu_{2/3}$**) in *Pitx3 aphakia* and control mice brains (cf. fig. 25).

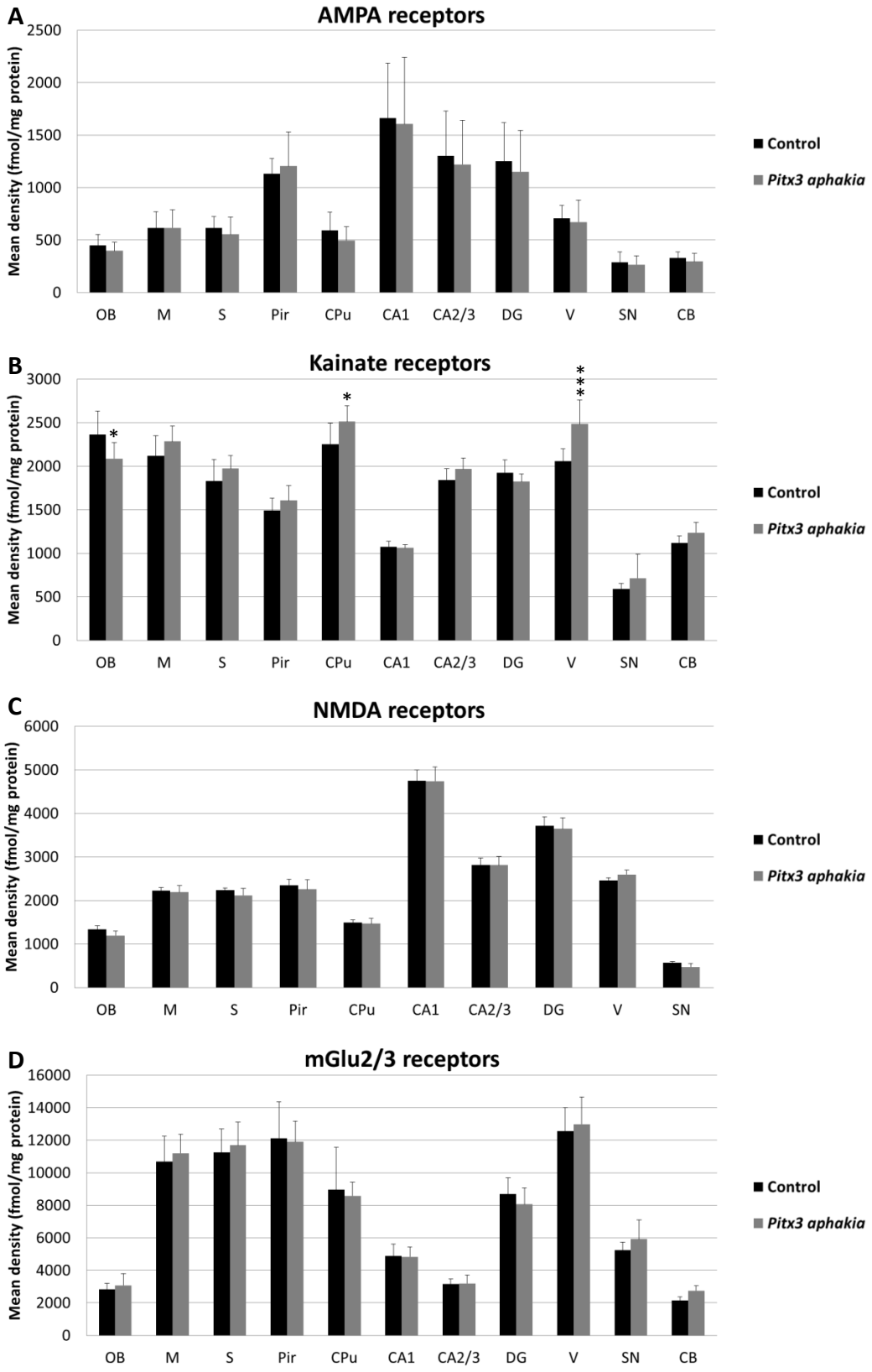

Fig.25 Bar charts of mean glutamatergic receptor densities including standard deviation in different brain regions of control (black) and *Pitx3 aphakia* mice (gray). Mean density is indicated as fmol/mg protein. Significant differences are indicated by *p<0.05 or ***p<0.01, respectively. The following [^{3}H]-ligands were used: AMPA (A); Kainate (B); MK 801 (C); LY341,495 (D). For contrast color coded images that visualize the regional distribution of the analyzed neurotransmitter receptors within the brain, see chapter 1. For a schematic overview of brain regions / abbreviations, see fig.3.

2.2. GABA receptors

$GABA_A$ receptor densities investigated by using the receptor *agonist* [^{3}H]-muscimol were significantly higher in the motor (31 %; $p<0.01$), the somatosensory (28 %; $p<0.01$) and the piriform cortex (23 %; $p<0.05$), as well as in the cerebellum (44 %; $p<0.01$) of *Pitx3 aphakia* mice compared to control animals (cf. fig. 26).
Mean **$GABA_A$** receptor densities investigated by using the receptor *antagonist* [^{3}H]-SR 95531 were significantly increased in *Pitx3 aphakia* brains in the three hippocampal regions, CA1 (21 %; $p<0.01$), CA2/3 (60 %; $p<0.01$) and dentate gyrus (69 %; $p<0.01$), as well as in the visual cortex (32 %; $p<0.01$) (cf. fig. 26).

The mean densities of $GABA_A$ associated benzodiazepine (**BZ**) binding sites were increased in all investigated brain regions of *Pitx3 aphakia* compared to control mice. These changes were statistically significant for all regions, except for the olfactory bulb and CA1, and reached from 19 to 56 % (motor / somatosensory cortex and striatum: $p<0.05$; piriform / visual cortex, CA2/3, dentate gyrus, substantia nigra and cerebellum: $p<0.01$) (cf. fig. 26).

$GABA_B$ receptor density changes between control and *Pitx3 aphakia* mice were found in the motor (21 %; $p<0.01$), piriform (21 %; $p<0.05$) and visual cortex (29 %; $p<0.01$), the dentate gyrus (12 %; $p<0.05$) and the substantia nigra (26 %; $p<0.01$). In each of these cases receptor densities were higher in the brains of *Pitx3 aphakia* mice than in corresponding control animals (cf. fig. 26).

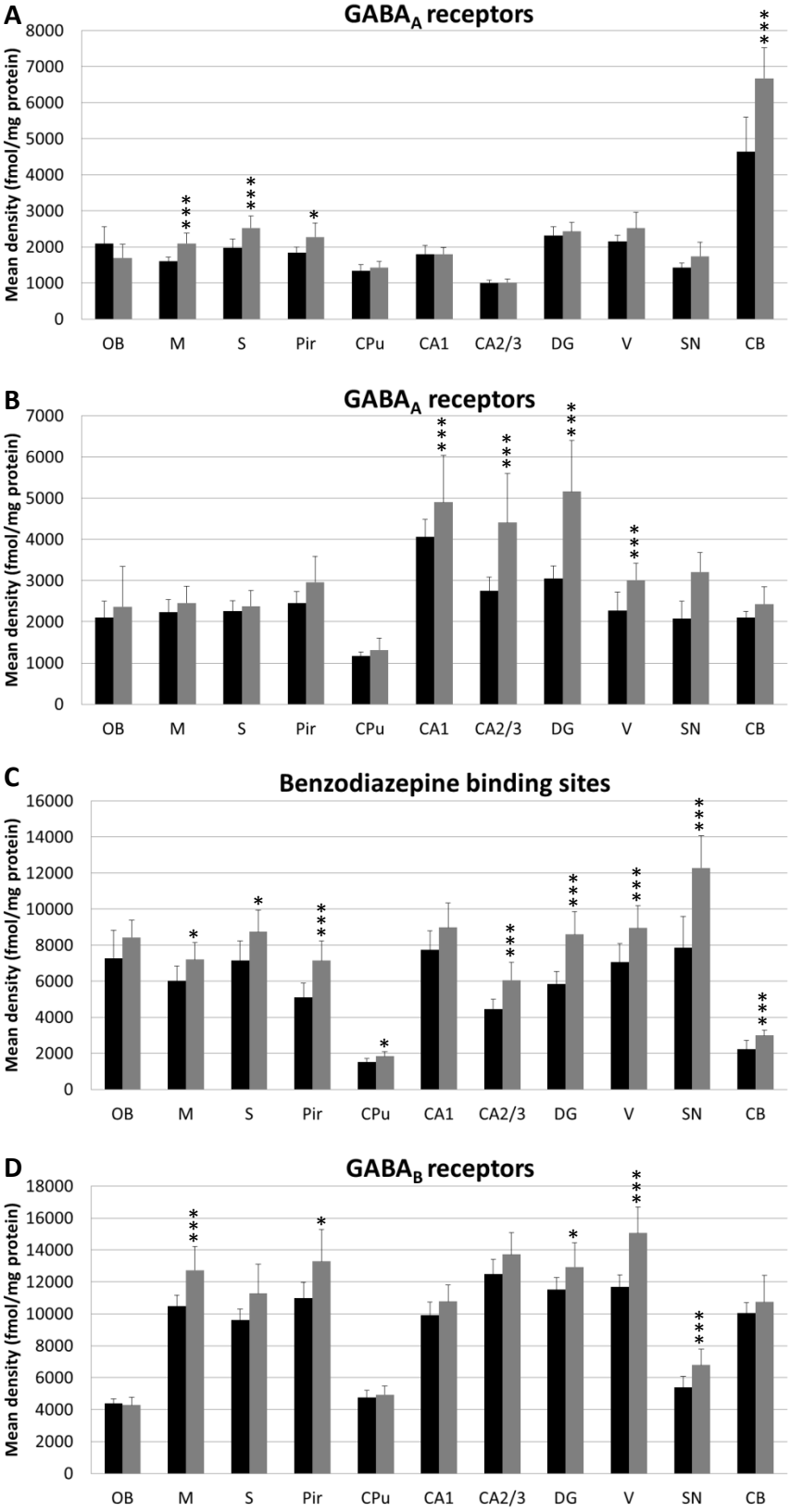

Fig.26 Bar charts of mean GABAergic receptor densities including standard deviation in different brain regions of control (black) and *Pitx3 aphakia* mice (gray). Mean density is indicated as fmol/mg protein. Significant differences are indicated by *p<0.05 or ***p<0.01, respectively. [^{3}H]-ligands: Muscimol (agonist) (A); SR 95531 (antagonist) (B); Flumazenil (C); CGP 54626 (D). For contrast color coded images that visualize the regional distribution of the analyzed neurotransmitter receptors within the brain, see chapter 1. For a schematic overview of brain regions / abbreviations, see fig.3.

2.3. Acetylcholine receptors

No significant differences of **M_1** receptor densities were observed between control and *Pitx3 aphakia* mice (cf. fig. 27).

The densities of **M_2** receptors revealed by the *agonist* [^{3}H]-oxotremorine-M were significantly decreased in the somatosensory cortex (-12 %; $p<0.01$) as well as in the striatum (-19 %; $p<0.01$) of *Pitx3 aphakia* mice, when compared to controls.
Binding of [^{3}H]-AF-DX 384, an *antagonist* of the **M_2** muscarinic acetylcholine receptor, did not demonstrate significant differences between *Pitx3 aphakia* and control mice (cf. fig. 27).

Mean **M_3** receptor densities were significantly increased in all cortical regions of *Pitx3 aphakia* mice, i.e. motor (21 %; $p<0.01$), somatosensory (13 %; $p<0.01$), piriform (14 %; $p<0.01$) and visual cortex (17 %; $p<0.01$), as well as in the CA1 (9 %; $p<0.05$) region of the hippocampus (cf. fig. 27).

Nicotinic acetylcholine receptor densities were significantly decreased in the striatum (-47 %; $p<0.01$), the CA2/3 region of the hippocampus (-15 %; $p<0.05$) and the dentate gyrus (-16 %; $p<0.01$) of *Pitx3 aphakia* mice compared to controls. The decrease of receptor density in the striatum reaches nearly 50%. (cf. fig. 27)

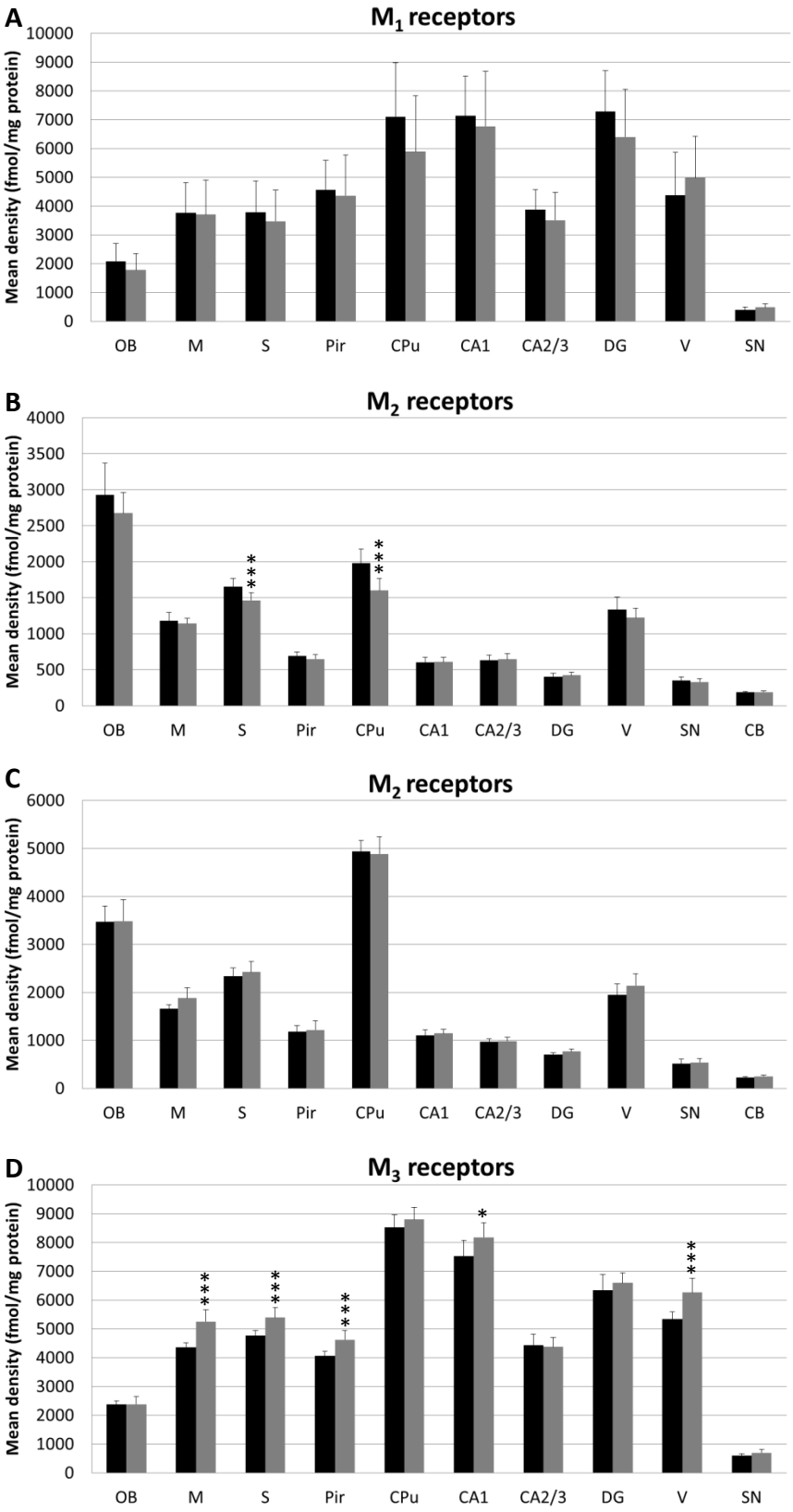

Fig.27 Bar charts of mean acetylcholinergic receptor densities including standard deviation in different brain regions of control (black) and *Pitx3 aphakia* mice (gray). Mean density is indicated as fmol/mg protein. Significant differences are indicated by *p<0.05 or ***p<0.01, respectively. [^{3}H]-ligands: Pirenzepine (A); Oxotremorine-M (agonist) (B); AF-DX 384 (antagonist) (C); 4-DAMP (D); Epibatidine (E). For contrast color coded images that visualize the regional distribution of the analyzed neurotransmitter receptors, see chapter 1. For a schematic overview of brain regions / abbreviations, see fig.3.

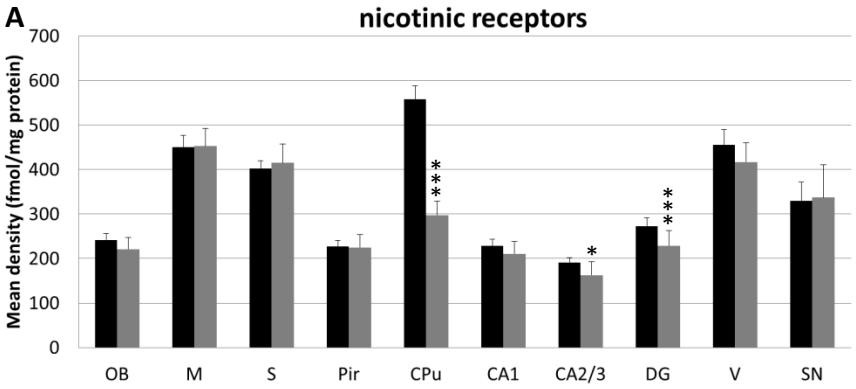

Fig.27 Continuation.
For explanation, see previous page.

2.4. Noradrenaline receptors

Statistical tests revealed significantly higher α_1 adrenergic receptor densities in the olfactory bulb (14 %; p<0.01), piriform cortex (15 %; p<0.01), striatum (7 %; p<0.05), the hippocampal regions CA1 (8 %; p<0.05), CA2/3 (13 %; p<0.01), and DG (11 %; p<0.01), and substantia nigra (19 %; p<0.01) of the *Pitx3 aphakia* group compared to controls (cf. fig. 28).

There was no significant difference of adrenergic α_2 receptor densities between control mice and *Pitx3 aphakia* mice in the investigated brain regions (cf. fig. 28).

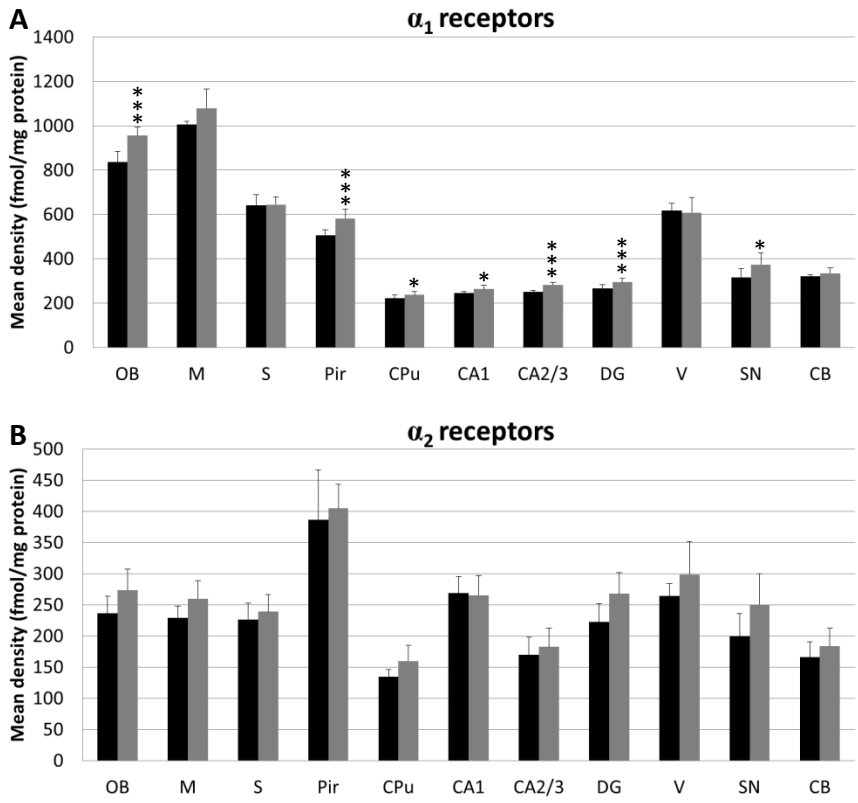

Fig.28 Bar charts of mean adrenergic receptor densities including standard deviation in different brain regions of control (black) and *Pitx3 aphakia* mice (gray). Mean density is indicated as fmol/mg protein. Significant differences are indicated by *p<0.05 or ***p<0.01, respectively. The following [^{3}H]-ligands were used: Prazosin (A); UK14,304 (B). For contrast color coded images that visualize the regional distribution of the analyzed neurotransmitter receptors within the brain, see chapter 1. For a schematic overview of brain regions / abbreviations, see fig.3.

2.5. Serotonin receptors

The *Pitx3 aphakia* mice showed a significant decrease of **5-HT$_{1A}$** receptor densities in the olfactory bulb (-13 %; p<0.05), the CA1 (-7 %; p<0.05) region of the hippocampus and the dentate gyrus (-12 %; p<0.05) compared to controls (cf. fig. 29 and fig. 30).

5-HT$_2$ receptor densities in the striatum of *Pitx3 aphakia* mice were approximately half of mean densities from control animals (-48 %; p<0.01) (cf. fig. 29 and fig. 30).

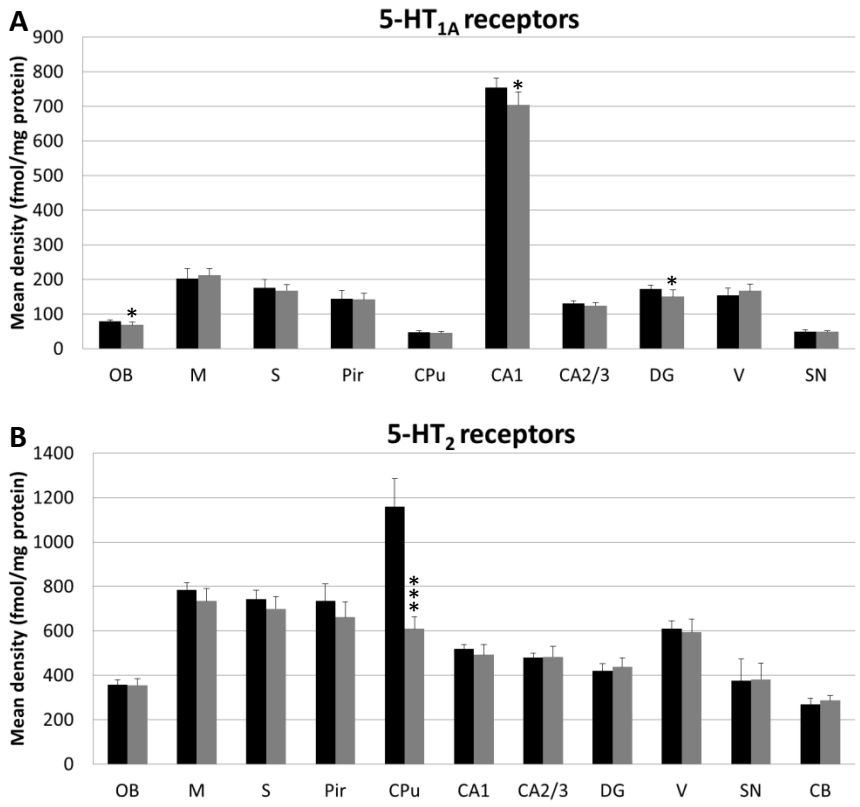

Fig.29 Bar charts of mean serotonergic receptor densities including standard deviation in different brain regions of control (black) and *Pitx3 aphakia* mice (gray). Mean density is indicated as fmol/mg protein. Significant differences are indicated by *p<0.05 or ***p<0.01, respectively. The following [^{3}H]-ligands were used: 8-OH-DPAT (A); Ketanserin (B). For contrast color coded images that visualize the regional distribution of the analyzed neurotransmitter receptors within the brain, see chapter 1. For a schematic overview of brain regions / abbreviations, see fig.3.

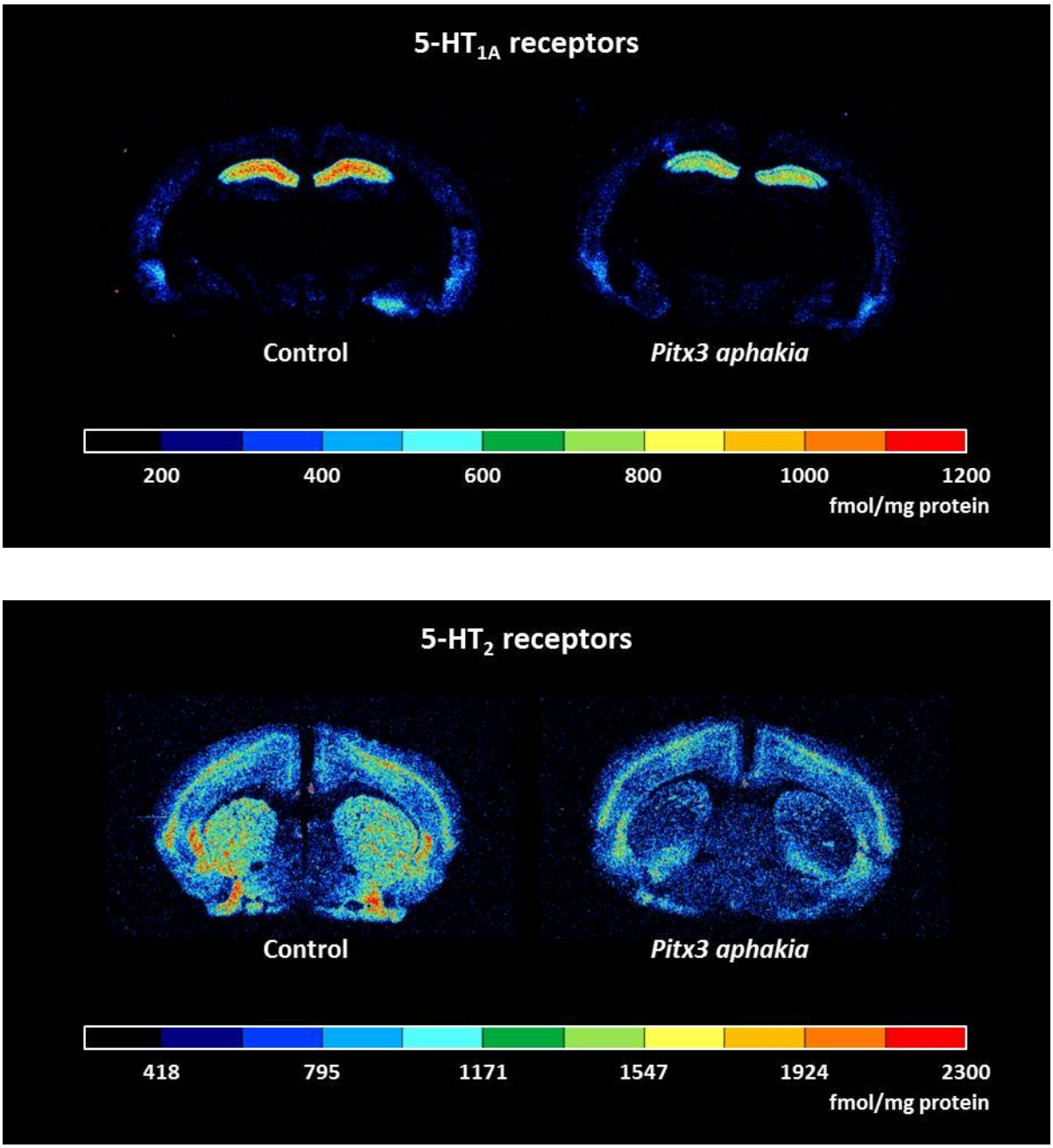

Fig. 30 Serotonergic 5-HT_{1A} receptor densities in the hippocampus and 5-HT_2 receptor densities in the striatum of *Pitx3 aphakia* (right) and control mice (left) presented as contrast color coded images (the color scale for 5-HT_{1A} receptors reached between 100 and 1200 fmol/mg protein; the color scale for 5-HT_2 receptors reached between 230 and 2300 fmol/mg protein).

2.6. Dopamine receptors

Although **D_1** receptor densities showed a tendency to higher values in *Pitx3 aphakia* mice, no significant difference between the two groups could be revealed by statistical tests (cf. fig. 32).

D_2 receptor densities were significantly higher in the striatum of *Pitx3 aphakia* mice compared to control mice (8%; $p<0.05$) (cf. fig. 31 and fig. 32).

D_2/D_3 receptor densities did not differ significantly between the two groups (cf. fig. 32).

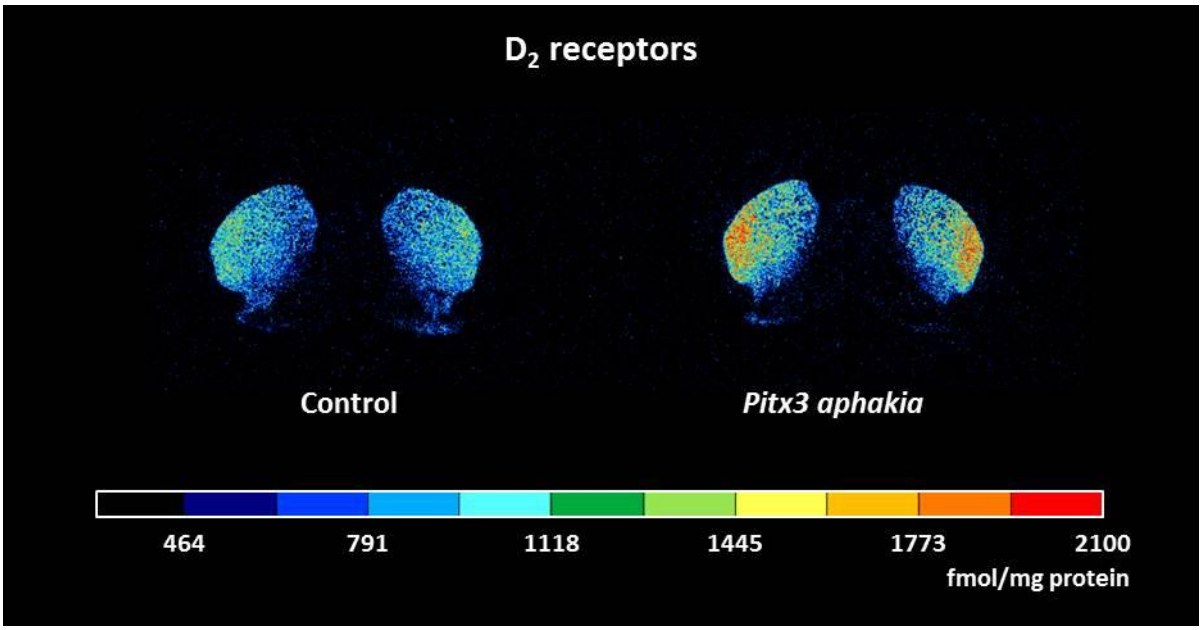

Fig. 31 Dopaminergic D_2 receptor densities in the striatum of *Pitx3 aphakia* (right) and control mice (left) presented as contrast color coded images (the color scale for D_2 receptors reached between 300 and 2100 fmol/mg protein).

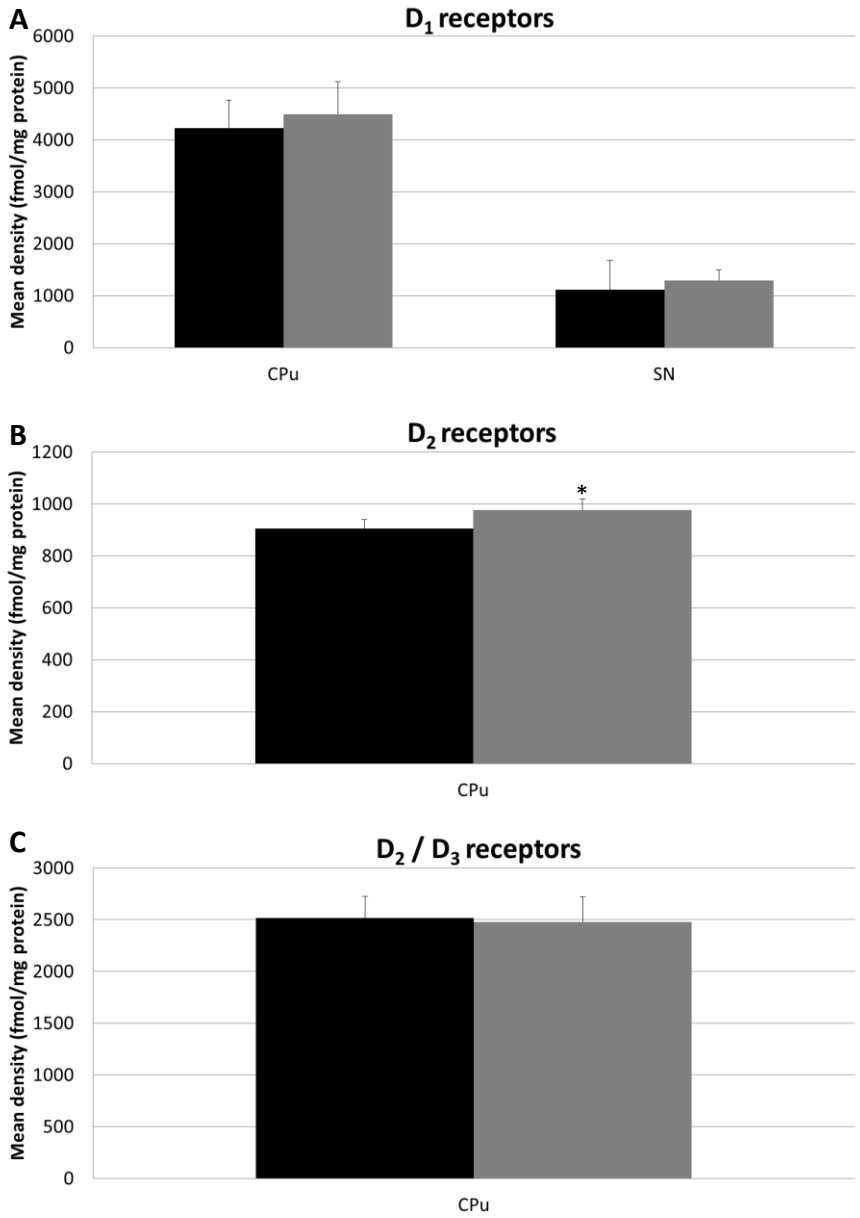

Fig.32 Bar charts of mean dopaminergic receptor densities including standard deviation in different brain regions of control (black) and *Pitx3 aphakia* mice (gray). Mean density is indicated as fmol/mg protein. Significant differences are indicated by *p<0.05 or ***p<0.01, respectively. The following [^{3}H]-ligands were used: SCH 23390 (A); Raclopride (B); Fallypride (C). For contrast color coded images that visualize the regional distribution of the analyzed neurotransmitter receptors within the brain, see chapter 1. For a schematic overview of brain regions / abbreviations, see fig.3.

2.7. Adenosine receptors

There was no significant difference between the $\mathbf{A_{2A}}$ receptor densities of control animals and *Pitx3 aphakia* mice (cf. fig. 33).

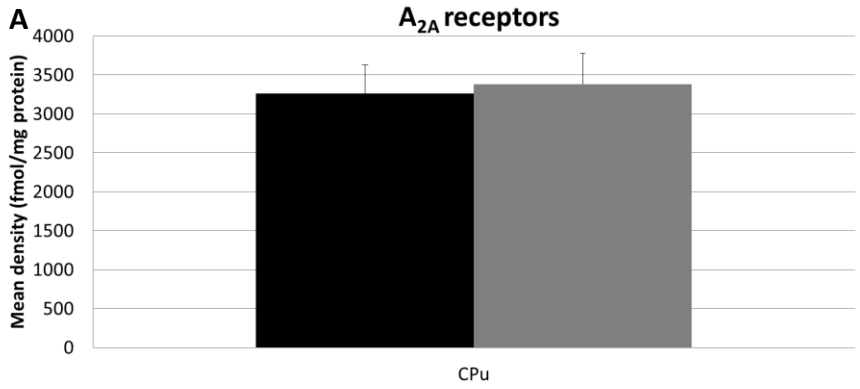

Fig.33 Bar charts of mean adenosine receptor densities including standard deviation in different brain regions of control (black) and *Pitx3 aphakia* mice (gray). Mean density is indicated as fmol/mg protein. Significant differences are indicated by *p<0.05 or ***p<0.01, respectively. The following [^{3}H]-ligand was used: ZM241 385 (A). For contrast color coded images that visualize the regional distribution of the analyzed neurotransmitter receptors within the brain, see chapter 1. For a schematic overview of brain regions / abbreviations, see fig.3.

2.8. Summary diagram

Changes in densities of receptors were found in all investigated brain regions of *Pitx3 aphakia* mice. Fig. 34 gives a comprehensive overview.

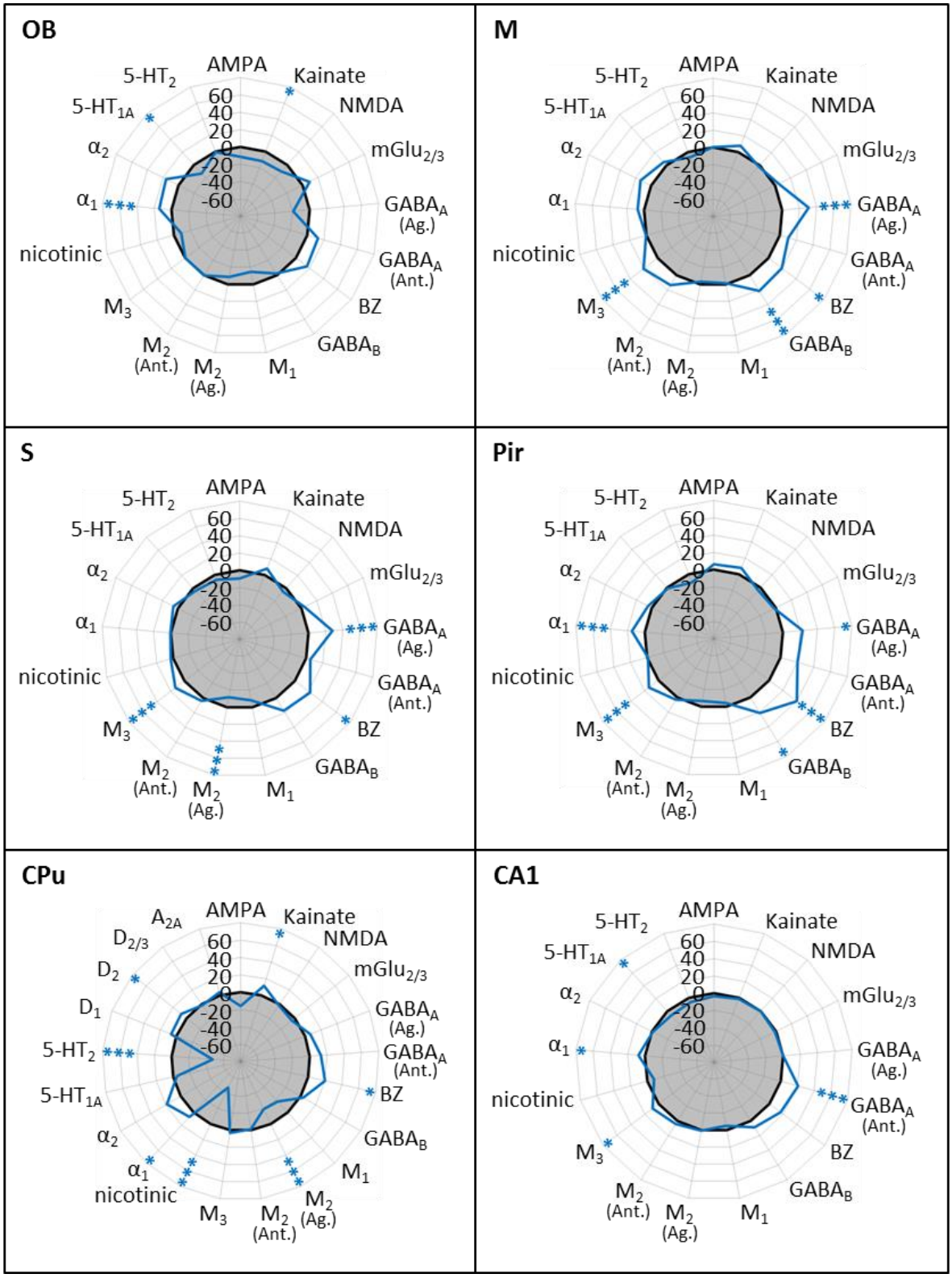

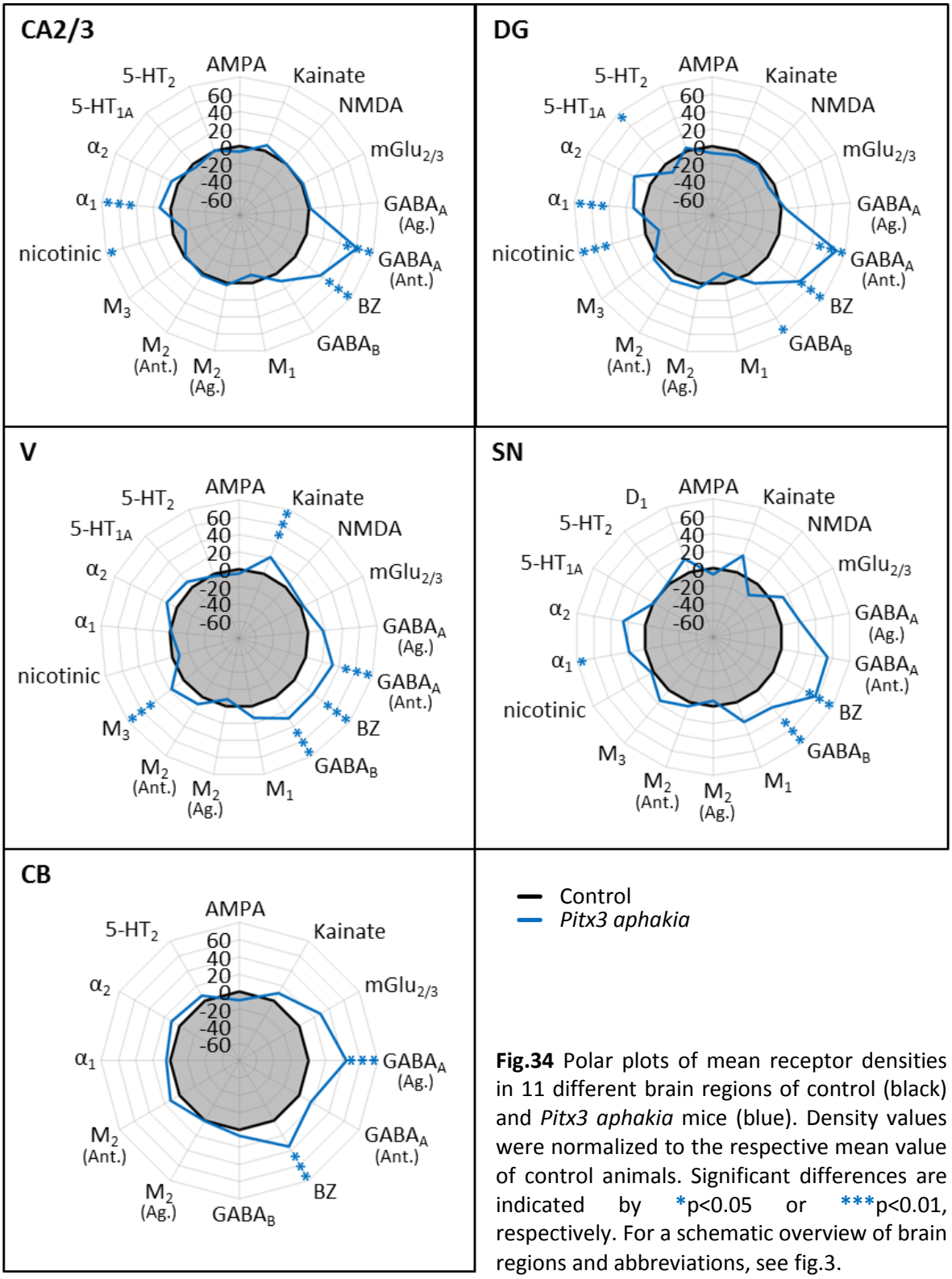

Fig.34 Polar plots of mean receptor densities in 11 different brain regions of control (black) and *Pitx3 aphakia* mice (blue). Density values were normalized to the respective mean value of control animals. Significant differences are indicated by *p<0.05 or ***p<0.01, respectively. For a schematic overview of brain regions and abbreviations, see fig.3.

3. Neurotransmitter receptor densities in *Parkin* and *DJ-1* knockout mouse brains

3.1. Glutamate receptors

AMPA receptor densities were significantly decreased in all hippocampal regions (CA1: -34 %; $p<0.05$; CA2/3: -24 %; $p<0.01$; dentate gyrus: -28 %; $p<0.01$), the visual cortex (-13 %; $p<0.05$) and the cerebellum (-41 %; $p<0.01$) of *Parkin* knockout mice compared to control animals. All other investigated brain regions in these mice demonstrated a similar trend, which however did not reach significance (cf. fig. 35).

In *Parkin* and *DJ-1* knockout mice brains, **kainate** receptor densities were increased between 13 and 28 % in the olfactory bulb ($p<0.05$), the motor ($p<0.01$), somatosensory ($p<0.01$), piriform ($p<0.01$) and visiual cortex ($p<0.01$) (cf. fig. 35).

Statistical tests revealed significantly higher **NMDA** receptor densities in the piriform cortex (10 %; $p<0.01$) and all hippocampal regions (CA1: 11%; $p<0.01$; CA2/3: 7 %; $p<0.01$; dentate gyrus: 7 %; $p<0.01$) of *Parkin* mice compared to control animals (cf. fig. 35).

No significant changes of metabotropic glutamate receptor (**$mGlu_{2/3}$**) densities were shown between control mice and *Parkin* or *DJ-1* knockout mice, respectively (cf. fig. 35).

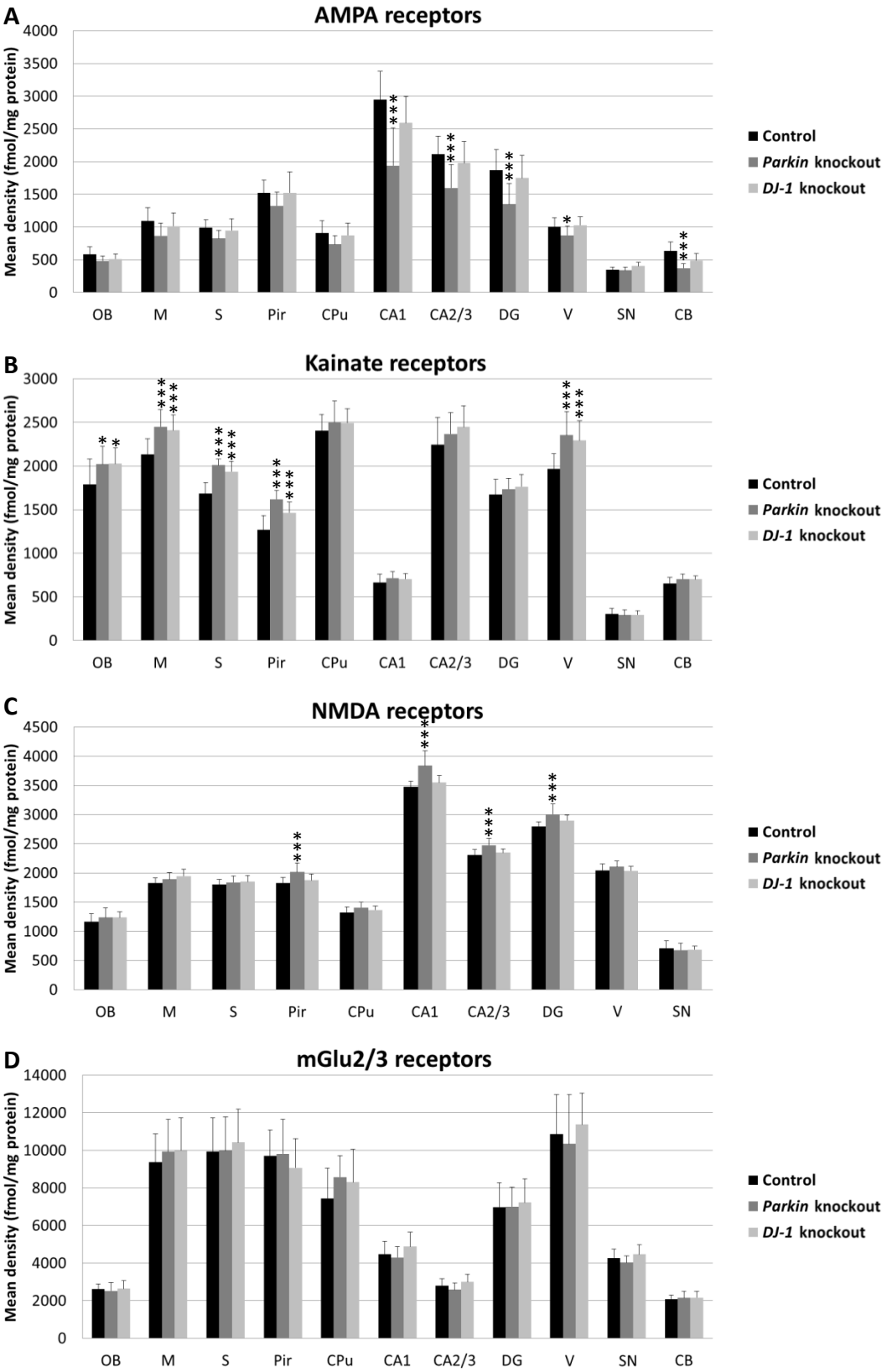

Fig.35 Bar charts of mean glutamatergic receptor densities including standard deviation in different brain regions of control (black), *Parkin* knockout (dark gray) and *DJ*-1 knockout mice (light gray). Mean density is indicated as fmol/mg protein. Significant differences are indicated by *p<0.05 or ***p<0.01, respectively. The following [^{3}H]-ligands were used: AMPA (A); Kainate (B); MK 801 (C); LY341,495 (D). For contrast color coded images that visualize the regional distribution of the analyzed neurotransmitter receptors within the brain, see chapter 2.

3.2. GABA receptors

Neither binding of the **$GABA_A$** receptor *agonist* [^{3}H]-muscimol, nor the receptor *antagonist* [^{3}H]-SR 95531 revealed significant differences of receptor densities between control mice and *Parkin* and *DJ-1* knockout mice, respectively (cf. fig. 36).

The densities of **BZ** binding sites were not changed in the brains *Parkin* and *DJ-1* knockout mice when compared to control animals (cf. fig. 36).

Both *Parkin* and *DJ-1* knockout mice exhibited significantly higher **$GABA_B$** receptor densities compared to controls in numerous brain regions. In case of *Parkin* mice, these regions were the piriform cortex (26 %; $p<0.01$), the striatum (13 %; $p<0.05$), the hippocampal regions (CA1: 18 %; $p<0.01$; CA2/3: 20 %; $p<0.01$; dentate gyrus: 19 %; $p<0.01$), the visual cortex (18 %; $p<0.01$) and the substantia nigra (15 %; $p<0.05$). In case of *DJ-1* mice, statistical tests revealed a significant (14-32 %; $p<0.01$) increase of receptor densities for all analyzed brain regions, except for the cerebellum (cf. fig. 36).

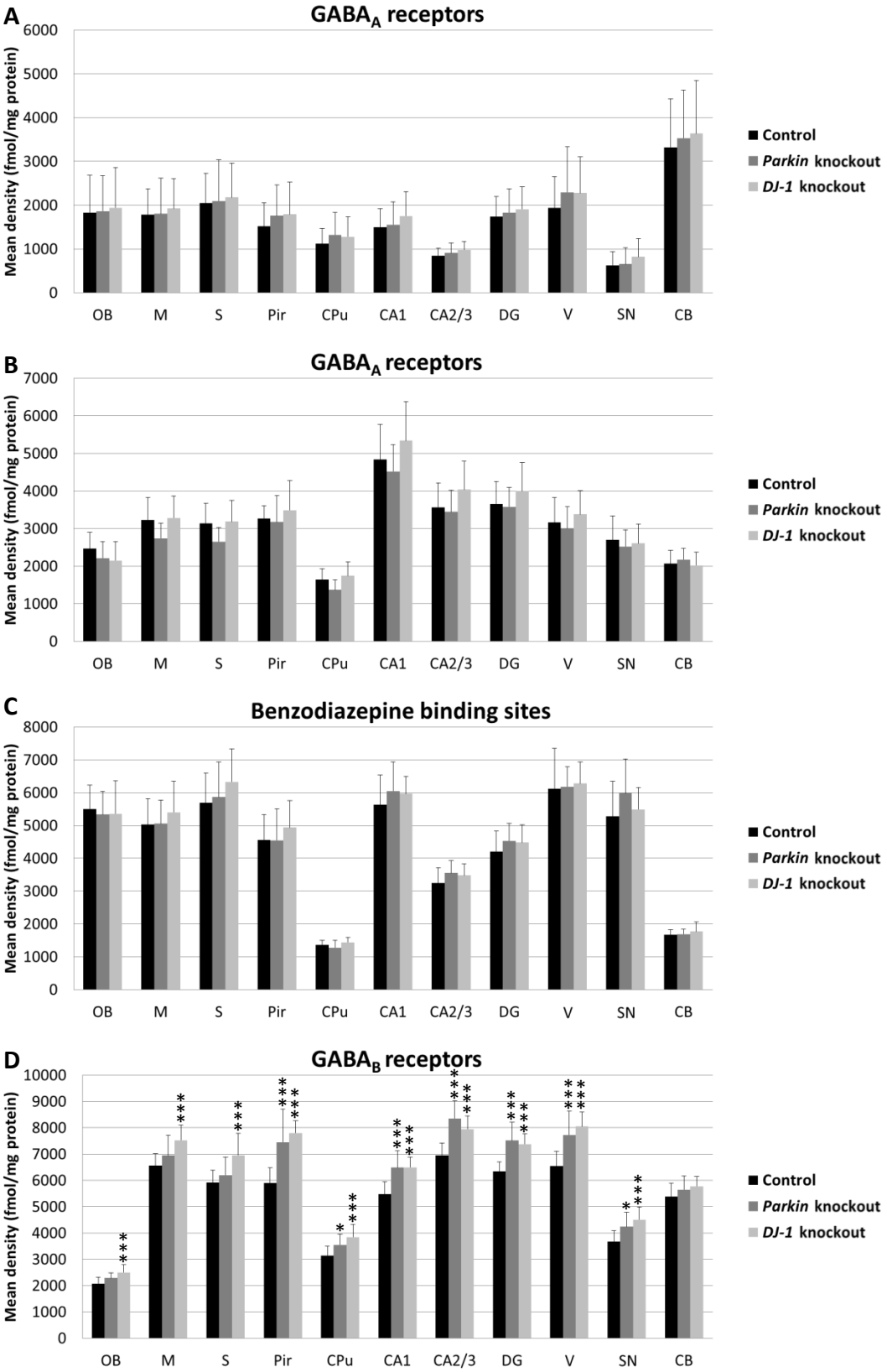

Fig.36 Bar charts of mean GABAergic receptor densities including standard deviation in different brain regions of control (black), *Parkin* knockout (dark gray) and *DJ*-1 knockout mice (light gray). Mean density is indicated as fmol/mg protein. Significant differences are indicated by *p<0.05 or ***p<0.01, respectively. [^{3}H]-ligands: Muscimol (agonist) (A); SR 95531 (antagonist) (B); Flumazenil (C); CGP 54626 (D). For contrast color coded images that visualize the regional distribution of the analyzed neurotransmitter receptors within the brain, see chapter 2.

3.3. Acetylcholine receptors

Statistical tests revealed significantly higher **M_1** acetylcholine receptor densities in the olfactory bulb (Parkin and *DJ-1* knockout: $p<0.01$), the striatum (*Parkin* knockout: $p<0.01$; *DJ-1* knockout: $p<0.05$) and the hippocampus (Parkin knockout: CA1 and dentate gyrus: $p<0.01$; CA2/3: $p<0.05$; DJ-1 knockout: CA1, CA2/3 and dentate gyrus: $p<0.01$) of both knockout models compared to control animals. The densities were increased by 24 – 47 %. The motor, somatosensory, piriform and visual cortex also exhibited a trend towards higher densities in the knockout mice, however this trend was not statistically significant (cf. fig. 37).

Binding experiments using [^{3}H]-oxotremorine-M, an *agonist* of the **M_2** muscarinic acetylcholine receptor, revealed numerous density alterations between control and *Parkin* and *DJ-1* knockout mice, respectively. *Parkin* knockout mice exhibited increased receptor densities in the olfactory bulb (16 %; $p<0.01$), somatosensory (9 %; $p<0.05$) and piriform cortex (22 %; $p<0.01$), striatum (28 %; $p<0.01$), substantia nigra (15 %; $p<0.05$), and the cerebellum (9 %; $p<0.05$). *DJ-1* knockout mice showed significantly higher densities in the olfactory bulb (10 %; $p<0.01$), motor (19 %; $p<0.01$), somatosensory (15 %; $p<0.01$), and piriform cortex (18 %; $p<0.01$), hippocampus (CA1: 14 %; $p<0.01$; CA2/3: 16 %; $p<0.01$; dentate gyrus: 18%; $p<0.01$), substantia nigra (13 %; $p<0.05$) and cerebellum (15 %; $p<0.01$) (cf. fig. 37).
In contrast, binding of the **M_2** receptor *antagonist* [^{3}H]-AF-DX 384 did not reveal statistically significant differences between the knockout mice and control animals (cf. fig. 37).

M_3 receptor densities did not differ significantly between control mice and *Parkin* or *DJ-1* knockout mice, respectively, in any of the brain regions (cf. fig. 37).

Nicotinic acetylcholine receptor densities were significantly increased in the motor (11 %; $p<0.01$), somatosensory (12 %; $p<0.01$), piriform (20 %; $p<0.01$), and visual cortex (12 %; $p<0.01$) of *Parkin* knockout mice compared to control mice (cf. fig. 37).

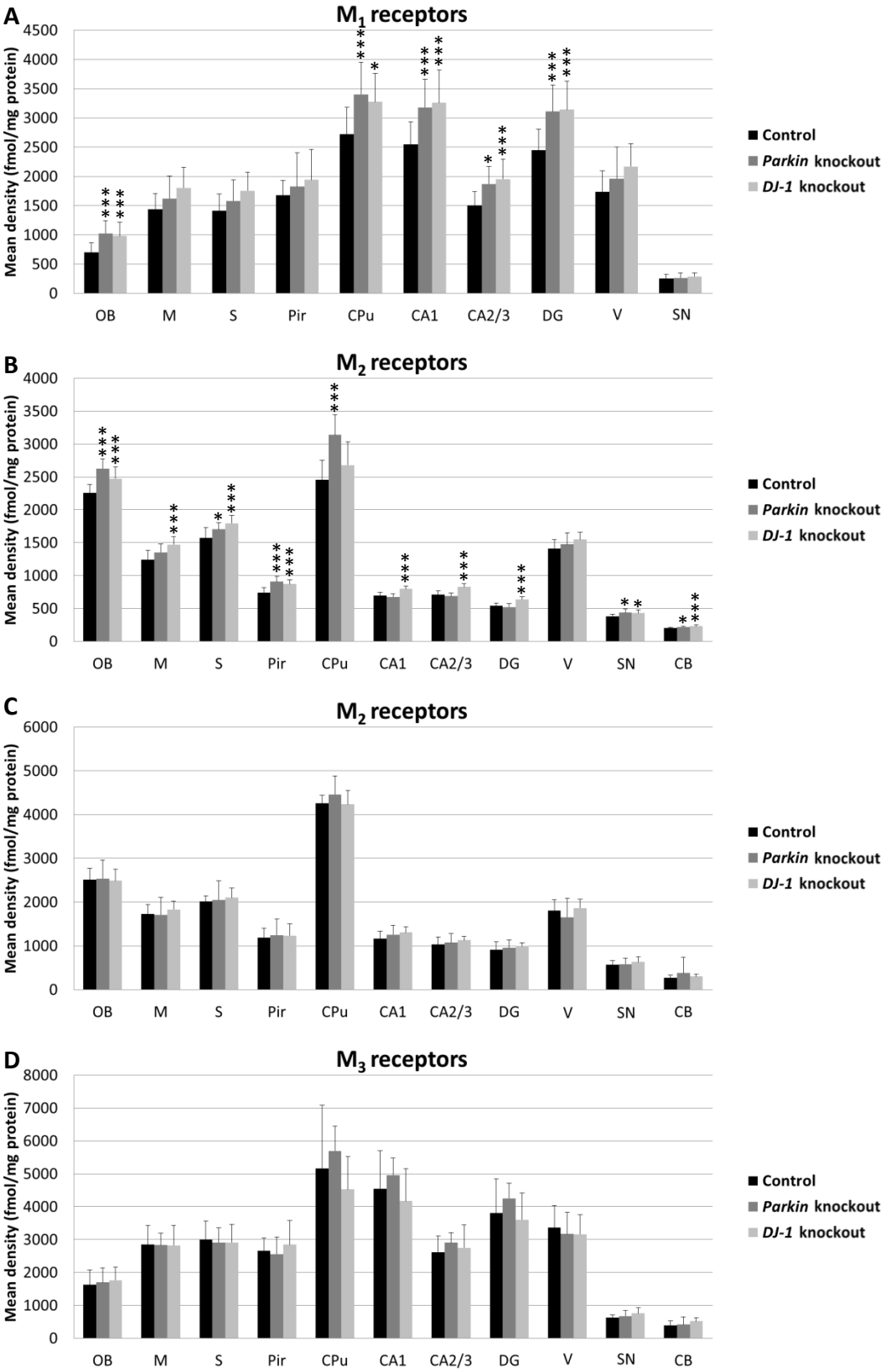

Fig.37 Bar charts of mean acetylcholinergic receptor densities including standard deviation in different brain regions of control (black), *Parkin* knockout (dark gray) and *DJ*-1 knockout mice (light gray). Mean density is indicated as fmol/mg protein. Significant differences are indicated by *p<0.05 or ***p<0.01, respectively. [^{3}H]-ligands: Pirenzepine (A); Oxotremorine-M (agonist) (B); AF-DX 384 (antagonist) (C); 4-DAMP (D); Epibatidine (E). For contrast color coded images that visualize the regional distribution of the analyzed neurotransmitter receptors within the brain, see chapter 2.

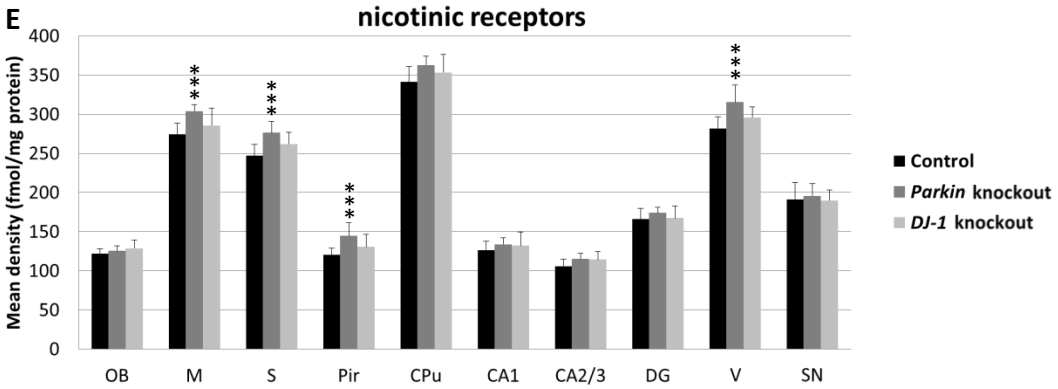

Fig.37 Continuation.
For explanation, see previous page.

3.4. Noradrenaline receptors

No significant differences of adrenergic α_1 receptor densities were found between control mice and *Parkin* or *DJ-1* knockout mice, respectively (cf. fig. 38).

Mean α_2 receptor densities were significantly increased in numerous brain regions of *Parkin* knockout mice compared to control animals, i.e. the olfactory bulb (42 %; p<0.01), the motor (19 %; p<0.05) and the piriform cortex (38 %; p<0.01), the striatum (30 %; p<0.05), the hippocampus (CA1: 37 %; p<0.01; CA2/3: 31%; p<0.05; dentate gyrus: 33 %; p<0.01) and the cerebellum (25 %; p<0.01). *DJ-1* knockout mice exhibited a tendency to increased receptor densities in all ROIs, however, this did not prove to be statistically significant (cf. fig. 38).

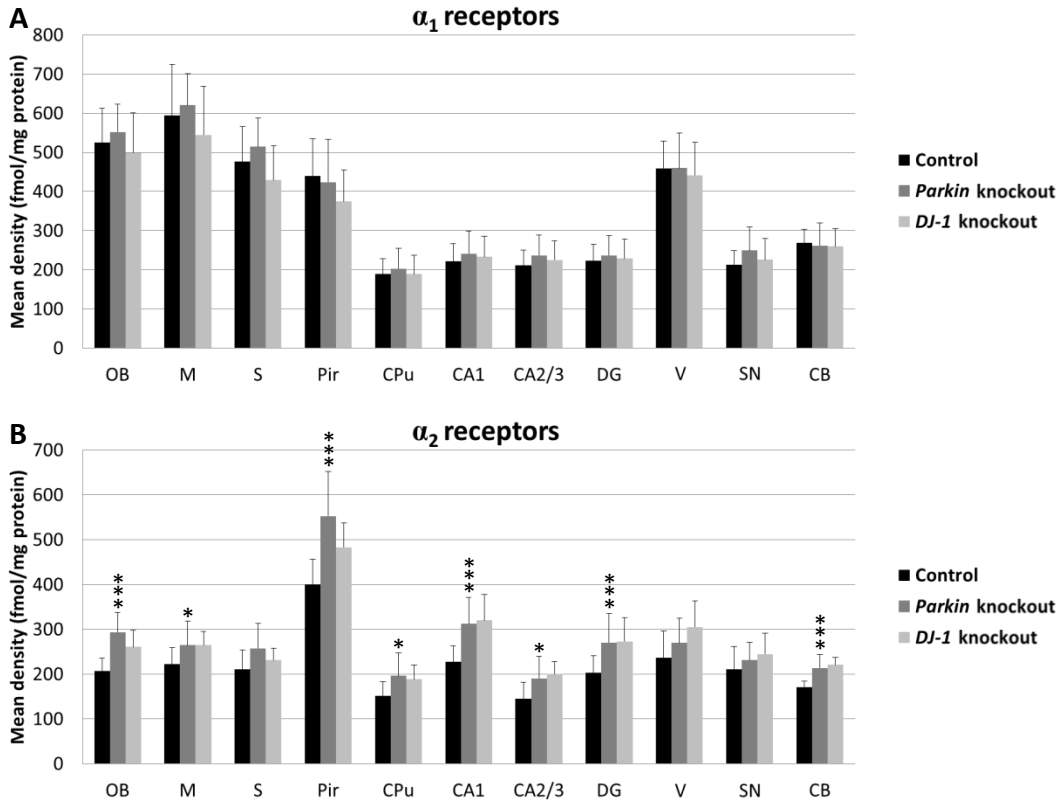

Fig.38 Bar charts of mean adrenergic receptor densities including standard deviation in different brain regions of control (black), *Parkin* knockout (dark gray) and *DJ*-1 knockout mice (light gray). Mean density is indicated as fmol/mg protein. Significant differences are indicated by *p<0.05 or ***p<0.01, respectively. The following [^{3}H]-ligands were used: Prazosin (A); UK14,304 (B). For contrast color coded images that visualize the regional distribution of the analyzed neurotransmitter receptors within the brain, see chapter 2.

3.5. Serotonin receptors

No significant differences were found regarding **5-HT$_{1A}$** receptor densities in the brains of *Parkin* and *DJ-1* knockout and corresponding control mice (cf. fig. 39).

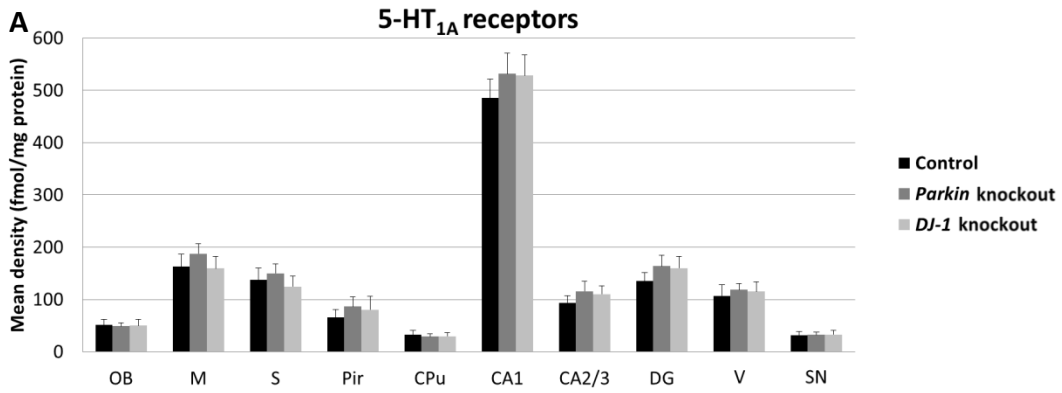

Fig.39 Bar charts of mean serotonergic receptor densities including standard deviation in different brain regions of control (black), *Parkin* knockout (dark gray) and *DJ*-1 knockout mice (light gray). Mean density is indicated as fmol/mg protein. Significant differences are indicated by *p<0.05 or ***p<0.01, respectively. The following [^{3}H]-ligand was used: 8-OH-DPAT (A). For contrast color coded images that visualize the regional distribution of the analyzed neurotransmitter receptors within the brain, see chapter 2.

3.6. Dopamine receptors

Dopamine **D_2** and **D_2/D_3** receptor densities in the striatum of *Parkin* and *DJ-1* knockout mice and control animals did not differ significantly (cf. fig. 40).

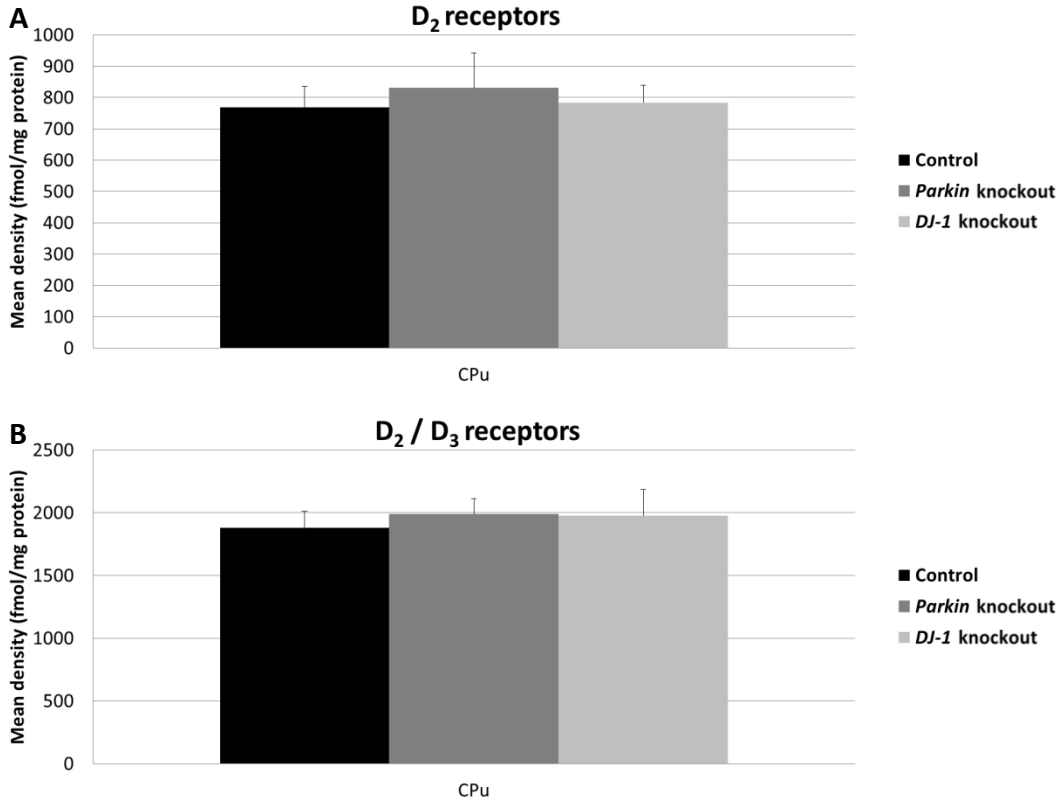

Fig.40 Bar charts of mean dopaminergic receptor densities including standard deviation in different brain regions of control (black), *Parkin* knockout (dark gray) and *DJ*-1 knockout mice (light gray). Mean density is indicated as fmol/mg protein. Significant differences are indicated by *p<0.05 or ***p<0.01, respectively. The following [^{3}H]-ligands were used: Raclopride (A); Fallyprid (B). For contrast color coded images that visualize the regional distribution of the analyzed neurotransmitter receptors within the brain, see chapter 2.

3.7. Adenosine receptors

Adenosine $\mathbf{A_{2A}}$ receptor density in the striatum of *DJ-1* knockout mice was significantly increased (9 %; p<0.01) compared to controls (cf. fig. 41).

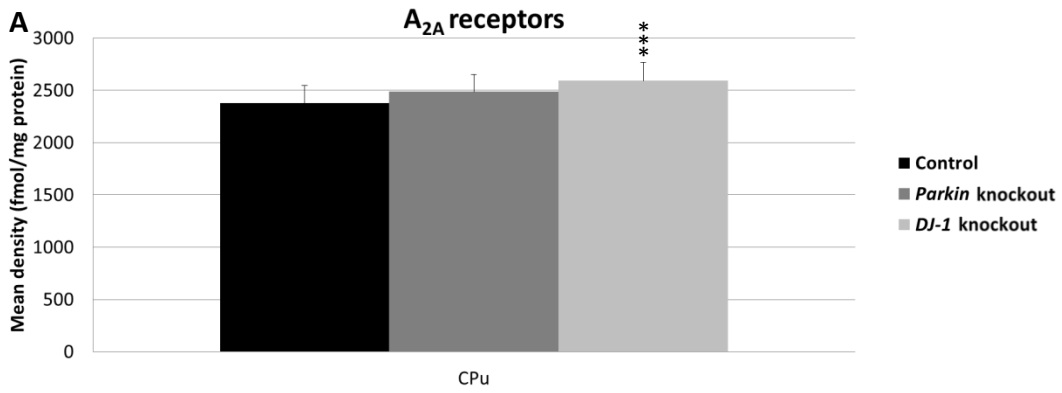

Fig.41 Bar charts of mean adenosine receptor densities including standard deviation in different brain regions of control (black), *Parkin* knockout (dark gray) and *DJ*-1 knockout mice (light gray). Mean density is indicated as fmol/mg protein. Significant differences are indicated by *p<0.05 or ***p<0.01, respectively. The following [^{3}H]-ligand was used: ZM241 385 (A). For contrast color coded images that visualize the regional distribution of the analyzed neurotransmitter receptors within the brain, please see chapter 2.

3.8. Summary diagram

Changes in densities of receptors were found in all investigated brain regions of *Parkin* and *DJ-1* knockout mice. Fig. 42 gives a comprehensive overview.

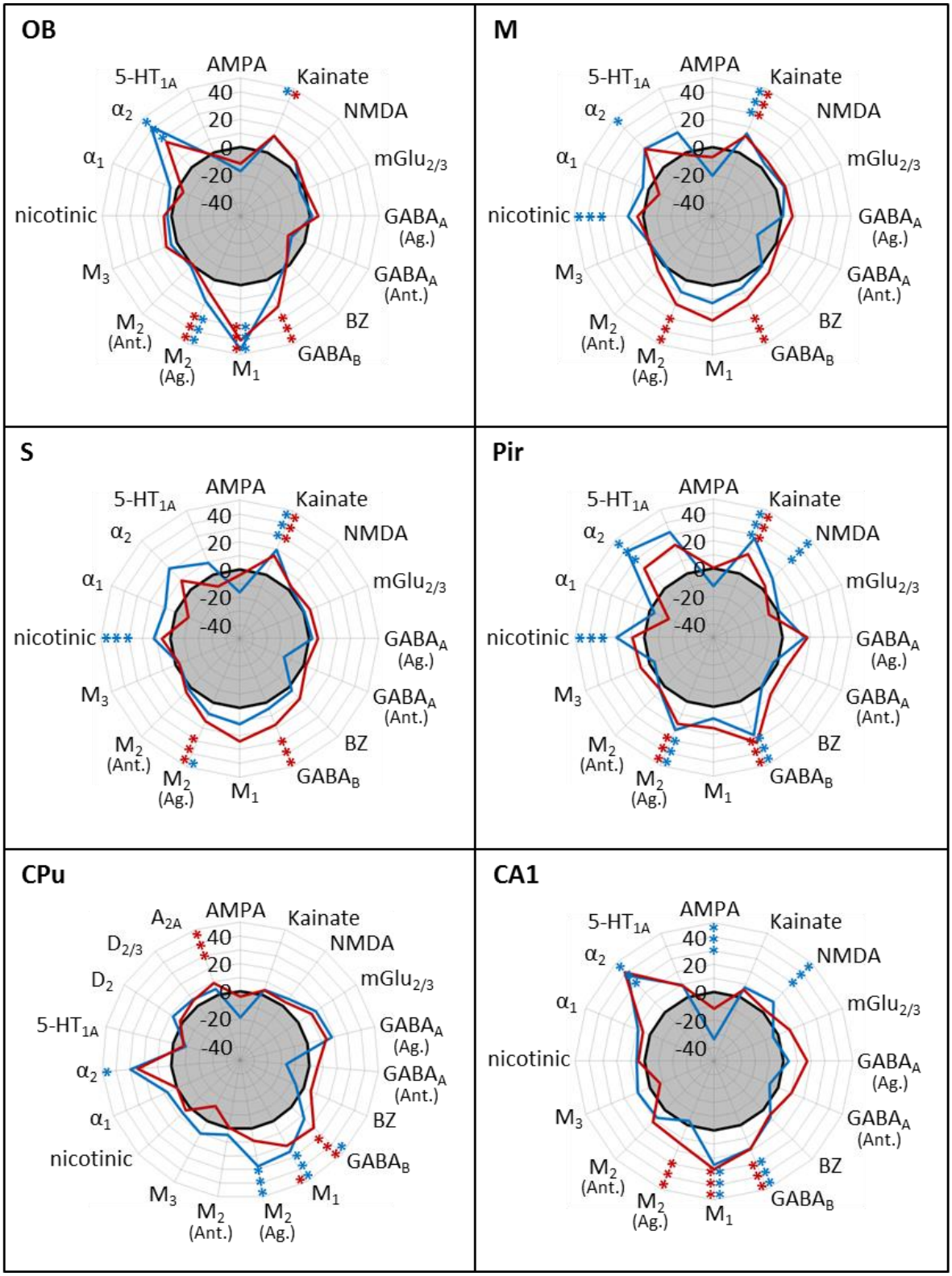

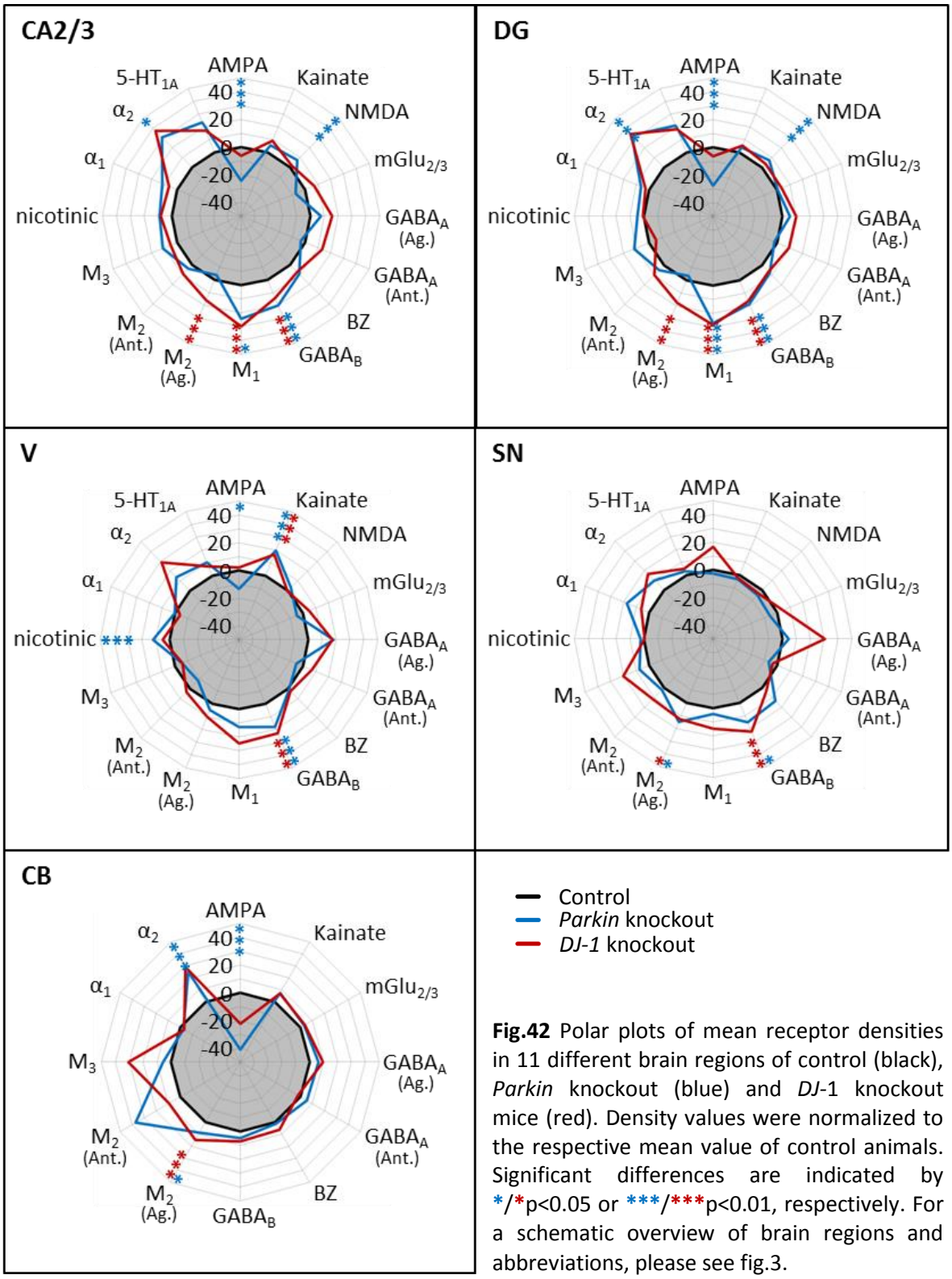

Fig.42 Polar plots of mean receptor densities in 11 different brain regions of control (black), *Parkin* knockout (blue) and *DJ*-1 knockout mice (red). Density values were normalized to the respective mean value of control animals. Significant differences are indicated by */*p<0.05 or ***/***p<0.01, respectively. For a schematic overview of brain regions and abbreviations, please see fig.3.

4. mRNA Levels of neurotransmitter receptors

4.1. KA2 receptor subunit mRNA

The mean mRNA levels of the KA2 kainate receptor subunit varied from 44 fmol x 10^{-3} / mg protein (CA1, *Parkin* knockout) to 93 fmol x 10^{-3} / mg protein (OB, Control). mRNA levels were homogeneously distributed between ROIs revealing comparable values for the motor, somatosensory and piriform cortex, the striatum and the CA1 region of the hippocampus, whereas the transcription levels in the olfactory bulb and the other hippocampal regions (CA2/3 and dentate gyrus) were slightly higher. Compared to controls, both knockout models exhibited a trend towards increased mRNA levels in the investigated brain areas, except for CA1 in *Parkin* knockout mice. However, these differences did not prove to be statistically significant.

The results are summarized in figure 43.

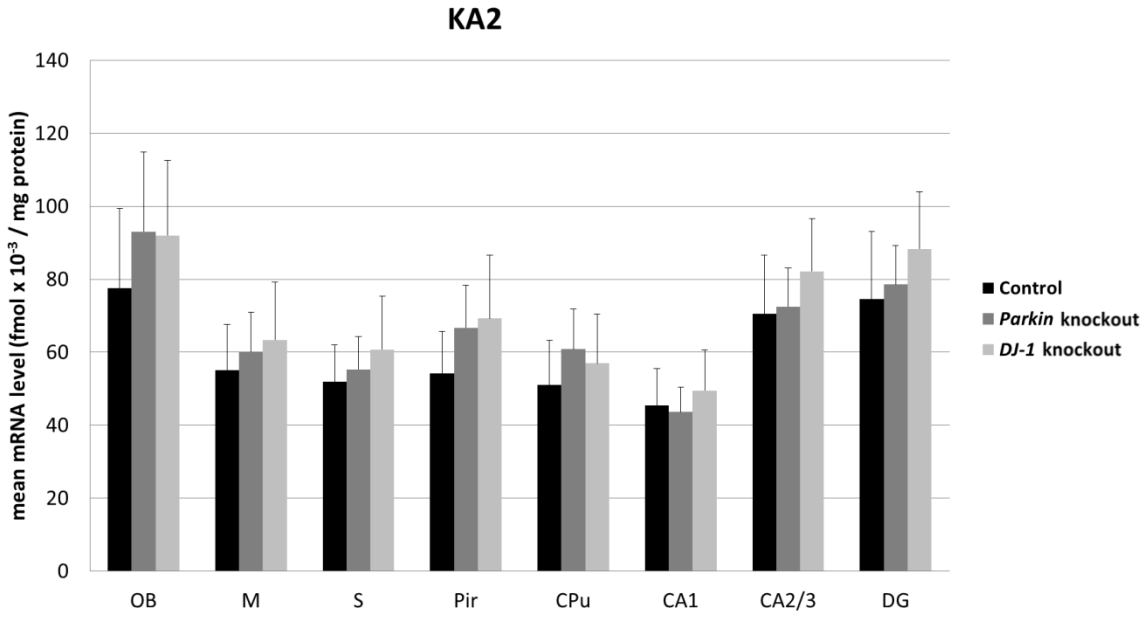

Fig.43 Bar chart of mean mRNA levels of the KA2 kainate receptor subunit including standard deviation in different brain regions of control (black), *Parkin* knockout (dark gray) and *DJ*-1 knockout mice (light gray). Mean mRNA level is indicated as fmol x 10^{-3} / mg protein.

4.2. $GABA_B$ receptor mRNA

$GABA_B$ receptor mean mRNA levels ranged between 6 fmol x 10^{-3} / mg protein (CPu, Control) and 64 fmol x 10^{-3} / mg protein (DG, *Parkin* knockout). mRNA levels were heterogeneously distributed above the investigated brain areas. The motor, somatosensory and piriform cortex, the CA2/3 region of the hippocampus as well as the dentate gyrus showed relatively high transcription levels. The CA1 region of the hippocampus revealed medium mRNA levels whereas the values of the olfactory bulb and the striatum were relatively low. As in the case of KA2 mRNA levels, the knockout mice showed a trend towards higher values than control mice in all analyzed brain regions, but these alterations did not reach statistical significance The results are summarized in figure 44.

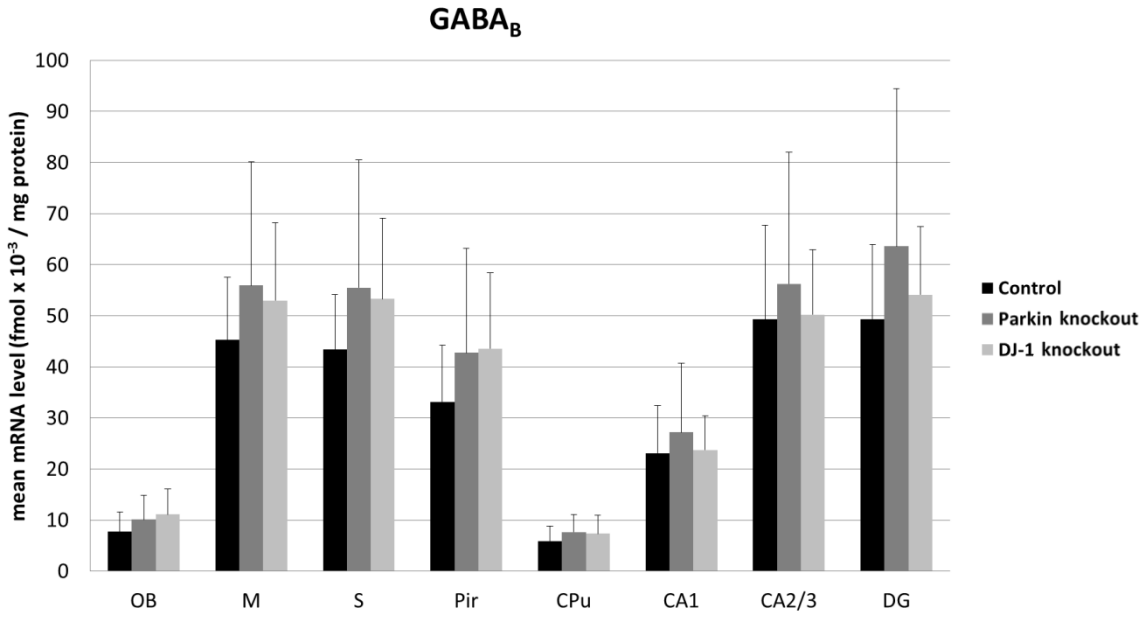

Fig.44 Bar chart of mean mRNA levels of the $GABA_B$ receptor including standard deviation in different brain regions of control (black), *Parkin* knockout (dark gray) and *DJ*-1 knockout mice (light gray). Mean mRNA level is indicated as fmol x 10^{-3} / mg protein.

Discussion

The occurrence of up to 21 different neurotransmitter receptor binding sites was analyzed by means of quantitative in vitro receptor autoradiography in the brains of three well established mouse models of Parkinson's disease (*Pitx3 aphakia, Parkin* and *DJ-1* knockout mice), and in controls. Differential changes of receptor densities in several neurotransmitter systems were demonstrated in all investigated mouse models. In figures 34 and 42 (see results section), the region-specific densities of each receptor type are presented as normalized values (mean value of control animals = 100 %) in the PD mouse models.

1. Glutamate receptors

Glutamate is the most important excitatory neurotransmitter in the vertebrate nervous system. In general, glutamate receptors can be subdivided into ionotropic AMPA, kainate and NMDA receptors and metabotropic receptors. Under physiological conditions glutamate receptors play a crucial role in long-term potentiation, a process of synaptic plasticity associated with learning and memory (Brown et al., 1988; Bliss and Collingridge, 1993; McEntee and Crook, 1993). Under pathological conditions excessive glutamate release or impaired uptake can result in excitotoxicity and subsequent neurodegenerative processes (Mattson and Kater, 1989). Therefore, an involvement of glutamate is assumed in the etiology of several neurodegenerative diseases like Huntington's, Alzheimer's or Parkinson's disease (Planells-Cases et al., 2006).

AMPA receptor densities were significantly decreased in the hippocampus, the visual cortex and the cerebellum of *Parkin* knockout mice. The decrease of AMPA receptors well corresponds to the intracellular *Parkin* function, which is involved in AMPA receptor trafficking mediated by ubiquitination-dependent interaction with C-kinase (PICK1) (Xia et al., 1999; Lu and Ziff, 2005; Joch et al., 2007). Thus, lack of *Parkin* expression might indirectly affect excitatory synaptic transmission in these brain regions. This hypothesis is further

supported in particular for the hippocampal regions, where a complex pattern of changes of synaptic physiology has been described in *Parkin* knockout mice (Hanson et al., 2010). The hypothesis of a role of Parkin in the regulation of receptor trafficking and synaptic transmission is additionally supported by the analysis of **NMDA** receptor densities. NMDA receptors were significantly increased in the piriform cortex and the hippocampus of *Parkin* knockout mice. Since the NMDA receptor mediate AMPA receptor endocytosis via Ca^{2+} influx (Hanley and Henley, 2005), the increased NMDA receptor density in *Parkin* knockout mice might additionally impair the normal AMPA receptor trafficking. The described increase of hippocampal NMDA receptor densities may furthermore explain the enhanced synaptic plasticity in *Parkin* knockout mice, revealed by significantly stronger long-term potentiation (Hanson et al., 2010).

The changes concerning glutamatergic receptor densities in the hippocampus of *Parkin* knockout mice give rise to the assumption that these mice might demonstrate deficits in learning and other cognitive processes, which would be an interesting topic of further investigation. Thus, the decreased AMPA receptor densities in the hippocampus of Parkin mice, could explain cognitive impairments in patients with Parkinson's disease (Aarsland et al., 2010; Ojo et al., 2012). In this case, AMPA receptor potentiators that were shown to enhance cognitive function (O'Neill et al., 2004) could be a promising target for therapeutic intervention in PD.

Glutamate induced excitotoxicity may play an important role in the pathogenesis of Parkinson's disease (Beal, 1998; Rodriguez et al., 1998). The up-regulation of NMDA receptor densities in *Parkin* knockout mice might trigger cytotoxic effects, since glutamate excitotoxicity is mainly mediated via NMDA receptors (Akaike et al., 1999). Thus, NMDA receptor antagonists could be a target for the treatment of PD. The present results support the studies examining the potential benefit of NMDA receptor antagonists, e.g. amantadine, in the treatment of Parkinson's disease (Lange et al., 1997; Hallett and Standaert, 2004; Planells-Cases et al., 2006). Besides the elevated densities of the NMDA receptor in *Parkin* knockout mice, the **kainate** receptor exhibited increased densities in the olfactory bulb and cortical regions (motor, somatosensory, piriform and visual cortex) of *Parkin* and *DJ-1* knockout mice, respectively, as well as in the striatum and the visual cortex of *Pitx3 aphakia* mice, compared to control mice. These alterations might also play a role in excitotoxic

processes leading to neurodegeneration. It was shown that *Parkin* protects cultured neurons from kainate induced excitotoxicity (Staropoli et al., 2003). These results might be of particular interest for further experimental investigation, since kainate receptors have largely been neglected in PD research so far.

Quantitative in situ hybridization did not reveal significant differences with respect to KA2 kainate receptor subunit mRNA levels in *Parkin* and *DJ-1* knockout mice, compared to control animals. Thus, we suggest that the density changes of kainate receptors are most likely caused by regulation mechanisms at the translational rather than the transcriptional level. However, it has to be noted that mRNA levels for neurotransmitter receptors were demonstrated to be comparatively rare, thus demanding a highly sensitive experimental approach, which might be challenging concerning the detection of subtle mRNA expression differences (Cremer et al., 2009).

2. GABA receptors

γ-Aminobutyric acid (GABA) is the most abundant inhibitory neurotransmitter in the vertebrate brain. GABA receptors can be classified into ionotropic $GABA_A$ and $GABA_C$ receptors and metabotropic $GABA_B$ receptors. The GABAergic system, and the $GABA_A$ receptor in particular, plays a role in memory processes (Chapouthier and Venault, 2002), anxiety (Sanders and Shekhar, 1995) and the induction of seizures (Roberts, 1984). $GABA_A$ receptors exhibit binding sites for benzodiazepine (BZ) molecules located between α_1 and γ_2 receptor subunits. Benzodiazepines enhance the action of GABA by binding to the allosteric side of the receptor and are therefore therapeutically used as sedatives, hypnotics and anxiolytics (Rudolph and Mohler, 2006). To date, little is known about the GABAergic system in the context of Parkinson's disease, although GABA levels were shown to be reduced in the brains of PD patients (de Jong et al., 1984; Gerlach et al., 1996).

Pitx3 aphakia mice exhibited statistically significant alterations concerning the $GABA_A$ and $GABA_B$ receptor as well as the benzodiazepine binding site densities. The **$GABA_A$** receptor

agonist muscimol revealed density increases in the motor, the somatosensory and the piriform cortex as well as in the cerebellum. Additionally, the $GABA_A$ receptor antagonist SR 95531 revealed density increases in the hippocampus (CA1, CA2/3 and dentate gyrus) as well as the visual cortex. Thus, muscimol and SR 95531 exhibited different regional binding profiles. This is explainable by different binding mechanisms between receptor agonists and antagonists in general (Jones et al., 2001) and different affinities in particular, since muscimol represents an agonist for high-affinity GABA sites, while SR 95531 on the contrary represents an antagonist binding mainly to low-affinity GABA sites (Olsen et al., 1990). Binding site densities of muscimol and SR 95531 were shown to be differentially changed in other studies as well, for example in the rat mesolimbic system after acute ethanol application (Cowen et al., 1998). **BZ** binding sites were increased in all investigated brain regions of *Pitx3 aphakia* mice, except for the olfactory bulb and the CA1 region of the hippocampus. Since BZ binding sites are associated with the $GABA_A$ receptor, these data are generally concordant to those described for the $GABA_A$ receptor. **$GABA_B$** receptor densities were significantly enhanced in the motor, piriform and visual cortex, the dentate gyrus and the substantia nigra of *Pitx3* aphakia mice compared to control animals. The $GABA_B$ receptor is the only receptor sigtnificantly changed in *Parkin* and *DJ-1* knockout mice. Its density is significantly increased in numerous brain regions of both knockout mice, with the exception of the cerebellum in *DJ-1* knockout mice, and the olfactory bulb, the motor and somatosensory cortex and the cerebellum in *Parkin* knockout mice. Notably, the densities of all GABAergic binding sites were consistently increased in the different investigated brain regions of *Pitx3 aphakia* mice and with regard to the $GABA_B$ receptor, also in the mouse models of hereditary PD. Thus, it would be interesting to investigate, whether reduced GABA levels occur in the mouse models, as have been found in PD patients. If so, the here described receptor density increases could represent an up-regulation to compensate the reduced level of GABA. To our knowledge, the densities of GABA receptors have not been investigated in PD patients so far. Our study, however, indicates that GABA receptor levels might be elevated in PD and, thus, the application of either GABA receptor agonists or antagonists could have beneficial effects.

3. Acetylcholine receptors

The first neurotransmitter ever discovered was acetylcholine in the 1920s. In 1921, Loewi demonstrated the action of a chemical transmitter at the vagus nerve endings in the heart (Loewi, 1921) that was later identified as acetylcholine (Loewi and Navratil, 1926). Acetylcholine binds to two receptor classes, either metabotropic muscarinic or ionotropic nicotinic receptors. Acetylcholine is a neuromodulator influencing neuronal excitability, synaptic transmission and synaptic plasticity depending on release-site, receptor subtype and neuronal population at the target site (Picciotto et al., 2012). The acetylcholine system of the brain modulates attention (Klinkenberg et al., 2011), and learning and memory (Hasselmo, 2006). Alterations of the cholinergic system occur in different pathologies, e.g. Alzheimer's disease (Burghaus et al., 2000), and Myasthenia gravis (Graus and De Baets, 1993). In PD patients reduced nicotinic acetylcholine receptor densities have been described in several brain regions (Burghaus et al., 2003; Oishi et al., 2007; Kas et al., 2009; Meyer et al., 2009).

In the present study, acetylcholine receptor **M_1** densities were increased in the olfactory bulb, the striatum and the hippocampus (CA1, CA2/3 and dentate gyrus) of *Parkin* and *DJ-1* knockout mice. **M_2** receptor densities were increased in the olfactory bulb, the somatosensory cortex, the piriform cortex, the striatum, the substantia nigra and the cerebellum of *Parkin* knockout mice as well as in all analyzed brain regions of *DJ-1* knockout mice, except for the striatum and the visual cortex. However, M_2 receptor densities were demonstrated to be decreased in the somatosensory cortex and the striatum of *Pitx3 aphakia* mice. The M_2 receptor densities were measured using the receptor agonist oxotremorine-M. Binding experiments using the receptor antagonist AF-DX 384 did not reveal significant alterations of M_2 receptor densities in any of the three mouse models studied here. This complex pattern of changes may at least partially be ascribed to different binding mechanisms and receptor affinities of agonists and antagonists. The comparable situation was already discussed above concerning $GABA_A$ receptor binding. **M_3** receptor densities were increased in the cortical regions (motor, somatosensory, piriform and visual cortex) and the CA1 region of the hippocampus in *Pitx3 aphakia* mice, whereas normal **M_3** receptor densities were found in the mouse models of hereditary PD. Taken together, the

densities of muscarinic acetylcholine receptors were differentially changed in all investigated mouse models.

While the **nicotinic** acetylcholine receptors were only slightly decreased in the CA2/3 region of the hippocampus and the dentate gyrus of *Pitx3 aphakia* mice, these receptors were massively reduced in the striatum. *Parkin* knockout mice exhibited a slight but significant increase of nicotinic receptor densities in some cortical regions (motor, somatosensory, piriform and visual cortex). Contrary to the muscarinic acetylcholine receptors, the nicotinic acetylcholine receptor has quite extensively been studied in PD. Reduced nicotinic acetylcholine receptor densities were reported in Parkinson's disease patients, particularly in cases with cognitive or depressive symptoms (Burghaus et al., 2003; Oishi et al., 2007; Kas et al., 2009; Meyer et al., 2009). Interestingly, the reductions of nicotinic receptor densities were found to be similar in Alzheimer's and Parkinson's diseases patients (Rinne et al., 1991). Thus, the present results in *Pitx3 aphakia* mice are in line with the results in human brains of PD patients, and, therefore provide further evidence for a correlation between nigrostriatal neurodegeneration and a reduction of nicotinic receptor densities. The question, whether neurodegenerative processes lead to the nicotinic receptor deficits or vice versa cannot be answered from the present data. However, numerous studies revealed a neuroprotective effect of nicotine treatment concerning nigrostriatal cell damage. Abin-Carriquiry et al. (2008) presented evidence that nicotine and nicotinic agonists have the potential to induce striatal protection after 6-hydroxydopamine injection, possibly due to their efficacy to stimulate striatal dopamine release. Furthermore, chronic oral nicotine application protected non-human primates against MPTP-induced striatal degeneration (Quik et al., 2006). Furthermore, an acute intermittent administration of nicotine was shown to exhibit a neuroprotective effect in 6-hydroxydopamine lesioned rats (Costa et al., 2001). Notably, nicotine seems to be neuroprotective rather than neurorestorative, since nigrostriatal damage is only reduced in rats and monkeys, if nicotine is administered before but not after neuronal damage (Huang et al., 2009). Since smoking exhibits an acute intermittent administration of low nicotine levels, a negative correlation with neurodegenerative processes for smokers could be assumed, and indeed smoking has been associated with a decreased incidence of PD (Allam et al., 2004; Ritz et al., 2007; Noyce et al., 2012). Taken together, nicotine and drugs acting on the nicotinic acetylcholine receptor

can be regarded as promising neuroprotective targets for the treatment of PD (Quik et al., 2012). Furthermore, acetylcholinesterase inhibitors could be tested with regard to beneficial effects based on elevated acetylcholine levels, since improvements of cognitive function in PD patients suffering from dementia were already demonstrated (Werber and Rabey, 2001).

4. Noradrenaline receptors

Adrenaline and noradrenaline are hormones and neurotransmitters, and play an important role in stimulating the sympathetic nervous system, e.g. in the context of the fight-or-flight response. The adrenergic receptors are G-protein coupled and can be subdivided into α (α_1 and α_2) and β receptors (β_1 – β_3). Under physiological conditions, the adrenergic system plays a role in attention (Clark et al., 1987; Devauges and Sara, 1990), olfaction (Firestein and Menini, 1999; Hall, 2011) and memory processing (Gold and van Buskirk, 1978; Sternberg et al., 1985). Under pathological conditions the adrenergic system is involved amongst others in the attention-deficit hyperactivity disorder (Mefford and Potter, 1989; Biederman, 2005), depression (Leonard, 1997; Fu et al., 2001) and dementia (Bondareff et al., 1982; Yu et al., 2011). Even though PD is often regarded as a neurodegenerative disease exclusively affecting the dopaminergic nigro-striatal system, neuronal degeneration has also been demonstrated in the nucleus basalis as well as in the locus coeruleus of PD patients (Bertrand et al., 1997; Zarow et al., 2003). Since the locus coeruleus is a major region of noradrenalinee synthesis in the brain (Benarroch, 2009), noradrenalinee concentrations were conclusively shown to be reduced in PD patients (Scatton et al., 1983; Tohgi et al., 1993).

Adrenergic $\boldsymbol{\alpha_2}$ receptor densities were significantly increased in numerous brain regions of *Parkin* knockout mice, i.e. the olfactory bulb, the motor and piriform cortices, the striatum, the cerebellum and the hippocampus. The brains of *DJ-1* knockout mice also exhibited a tendency towards higher densities, however, these changes did not prove to be statistically significant. Adrenergic $\boldsymbol{\alpha_1}$ receptor densities were increased in the olfactory bulb, the piriform cortex, the striatum, and the hippocampus of *Pitx3 aphakia* mice. In general, these

increases of receptor densities may reflect compensatory receptor up-regulations resulting from a reduced adrenergic innervation. To date, there is sparse evidence concerning the regulation of adrenergic receptor expression in PD patients, though the present findings suggest, that this might be a promising target for future research. The treatment of noradrenergic deficits might complement current PD therapeutic approaches that mainly focus on the dopaminergic deficits (e.g. L-DOPA), especially with regard to the PD comorbidity depression. For example, the serotonin/noradrenaline reuptake inhibitor venlafaxine turned out to improve depression in PD patients (Richard et al., 2012). Furthermore, the noradrenaline/dopamine reuptake inhibitor bupropion was proposed as the treatment of choice in depression associated with PD, avoiding the serotonin associated side effects of standard medication (Stahl et al., 2004; Raskin and Durst, 2010).

5. Serotonin receptors

In 1948, a substance in the serum that influences the vascular tone was detected and named accordingly “serotonin” (Rapport et al., 1948). Serotonin receptors can be subdivided into seven families 5-HT_1 to 5-HT_7, each with one to five receptor subtypes, respectively. The serotonergic system is involved in neuronal processes concerning learning and memory (Matsukawa et al., 1997), sleep (Ursin, 2002) or pain (Messing and Lytle, 1977). Alterations of the serotonin system were described in numerous neurological and psychiatric disorders, amongst others migraine (Hamel, 2007), depression (Meltzer, 1990; Mann, 1999), Alzheimer’s disease (Cross, 1990) and schizophrenia (Gurevich and Joyce, 1997). To date, little is known about the serotonergic system in PD patients, however, there is some evidence suggesting a serotonergic affection. For example, densities of serotonin transporters were shown to be reduced in the striatum of PD patients (Kerenyi et al., 2003). Furthermore depression, a disorder which is associated with impaired serotonergic neurotransmission, is a very frequent comorbidity of Parkinson’s disease (Cummings and Masterman, 1999).

Parkin and *DJ-1* knockout mice did not show alterations of serotonin receptor densities in the investigated brain regions. The brains of *Pitx3 aphakia* mice exhibited significantly decreased 5-HT_{1A} receptor densities in the olfactory bulb, the CA1 region of the hippocampus and the dentate gyrus as well as a severe reduction (nearly 50%) of 5-HT_2 receptor densities in the striatum (cf. Results: fig. 30). The data for 5-HT_2 receptors is in concordance with previous results that revealed a similar downregulation of this receptor type in 6-hydroxydopamine-induced parkinsonian rats (Li et al., 2010). Together, these data suggest a role for 5-HT_2 receptors in PD. The here described changes of serotonin receptors and consequently serotonergic transmission might be indicators of concomitant cognitive dysfunction in PD. Reduced serotonergic receptor densities might also play a role in the occurrence of depression as comorbidity of PD. Accordingly, 5-HT_{1A} receptor dysfunction was described to be associated with PD and to differ between depressive and non-depressive PD patients (Ballanger et al., 2012). Furthermore, serotonin transporter densities were shown to be reduced in PD (Cash et al., 1985; Kerenyi et al., 2003). Depression severely impairs the quality of life in PD patients (Committee, 2002), and therefore potential targets for therapeutic intervention are demanded. The dopamine agonist pramipexole (Barone et al., 2010) as well as the selective serotonin reuptake inhibitor paroxetine (Richard et al., 2012) were effective in treating PD associated depression. On the other hand, the dual reuptake inhibitor nortriptyline was found to be superior to paroxetine (Menza et al., 2009). However, placebo-controlled studies with larger numbers of patients that compare the efficaciousness of different compounds are needed to establish an ideal treatment of depression in PD. Our study indicates that serotonergic receptor agonists could be a relevant starting point for therapeutic intervention, due to the fact that such agonists act specifically on one receptor type instead of influencing the whole serotonergic system by inhibiting the reuptake process.

The relationship between deficits of the serotonergic neurotransmitter system and anxiety-like behavior has been extensively studied. Knockout mouse models of different 5-HT receptor types, e.g. the 5-HT_{1A} and the 5-HT_{2C} receptor, exhibited altered anxiety behavior compared to control animals (Heisler et al., 1998; Parks et al., 1998; Ramboz et al., 1998; Heisler et al., 2007). Knockout of the 5-HT_{1A} receptor was shown to elevate anxiety-like behavior and knockout of the 5-HT_{2C} receptor was demonstrated to have anxiolytic effects.

Due to changes concerning serotonin receptor densities, the anxiety-like behavior of *Pitx3 aphakia* mice is an interesting aspect for future research and could be verified by various tests in mice, e.g. elevated zero maze, open-field or novel object (Heisler et al., 2007).

In the present study, alterations regarding the serotonergic system only occurred in *Pitx3 aphakia* mice but not in *Parkin* or *DJ-1* knockout mice. Thus, it is tempting to speculate that deficits of the serotonergic system might be correlated with the loss of dopaminergic neurons in the substantia nigra, since this is the major difference between *Pitx3 aphakia* mice and the mouse models of hereditary Parkinsonism. Recently, it was shown that partial lesions of the striatal dopaminergic innervation can induce "depressive-like" behavior in rats, evaluated by a forced swimming test (Kuter et al., 2011). The forced swimming test would be a suitable test to evaluate the "depressive-like" behavior in PD mouse models. We hypothesize that the behavior of *Pitx3 aphakia* mice should be impaired, whereas the performance of *Parkin* and *DJ-1* knockout mice should likely be comparable to those of controls. Furthermore, it would be interesting to evaluate, if there are differences concerning the frequency of depression as a comorbidity of either sporadic or hereditary Parkinsonism in humans. With regard to our results, it could be assumed that the percentage of PD patients suffering additionally from depression is higher in the sporadic group than in the hereditary one.

6. Dopamine receptors

The neurotransmitter dopamine is synthesized in the ventral tegmental area and the substantia nigra, both located in the mesencephalon. There are five different dopamine receptors, D_1 to D_5, that are all coupled to a G-protein and influence the intracellular levels of cyclic adenosine monophosphate (cAMP), acting as an important and ubiquitous second messenger. Dopamine plays a crucial role in cognitive processes, motor functions and reward-related mechanisms (Egerton et al., 2009). Dysfunctions of the dopaminergic systems are associated with neurological disorders like Parkinson's disease (Ehringer and Hornykiewicz, 1960), attention-deficit hyperactivity disorder (Biederman, 2005; Wu et al.,

2012) or schizophrenia (Breier et al., 1997; Abi-Dargham et al., 1998). In the case of Parkinson's disease, degenerative processes affecting the dopaminergic neurons of the substantia nigra cause deficiencies of striatal dopamine concentration and the dopaminergic system in general (Fahn, 2003).

Dopamine **D_2** receptor densities exhibited a significant increase in the striatum of *Pitx3 aphakia* mice (cf. Results: fig. 31). This alteration may reflect a compensatory up-regulation of D_2 receptors induced by the described loss of nigrostriatal dopaminergic innervation. Lower concentrations of dopamine in the striatum may at least in part be compensated through elevated receptor densities. Dopamine receptors were extensively studied in PD patients and similar to our results for *Pitx3 aphakia* mice, the literature generally describes an increase of D_2 receptor density in the striatum of PD patients, while the density of D_1 receptors is not or only slightly altered (Rinne et al., 1990a; Rinne et al., 1990b; Piggott et al., 1999; Hurley and Jenner, 2006). The fact that no significant changes concerning dopamine receptor densities were found in *Parkin* and *DJ-1* knockout mice, can be explained by the absence of neurodegenerative processes in these PD mouse models.

7. Adenosine receptors

The adenosine compounds adenosine triphosphate and adenosine diphosphate play a crucial role in the cellular energy metabolism, whereas cyclic adenosine monophosphate is a second messenger and involved in signal transduction processes. There are four types of adenosine receptors, i.e. A_1, A_{2A}, A_{2B} and A_3 receptors. Adenosine was shown to regulate sleep (Porkka-Heiskanen et al., 1997; Porkka-Heiskanen, 1999), cerebral blood flow (Winn et al., 1981; Hylland et al., 1994) and locomotor behavior (El Yacoubi et al., 2000). Furthermore, adenosine exhibits neuroprotective effects in hypoxia (Gribkoff et al., 1990) and ischemia (Deckert and Gleiter, 1994; Latini et al., 1999) and anticonvulsant effects in seizure models, an observation which is especially interesting with regard to epilepsy (Dragunow, 1988).

Adenosine **A_{2A}** receptor densities were slightly but significantly increased in the striatum of *DJ-1* knockout mice. These results are in line with a study of Varani et al. which demonstrated that A_{2A} receptors are overexpressed in the putamen of PD patients and these changes correlate with motor symptoms (Varani et al., 2010). Thus, upregulation of A_{2A} receptor densities in the brains of PD mouse models as well as PD patients might in part explain the beneficial effects concerning motor symptoms and dyskinesia that were reported for adenosine A_{2A} receptor agonists (Cieslak et al., 2008; Hickey and Stacy, 2012).

8. Striatum associated alterations of neurotransmitter receptor densities

The striatum is strongly innervated by neurons of the substantia nigra and the function of the nigrostriatal pathway in mice is experimentally accessible via numerous behavioral tests. For example, the challenging beam and the pole test provide sensitive measurements of deficits of the nigrostriatal system (Ogawa et al., 1985; Drucker-Colin and Garcia-Hernandez, 1991; Matsuura et al., 1997). All three PD mouse models that were investigated in this study exhibited deficits with regard to behavioral tasks sensitive to nigrostriatal dysfunction (Goldberg et al., 2003; Goldberg et al., 2005; Hwang et al., 2005).

The densities of numerous neurotransmitter receptors were significantly changed in the striatum of the investigated mouse models (cf. fig. 34 and 42). *Parkin* knockout mice exhibited higher $GABA_B$, M_1, M_2 and α_2 receptor densities in the striatum compared to control animals, whereas *DJ-1* knockout mice showed elevated AMPA, $GABA_B$ and M_1 receptor densities. In the case of *Pitx3 aphakia* mice, kainate, α_1 and D_2 receptor as well as BZ binding site densities were elevated, while M_2, nicotinic and 5-HT_2 receptor densities were decreased in the striatum. Thus, the analyzed PD mouse models exhibited a complex pattern of changes concerning neurotransmitter receptor densities in the striatum, which is likely to be associated with nigrostriatal deficits described for these mice. However, further investigation in this field will be necessary to unravel these correlations. Electrophysiological experiments, investigations of the levels of different neurotransmitters or behavioral testing

after application of agonists and antagonists of the respective receptor types would be interesting topics to address in the future.

The differential receptor density changes in the striatum of PD mouse models, particularly those found in *Pitx3 aphakia* mice, underline the importance of comprehensive methodological approaches for investigations on neurotransmitter receptors. Although PD primarily affects dopamine producing neurons and thereby the dopaminergic system, six of seven neurotransmitter systems tested were affected in the striatum of *Pitx3 aphakia* mice with regard to receptor densities (i.e. the glutamatergic, GABAergic, acetylcholinergic, adrenergic, serotonergic and dopaminergic system). However, the changes in the dopaminergic system were moderate including a slight but significant increase of D_2 receptor densities. On the contrary, nicotinic acetylcholine and 5-HT_2 receptor densities for example were massively decreased by nearly 50 %. This example illustrates how different neurotransmitter systems strongly interact and changes of a single receptor system are most often accompanied by changes in other systems. Thus, comprehensive investigations of neurotransmitter receptors present a holistic image that could enhance the understanding of the diseases' etiology.

9. Olfaction in Parkinson's disease

One of the major difficulties in the treatment of PD is the fact that at the time of the first clinical diagnosis, many of the dopaminergic neurons are already lost. Since neuroprotective therapies should start, however, as early as possible, a diagnosis before the onset of clinically relevant symptoms would improve the chance of neuroprotective treatment.
Olfactory dysfunction is a very frequent non-motor symptom of Parkinson's disease (Doty et al., 1988; Hawkes et al., 1997). Impaired olfaction was shown to appear at an early disease stage and can precede motor symptoms of PD by four years (Ross et al., 2008). An increased risk to develop Parkinson's disease for people with idiopathic olfactory dysfunction was reported (Ponsen et al., 2004). Olfactory performance is clinically accessible via numerous well-established test conditions, e.g. the University of Pennsylvania Smell Identification Test

(UPSIT) (Doty et al., 1984) that was used in the studies of Doty et al. (1988) and Hawkes et al. (1997). Such tests are comparably fast, cheap and simple, and would be a promising tool for PD screening even of large group sizes.

Odorant molecules are recognized in the olfactory bulb and the information is further analyzed in the piriform cortex, the olfactory tubercle and the amygdala. In the present study, the densities of various neurotransmitter receptors were found to be changed in the olfactory bulb and the piriform cortex of PD mouse models, as summarized in figure 34 and 42. Such alterations may underly the olfactory dysfunction in PD patients. To our knowledge, this issue has not been studied in detail so far. Therefore, neurotransmitter receptors in the olfactory system of PD patients would be an interesting topic for future research.

The pattern of neurotransmitter density changes in the olfactory bulb and the piriform cortex was quite similar between *Parkin* and *DJ-1* knockout mice. The densities of kainate, $GABA_B$, M_1, M_2 and α_2 receptors were increased compared to controls in the olfactory bulb of these mice. Additionally, kainate, NMDA, $GABA_B$, M_2, nicotinic and α_2 receptor densities were increased in the piriform cortex. On the contrary, *Pitx3 aphakia* mice exhibited decreased kainate and 5-HT_{1A} and increased α_1 receptor densities, respectively, in the olfactory bulb, whereas $GABA_A$, $GABA_B$, M_3 and α_1 receptor as well as BZ binding site densities were increased in the piriform cortex. Thus, neurotransmitter receptor densities were differentially changed in the investigated knockout mouse models of hereditary Parkinsonism compared to *Pitx3 aphakia* mice. Interestingly, PD patients with mutations in the *Parkin* or the *DJ-1* gene were demonstrated to have smell identification scores comparable to healthy individuals, or at least higher than PD patients without the respective mutations (Khan et al., 2004; Verbaan et al., 2008; Kertelge et al., 2010). It is tempting to speculate that our results suggest a compensating mechanism maintaining olfactory perception in mutations associated to hereditary Parkinsonism. However, to our knowledge, the smell discrimination abilities of *Parkin* and *DJ-1* knockout mice have not been experimentally analyzed so far and, thus, would be an interesting topic of further investigation.

Summary

Parkinson's disease (PD) is the second most common neurodegenerative disorder. Despite ongoing efforts, the knowledge of the etiology and underlying mechanisms resulting in the neurodegenerative processes (e.g., loss of dopaminergic neurons) remains incomplete. Since therapeutic intervention is still limited to symptomatic relief and mainly focused on the dopamine system, the understanding of the role of other, non-dopaminergic systems during pathogenesis of PD has to be improved for identifying new targets for treatment. Neurotransmitter receptors are major targets for pharmaceutical interventions in numerous neurological and psychiatric disorders, since distinct changes of receptors are often found in such diseases. In case of PD, the dominant role of changes in dopaminergic neurotransmission is well known. The possible involvement of other transmitter systems and their receptors, however, is not well understood.

Therefore, the aim of this study was the analysis of the density and distribution of neurotransmitter receptors for glutamate, GABA, acetylcholine, adrenaline, serotonin, dopamine and adenosine in the brains of three well established mouse models of PD.

The *Pitx3 aphakia* mouse served as a model exhibiting crucial hallmarks of PD on the neuropathological, symptomatic and pharmacological level. Additionally, *Parkin* and *DJ-1* knockout mice were analyzed as models for hereditary parkinsonism by exhibiting PD associated gene mutations. Quantitative receptor autoradiography was used to comprehensively investigate the density and distribution of glutamate, GABA, acetylcholine, adrenaline, serotonin, dopamine and adenosine receptors in eleven different brain regions (i.e., the olfactory bulb, the motor, somatosensory, piriform and visual cortices, the hippocampal regions CA1, CA2/3 and dentate gyrus, the striatum, the substantia nigra and the cerebellum).

Differential quantitative changes of neurotransmitter receptor densities were demonstrated for the three different animal models of PD compared to controls. In general, receptor density changes were similar between *Parkin* and *DJ-1* knockout mice, indicating pathologic mechanisms occurring likewise in both models. $GABA_B$ receptor densities were increased in several regions of all investigated PD models (i.e., the piriform cortex, the dentate gyrus, the visual cortex and the substantia nigra). Thus, the increase in $GABA_B$ receptors seems to be a common reaction during pathogenesis of PD. The densities of nicotinic acetylcholine, serotonergic 5-HT_{1A} and 5-HT_2 receptors were demonstrated to be considerably reduced in *Pitx3 aphakia* mouse brains (i.e., the nicotinic acetylcholine receptor in the striatum, CA2/3 and the dentate gyrus; the serotonergic 5-HT_{1A} receptor in the olfactory bulb, CA1 and the dentate gyrus; the 5-HT_2 receptor in the striatum). A complex pattern of receptor changes in the striatum of *Pitx3 aphakia*, *Parkin* and *DJ-1* knockout mice, respectively, correlates with the behavioral findings in these mice, and indicates differential interactions and dependencies between the different receptor systems in PD.

Taken together, the present findings of neurotransmitter receptor density changes in *Pitx3 aphakia*, *Parkin* and *DJ-1* knockout mice, respectively, provide novel data on the up- and down-regulation of GABA, acetylcholine, and 5-HT receptor expression in animal models of PD, and thereby highlight the often neglected impact of non-dopaminergic systems in the molecular pathology of Parkinson's disease.

Neurotransmitterrezeptoren in drei Nagetiermodellen der Parkinson-Krankheit – Eine quantitative Multirezeptorstudie

Zusammenfassung

Die Parkinson-Krankheit ist die zweithäufigste neurodegenerative Erkrankung des Menschen. Trotz intensiven Bestrebens, bleibt das Wissen über die Ätiologie und die zugrundeliegenden Mechanismen, welche zu den neurodegenerativen Prozessen führen (z.B. Verlust dopaminerger Neurone) bis heute unvollständig. Da die Behandlung immer noch auf symptomatische Linderung beschränkt ist und hauptsächlich auf das dopaminerge System fokussiert, muss das Verständnis der Rolle anderer, nicht-dopaminerger Systeme während der Pathogenese der Parkinson-Krankheit verbessert werden, um neue Ansatzpunkte für die Behandlung identifizieren zu können. Neurotransmitterrezeptoren sind wichtige Zielstrukturen pharmakologischer Behandlung zahlreicher neurologischer und psychiatrischer Erkrankungen, da spezifische Rezeptorveränderungen häufig mit diesen Krankheiten korrelieren. Im Fall der Parkinson-Krankheit ist die dominierende Rolle der Veränderungen der dopaminergen Neurotransmission wohlbekannt. Die mögliche Beteiligung anderer Transmittersysteme und ihrer Rezeptoren ist jedoch bisher nicht im Detail verstanden.

Ziel dieser Studie war daher die Analyse der Dichte und Verteilung von Neurotransmitterrezeptoren für Glutamat, GABA, Acetylcholin, Adrenalin, Serotonin, Dopamin und Adenosin in den Gehirnen von drei etablierten Mausmodellen der Parkinson-Krankheit.

Die *Pitx3 aphakia* Maus diente dabei als Modell, welches die entscheidenden Merkmale der Parkinson-Krankheit auf neuropathologischer, symptomatischer und pharmakologischer Ebene zeigt. Zusätzlich wurden *Parkin* und *DJ-1* Knockout Mäuse, die Parkinson-assoziierte Genmutationen aufweisen, als Modelle für erbliche Formen der Parkinson-Krankheit analysiert. Die quantitative Rezeptorautoradiographie wurde als methodisches Werkzeug für eine umfassende Untersuchung der Dichte und Verteilung von Glutamat-, GABA-, Acetylcholin-, Adrenalin-, Serotonin-, Dopamin- und Adenosin-Rezeptoren in elf verschiedenen Gehirnregionen (dem Bulbus olfactorius, dem motorischen, somatosensorischen, piriformen und visuellen Cortex, den hippocampalen Regionen CA1, CA2/3 und Gyrus dentatus, dem Striatum, der Substantia nigra und dem Cerebellum) genutzt.

In den drei unterschiedlichen Tiermodellen der Parkinson-Krankheit wurden verglichen mit den entsprechenden Kontrollen differenzierte, quantitative Veränderungen der Neurotransmitterrezeptordichten nachgewiesen. Dabei waren insgesamt die Rezeptordichteveränderungen bei *Parkin* und *DJ-1* Knockout Mäusen ähnlich, was darauf hindeutet, dass es pathologische Mechanismen gibt, die gleichermaßen in beiden Modellen auftreten. Die $GABA_B$-Rezeptordichten waren in mehreren Regionen aller untersuchten Modelle erhöht (dem piriformen Cortex, dem Gyrus dentatus, dem visuellen Cortex und der Substantia nigra). Daher kann angenommen werden, dass die Erhöhung der $GABA_B$-Rezeptordichte eine grundsätzliche Reaktion während der Pathogenese der Parkinson-Krankheit darstellt. Es wurde gezeigt, dass die Dichten der nikotinischen Acetylcholinrezeptoren, sowie der serotonergen 5-HT_{1A}- und 5-HT_2- Rezeptoren in den Gehirnen von *Pitx3 aphakia* Mäusen beträchtlich verringert sind (der nikotinische Acetylcholinrezeptor im Striatum, CA2/3 und dem Gyrus dentatus; der serotonerge 5-HT_{1A}-Rezeptor im Bulbus olfactorius, CA1 und dem Gyrus dentatus; der serotonerge 5-HT_2-Rezeptor im Striatum). Das komplexe Bild der Rezeptorveränderungen im Striatum von *Pitx3 aphakia, Parkin* und *DJ-1* Knockout Mäusen entspricht den Verhaltensbefunden dieser Mäuse und deutet auf differenzierte Interaktionen und Abhängigkeiten zwischen den unterschiedlichen Rezeptorsystemen im Rahmen der Parkinsonschen Erkrankung hin.

Zusammengefasst liefern die vorliegenden Ergebnisse zu den Dichteveränderungen von Neurotransmitterrezeptoren in *Pitx3 aphakia, Parkin* und *DJ-1* Knockout Mäusen neue Informationen über Veränderungen der GABA-, Acetylcholin- und 5-HT-Rezeptorexpression in Tiermodellen der Parkinson-Krankheit und betonen dadurch den häufig vernachlässigten Einfluss der nicht-dopaminergen Systeme im Rahmen der molekularen Pathologie der Parkinson-Krankheit.

References

Aarsland D, Bronnick K, Williams-Gray C, Weintraub D, Marder K, Kulisevsky J, Burn D, Barone P, Pagonabarraga J, Allcock L, Santangelo G, Foltynie T, Janvin C, Larsen JP, Barker RA, Emre M (2010) Mild cognitive impairment in Parkinson disease: a multicenter pooled analysis. Neurology 75:1062-1069.

Abi-Dargham A, Gil R, Krystal J, Baldwin RM, Seibyl JP, Bowers M, van Dyck CH, Charney DS, Innis RB, Laruelle M (1998) Increased striatal dopamine transmission in schizophrenia: confirmation in a second cohort. The American Journal of Psychiatry 155:761-767.

Abin-Carriquiry JA, Costa G, Urbanavicius J, Cassels BK, Rebolledo-Fuentes M, Wonnacott S, Dajas F (2008) In vivo modulation of dopaminergic nigrostriatal pathways by cytisine derivatives: implications for Parkinson's Disease. European Journal of Pharmacology 589:80-84.

Abou-Sleiman PM, Muqit MM, Wood NW (2006) Expanding insights of mitochondrial dysfunction in Parkinson's disease. Nature Reviews Neuroscience 7:207-219.

Abou-Sleiman PM, Healy DG, Quinn N, Lees AJ, Wood NW (2003) The role of pathogenic DJ-1 mutations in Parkinson's disease. Annals of Neurology 54:283-286.

Akaike A, Katsuki H, Kume T, Maeda T (1999) Reactive oxygen species in NMDA receptor-mediated glutamate neurotoxicity. Parkinsonism & Related Disorders 5:203-207.

Allam MF, Campbell MJ, Hofman A, Del Castillo AS, Fernandez-Crehuet Navajas R (2004) Smoking and Parkinson's disease: systematic review of prospective studies. Movement Disorders 19:614-621.

Ardayfio P, Moon J, Leung KK, Youn-Hwang D, Kim KS (2008) Impaired learning and memory in Pitx3 deficient aphakia mice: a genetic model for striatum-dependent cognitive symptoms in Parkinson's disease. Neurobiology of Disease 31:406-412.

Ballanger B, Klinger H, Eche J, Lerond J, Vallet AE, Le Bars D, Tremblay L, Sgambato-Faure V, Broussolle E, Thobois S (2012) Role of serotonergic 1A receptor dysfunction in depression associated with Parkinson's disease. Movement Disorders 27:84-89.

Barone P, Poewe W, Albrecht S, Debieuvre C, Massey D, Rascol O, Tolosa E, Weintraub D (2010) Pramipexole for the treatment of depressive symptoms in patients with Parkinson's disease: a randomised, double-blind, placebo-controlled trial. Lancet Neurology 9:573-580.

Bauer RB, Stevens C, Reveno WS, Rosenbaum H (1982) L-dopa treatment of Parkinson's disease: a ten-year follow up study. Journal of the American Geriatrics Society 30:322-325.

Beal MF (1998) Excitotoxicity and nitric oxide in Parkinson's disease pathogenesis. Annals of Neurology 44:S110-114.

Benarroch EE (2009) The locus ceruleus norepinephrine system: functional organization and potential clinical significance. Neurology 73:1699-1704.

Bertrand E, Lechowicz W, Szpak GM, Dymecki J (1997) Qualitative and quantitative analysis of locus coeruleus neurons in Parkinson's disease. Folia Neuropathologica / Association of Polish Neuropathologists and Medical Research Centre, Polish Academy of Sciences 35:80-86.

Biederman J (2005) Attention-deficit/hyperactivity disorder: a selective overview. Biological Psychiatry 57:1215-1220.

Bliss TVP, Collingridge GL (1993) A synaptic model of memory: long-term potentiation in the hippocampus. Nature 361:31-39.

Bondareff W, Mountjoy CQ, Roth M (1982) Loss of neurons of origin of the adrenergic projection to cerebral cortex (nucleus locus ceruleus) in senile dementia. Neurology 32:164-168.

Bonifati V, Rizzu P, van Baren MJ, Schaap O, Breedveld GJ, Krieger E, Dekker MC, Squitieri F, Ibanez P, Joosse M, van Dongen JW, Vanacore N, van Swieten JC, Brice A, Meco G, van Duijn CM, Oostra BA, Heutink P (2003) Mutations in the DJ-1 gene associated with autosomal recessive early-onset parkinsonism. Science 299:256-259.

Breier A, Su TP, Saunders R, Carson RE, Kolachana BS, de Bartolomeis A, Weinberger DR, Weisenfeld Medical N, Malhotra AK, Eckelman WC, Pickar D (1997) Schizophrenia is associated with

elevated amphetamine-induced synaptic dopamine concentrations: evidence from a novel positron emission tomography method. Proceedings of the National Academy of Sciences of the United States of America 94:2569-2574.

Brown TH, Chapman PF, Kairiss EW, Keenan CL (1988) Long-term synaptic potentiation. Science 242:724-728.

Burghaus L, Schutz U, Krempel U, Lindstrom J, Schroder H (2003) Loss of nicotinic acetylcholine receptor subunits alpha4 and alpha7 in the cerebral cortex of Parkinson patients. Parkinsonism & Related Disorders 9:243-246.

Burghaus L, Schutz U, Krempel U, de Vos RA, Jansen Steur EN, Wevers A, Lindstrom J, Schroder H (2000) Quantitative assessment of nicotinic acetylcholine receptor proteins in the cerebral cortex of Alzheimer patients. Brain Research. Molecular Brain Research 76:385-388.

Cash R, Raisman R, Ploska A, Agid Y (1985) High and low affinity [3H]imipramine binding sites in control and parkinsonian brains. European Journal of Pharmacology 117:71-80.

Chandran JS, Lin X, Zapata A, Hoke A, Shimoji M, Moore SO, Galloway MP, Laird FM, Wong PC, Price DL, Bailey KR, Crawley JN, Shippenberg T, Cai H (2008) Progressive behavioral deficits in DJ-1-deficient mice are associated with normal nigrostriatal function. Neurobiology of Disease 29:505-514.

Chapouthier G, Venault P (2002) GABA-A receptor complex and memory processes. Current Topics in Medicinal Chemistry 2:841-851.

Chen L, Cagniard B, Mathews T, Jones S, Koh HC, Ding Y, Carvey PM, Ling Z, Kang UJ, Zhuang X (2005) Age-dependent motor deficits and dopaminergic dysfunction in DJ-1 null mice. The Journal of Biological Chemistry 280:21418-21426.

Ciechanover A, Brundin P (2003) The ubiquitin proteasome system in neurodegenerative diseases: sometimes the chicken, sometimes the egg. Neuron 40:427-446.

Cieslak M, Komoszynski M, Wojtczak A (2008) Adenosine A(2A) receptors in Parkinson's disease treatment. Purinergic Signalling 4:305-312.

Clark CR, Geffen GM, Geffen LB (1987) Catecholamines and attention. I: Animal and clinical studies. Neuroscience and Biobehavioral Reviews 11:341-352.

Committee GPsDSS (2002) Factors impacting on quality of life in Parkinson's disease: results from an international survey. Movement Disorders 17:60-67.

Costa G, Abin-Carriquiry JA, Dajas F (2001) Nicotine prevents striatal dopamine loss produced by 6-hydroxydopamine lesion in the substantia nigra. Brain Research 888:336-342.

Cowen M, Chen F, Jarrott B, Lawrence AJ (1998) Effects of acute ethanol on GABA release and GABA(A) receptor density in the rat mesolimbic system. Pharmacology, Biochemistry, and Behavior 59:51-57.

Cremer C (2011) Neurotransmitter receptors in animal models of neurodegeneration: anatomy, pharmacology and molecular properties. Südwestdeutscher Verlag für Hochschulschriften: Heinrich-Heine-University Düsseldorf.

Cremer CM, Cremer M, Escobar JL, Speckmann EJ, Zilles K (2009) Fast, quantitative in situ hybridization of rare mRNAs using 14C-standards and phosphorus imaging. Journal of Neuroscience Methods 185:56-61.

Cremer CM, Bidmon HJ, Gorg B, Palomero-Gallagher N, Escobar JL, Speckmann EJ, Zilles K (2010) Inhibition of glutamate/glutamine cycle in vivo results in decreased benzodiazepine binding and differentially regulated GABAergic subunit expression in the rat brain. Epilepsia 51:1446-1455.

Cross AJ (1990) Serotonin in Alzheimer-type dementia and other dementing illnesses. Annals of the New York Academy of Sciences 600:405-415.

Cummings JL, Masterman DL (1999) Depression in patients with Parkinson's disease. International Journal of Geriatric Psychiatry 14:711-718.

de Jong PJ, Lakke JP, Teelken AW (1984) CSF GABA levels in Parkinson's disease. Advances in Neurology 40:427-430.

Deckert J, Gleiter CH (1994) Adenosine--an endogenous neuroprotective metabolite and neuromodulator. Journal of Neural Transmission. Supplementum 43:23-31.

Devauges V, Sara SJ (1990) Activation of the noradrenergic system facilitates an attentional shift in the rat. Behavioural Brain Research 39:19-28.

Ding Y, Restrepo J, Won L, Hwang DY, Kim KS, Kang UJ (2007) Chronic 3,4-dihydroxyphenylalanine treatment induces dyskinesia in aphakia mice, a novel genetic model of Parkinson's disease. Neurobiology of Disease 27:11-23.

Doty RL, Shaman P, Dann M (1984) Development of the University of Pennsylvania Smell Identification Test: a standardized microencapsulated test of olfactory function. Physiology & Behavior 32:489-502.

Doty RL, Deems DA, Stellar S (1988) Olfactory dysfunction in parkinsonism: a general deficit unrelated to neurologic signs, disease stage, or disease duration. Neurology 38:1237-1244.

Dragunow M (1988) Purinergic mechanisms in epilepsy. Progress in Neurobiology 31:85-108.

Drucker-Colin R, Garcia-Hernandez F (1991) A new motor test sensitive to aging and dopaminergic function. Journal of Neuroscience Methods 39:153-161.

Egerton A, Mehta MA, Montgomery AJ, Lappin JM, Howes OD, Reeves SJ, Cunningham VJ, Grasby PM (2009) The dopaminergic basis of human behaviors: A review of molecular imaging studies. Neuroscience and Biobehavioral Reviews 33:1109-1132.

Ehringer H, Hornykiewicz O (1960) Verteilung von Noradrenalin und Dopamin (3-Hydroxytyramin) im Gehirn des Menschen und ihr Verhalten bei Erkrankungen des extrapyramidalen Systems. Klinische Wochenschrift 38:1236-1239.

El Yacoubi M, Ledent C, Menard JF, Parmentier M, Costentin J, Vaugeois JM (2000) The stimulant effects of caffeine on locomotor behaviour in mice are mediated through its blockade of adenosine A(2A) receptors. British Journal of Pharmacology 129:1465-1473.

Fahn S (2003) Description of Parkinson's disease as a clinical syndrome. Annals of the New York Academy of Sciences 991:1-14.

Firestein S, Menini A (1999) The smell of adrenaline. Nature Neuroscience 2:106-108.

Fu CH, Reed LJ, Meyer JH, Kennedy S, Houle S, Eisfeld BS, Brown GM (2001) Noradrenergic dysfunction in the prefrontal cortex in depression: an [15O] H2O PET study of the neuromodulatory effects of clonidine. Biological Psychiatry 49:317-325.

Fuchs J, Mueller JC, Lichtner P, Schulte C, Munz M, Berg D, Wullner U, Illig T, Sharma M, Gasser T (2009) The transcription factor PITX3 is associated with sporadic Parkinson's disease. Neurobiology of Aging 30:731-738.

Gerlach M, Gsell W, Kornhuber J, Jellinger K, Krieger V, Pantucek F, Vock R, Riederer P (1996) A post mortem study on neurochemical markers of dopaminergic, GABA-ergic and glutamatergic neurons in basal ganglia-thalamocortical circuits in Parkinson syndrome. Brain Research 741:142-152.

Giasson BI, Lee VM (2003) Are ubiquitination pathways central to Parkinson's disease? Cell 114:1-8.

Glickman MH, Ciechanover A (2002) The ubiquitin-proteasome proteolytic pathway: destruction for the sake of construction. Physiological Reviews 82:373-428.

Gold PE, van Buskirk R (1978) Posttraining brain norepinephrine concentrations: correlation with retention performance of avoidance training and with peripheral epinephrine modulation of memory processing. Behavioral Biology 23:509-520.

Goldberg MS, Pisani A, Haburcak M, Vortherms TA, Kitada T, Costa C, Tong Y, Martella G, Tscherter A, Martins A, Bernardi G, Roth BL, Pothos EN, Calabresi P, Shen J (2005) Nigrostriatal dopaminergic deficits and hypokinesia caused by inactivation of the familial Parkinsonism-linked gene DJ-1. Neuron 45:489-496.

Goldberg MS, Fleming SM, Palacino JJ, Cepeda C, Lam HA, Bhatnagar A, Meloni EG, Wu N, Ackerson LC, Klapstein GJ, Gajendiran M, Roth BL, Chesselet MF, Maidment NT, Levine MS, Shen J (2003) Parkin-deficient mice exhibit nigrostriatal deficits but not loss of dopaminergic neurons. The Journal of Biological Chemistry 278:43628-43635.

Graus YM, De Baets MH (1993) Myasthenia gravis: an autoimmune response against the acetylcholine receptor. Immunologic Research 12:78-100.

Graw J (1999) Cataract mutations and lens development. Progress in Retinal and Eye Research 18:235-267.

Greenfield JG, Bosanquet FD (1953) The brain-stem lesions in Parkinsonism. Journal of Neurology, Neurosurgery, and Psychiatry 16:213-226.

Gribkoff VK, Bauman LA, VanderMaelen CP (1990) The adenosine antagonist 8-cyclopentyltheophylline reduces the depression of hippocampal neuronal responses during hypoxia. Brain Research 512:353-357.

Grimm C, Chatterjee B, Favor J, Immervoll T, Loster J, Klopp N, Sandulache R, Graw J (1998) Aphakia (ak), a mouse mutation affecting early eye development: fine mapping, consideration of candidate genes and altered Pax6 and Six3 gene expression pattern. Developmental Genetics 23:299-316.

Gurevich EV, Joyce JN (1997) Alterations in the cortical serotonergic system in schizophrenia: a postmortem study. Biological Psychiatry 42:529-545.

Hague S, Rogaeva E, Hernandez D, Gulick C, Singleton A, Hanson M, Johnson J, Weiser R, Gallardo M, Ravina B, Gwinn-Hardy K, Crawley A, St George-Hyslop PH, Lang AE, Heutink P, Bonifati V, Hardy J, Singleton A (2003) Early-onset Parkinson's disease caused by a compound heterozygous DJ-1 mutation. Annals of Neurology 54:271-274.

Hall RA (2011) Autonomic modulation of olfactory signaling. Science Signaling 4:pe1.

Hallett PJ, Standaert DG (2004) Rationale for and use of NMDA receptor antagonists in Parkinson's disease. Pharmacology & Therapeutics 102:155-174.

Hamel E (2007) Serotonin and migraine: biology and clinical implications. Cephalalgia 27:1293-1300.

Hanley JG, Henley JM (2005) PICK1 is a calcium-sensor for NMDA-induced AMPA receptor trafficking. The EMBO Journal 24:3266-3278.

Hanson JE, Orr AL, Madison DV (2010) Altered hippocampal synaptic physiology in aged parkin-deficient mice. Neuromolecular Medicine 12:270-276.

Hasselmo ME (2006) The role of acetylcholine in learning and memory. Current Opinion in Neurobiology 16:710-715.

Haubenberger D, Reinthaler E, Mueller JC, Pirker W, Katzenschlager R, Froehlich R, Bruecke T, Daniel G, Auff E, Zimprich A (2011) Association of transcription factor polymorphisms PITX3 and EN1 with Parkinson's disease. Neurobiology of Aging 32:302-307.

Hawkes CH, Shephard BC, Daniel SE (1997) Olfactory dysfunction in Parkinson's disease. Journal of Neurology, Neurosurgery, and Psychiatry 62:436-446.

Hayashi S, Wakabayashi K, Ishikawa A, Nagai H, Saito M, Maruyama M, Takahashi T, Ozawa T, Tsuji S, Takahashi H (2000) An autopsy case of autosomal-recessive juvenile parkinsonism with a homozygous exon 4 deletion in the parkin gene. Movement Disorders 15:884-888.

Heisler LK, Zhou L, Bajwa P, Hsu J, Tecott LH (2007) Serotonin 5-HT(2C) receptors regulate anxiety-like behavior. Genes, Brain, and Behavior 6:491-496.

Heisler LK, Chu HM, Brennan TJ, Danao JA, Bajwa P, Parsons LH, Tecott LH (1998) Elevated anxiety and antidepressant-like responses in serotonin 5-HT1A receptor mutant mice. Proceedings of the National Academy of Sciences of the United States of America 95:15049-15054.

Henchcliffe C, Beal MF (2008) Mitochondrial biology and oxidative stress in Parkinson disease pathogenesis. Nature Clinical Practice Neurology 4:600-609.

Hickey P, Stacy M (2012) Adenosine A2A antagonists in Parkinson's disease: what's next? Current Neurology and Neuroscience Reports 12:376-385.

Huang LZ, Parameswaran N, Bordia T, Michael McIntosh J, Quik M (2009) Nicotine is neuroprotective when administered before but not after nigrostriatal damage in rats and monkeys. Journal of Neurochemistry 109:826-837.

Hurley MJ, Jenner P (2006) What has been learnt from study of dopamine receptors in Parkinson's disease? Pharmacology & Therapeutics 111:715-728.

Hwang DY, Ardayfio P, Kang UJ, Semina EV, Kim KS (2003) Selective loss of dopaminergic neurons in the substantia nigra of Pitx3-deficient aphakia mice. Brain Research. Molecular Brain Research 114:123-131.

Hwang DY, Fleming SM, Ardayfio P, Moran-Gates T, Kim H, Tarazi FI, Chesselet MF, Kim KS (2005) 3,4-dihydroxyphenylalanine reverses the motor deficits in Pitx3-deficient aphakia mice: behavioral characterization of a novel genetic model of Parkinson's disease. The Journal of Neuroscience 25:2132-2137.

Hylland P, Nilsson GE, Lutz PL (1994) Time course of anoxia-induced increase in cerebral blood flow rate in turtles: evidence for a role of adenosine. Journal of Cerebral Blood Flow & Metabolism 14:877-881.

Imai Y, Soda M, Takahashi R (2000) Parkin suppresses unfolded protein stress-induced cell death through its E3 ubiquitin-protein ligase activity. The Journal of Biological Chemistry 275:35661-35664.

Joch M, Ase AR, Chen CX, MacDonald PA, Kontogiannea M, Corera AT, Brice A, Seguela P, Fon EA (2007) Parkin-mediated monoubiquitination of the PDZ protein PICK1 regulates the activity of acid-sensing ion channels. Molecular Biology of the Cell 18:3105-3118.

Jones MV, Jonas P, Sahara Y, Westbrook GL (2001) Microscopic kinetics and energetics distinguish GABA(A) receptor agonists from antagonists. Biophysical Journal 81:2660-2670.

Kas A, Bottlaender M, Gallezot JD, Vidailhet M, Villafane G, Gregoire MC, Coulon C, Valette H, Dolle F, Ribeiro M-J, Hantraye P, Remy P (2009) Decrease of nicotinic receptors in the nigrostriatal system in Parkinson's disease. Journal of Cerebral Blood Flow & Metabolism 29:1601-1608.

Kerenyi L, Ricaurte GA, Schretlen DJ, McCann U, Varga J, Mathews WB, Ravert HT, Dannals RF, Hilton J, Wong DF, Szabo Z (2003) Positron emission tomography of striatal serotonin transporters in Parkinson disease. Archives of Neurology 60:1223-1229.

Kertelge L, Bruggemann N, Schmidt A, Tadic V, Wisse C, Dankert S, Drude L, van der Vegt J, Siebner H, Pawlack H, Pramstaller PP, Behrens MI, Ramirez A, Reichel D, Buhmann C, Hagenah J, Klein C, Lohmann K, Kasten M (2010) Impaired sense of smell and color discrimination in monogenic and idiopathic Parkinson's disease. Movement Disorders 25:2665-2669.

Khan NL, Katzenschlager R, Watt H, Bhatia KP, Wood NW, Quinn N, Lees AJ (2004) Olfaction differentiates parkin disease from early-onset parkinsonism and Parkinson disease. Neurology 62:1224-1226.

Kitada T, Asakawa S, Matsumine H, Hattori N, Shimura H, Minoshima S, Shimizu N, Mizuno Y (2000) Progress in the clinical and molecular genetics of familial parkinsonism. Neurogenetics 2:207-218.

Kitada T, Asakawa S, Hattori N, Matsumine H, Yamamura Y, Minoshima S, Yokochi M, Mizuno Y, Shimizu N (1998) Mutations in the parkin gene cause autosomal recessive juvenile parkinsonism. Nature 392:605-608.

Kitada T, Pisani A, Karouani M, Haburcak M, Martella G, Tscherter A, Platania P, Wu B, Pothos EN, Shen J (2009) Impaired dopamine release and synaptic plasticity in the striatum of parkin-/- mice. Journal of Neurochemistry 110:613-621.

Klein C, Schlossmacher MG (2006) The genetics of Parkinson disease: Implications for neurological care. Nature Clinical Practice Neurology 2:136-146.

Klein C, Schlossmacher MG (2007) Parkinson disease, 10 years after its genetic revolution: multiple clues to a complex disorder. Neurology 69:2093-2104.

Klinkenberg I, Sambeth A, Blokland A (2011) Acetylcholine and attention. Behavioural Brain Research 221:430-442.

Kuter K, Kolasiewicz W, Golembiowska K, Dziubina A, Schulze G, Berghauzen K, Wardas J, Ossowska K (2011) Partial lesion of the dopaminergic innervation of the ventral striatum induces "depressive-like" behavior of rats. Pharmacological Reports : PR 63:1383-1392.

Lange KW, Kornhuber J, Riederer P (1997) Dopamine/glutamate interactions in Parkinson's disease. Neuroscience and Biobehavioral Reviews 21:393-400.

Latini S, Bordoni F, Pedata F, Corradetti R (1999) Extracellular adenosine concentrations during in vitro ischaemia in rat hippocampal slices. British Journal of Pharmacology 127:729-739.

Le W, Nguyen D, Lin XW, Rawal P, Huang M, Ding Y, Xie W, Deng H, Jankovic J (2011) Transcription factor PITX3 gene in Parkinson's disease. Neurobiology of Aging 32:750-753.

Leonard BE (1997) The role of noradrenalinee in depression: a review. Journal of Psychopharmacology 11:S39-47.

Li Y, Huang XF, Deng C, Meyer B, Wu A, Yu Y, Ying W, Yang GY, Yenari MA, Wang Q (2010) Alterations in 5-HT2A receptor binding in various brain regions among 6-hydroxydopamine-induced Parkinsonian rats. Synapse 64:224-230.

Loewi O (1921) Über humorale Übertragbarkeit der Herznervenwirkung - I. Mitteilung. Pflügers Archiv für die Gesamte Physiologie des Menschen und der Tiere 189:239-242.

Loewi O, Navratil E (1926) Über humorale Übertragbarkeit der Herznervenwirkung - X. Mitteilung. Über das Schicksal des Vagusstoffs. Pflügers Archiv für die Gesamte Physiologie des Menschen und der Tiere 214:678-688.

Lu W, Ziff EB (2005) PICK1 interacts with ABP/GRIP to regulate AMPA receptor trafficking. Neuron 47:407-421.

Lucking CB, Durr A, Bonifati V, Vaughan J, De Michele G, Gasser T, Harhangi BS, Meco G, Denefle P, Wood NW, Agid Y, Brice A (2000) Association between early-onset Parkinson's disease and mutations in the parkin gene. The New England Journal of Medicine 342:1560-1567.

Mann JJ (1999) Role of the serotonergic system in the pathogenesis of major depression and suicidal behavior. Neuropsychopharmacology 21:99S-105S.

Matsukawa M, Ogawa M, Nakadate K, Maeshima T, Ichitani Y, Kawai N, Okado N (1997) Serotonin and acetylcholine are crucial to maintain hippocampal synapses and memory acquisition in rats. Neuroscience Letters 230:13-16.

Matsuura K, Kabuto H, Makino H, Ogawa N (1997) Pole test is a useful method for evaluating the mouse movement disorder caused by striatal dopamine depletion. Journal of Neuroscience Methods 73:45-48.

Mattson MP, Kater SB (1989) Development and selective neurodegeneration in cell cultures from different hippocampal regions. Brain Research 490:110-125.

McEntee WJ, Crook TH (1993) Glutamate: its role in learning, memory, and the aging brain. Psychopharmacology 111:391-401.

Mefford IN, Potter WZ (1989) A neuroanatomical and biochemical basis for attention deficit disorder with hyperactivity in children: a defect in tonic adrenaline mediated inhibition of locus coeruleus stimulation. Medical Hypotheses 29:33-42.

Meltzer HY (1990) Role of serotonin in depression. Annals of the New York Academy of Sciences 600:486-499.

Menza M, Dobkin RD, Marin H, Mark MH, Gara M, Buyske S, Bienfait K, Dicke A (2009) A controlled trial of antidepressants in patients with Parkinson disease and depression. Neurology 72:886-892.

Messing RB, Lytle LD (1977) Serotonin-containing neurons: their possible role in pain and analgesia. Pain 4:1-21.

Meyer PM, Strecker K, Kendziorra K, Becker G, Hesse S, Woelpl D, Hensel A, Patt M, Sorger D, Wegner F, Lobsien D, Barthel H, Brust P, Gertz HJ, Sabri O, Schwarz J (2009) Reduced alpha4beta2*-nicotinic acetylcholine receptor binding and its relationship to mild cognitive and depressive symptoms in Parkinson disease. Archives of General Psychiatry 66:866-877.

Noyce AJ, Bestwick JP, Silveira-Moriyama L, Hawkes CH, Giovannoni G, Lees AJ, Schrag A (2012) Meta-analysis of early nonmotor features and risk factors for Parkinson disease. Annals of Neurology 72:893-901.

Nunes I, Tovmasian LT, Silva RM, Burke RE, Goff SP (2003) Pitx3 is required for development of substantia nigra dopaminergic neurons. Proceedings of the National Academy of Sciences of the United States of America 100:4245-4250.

Nunomura A, Moreira PI, Lee HG, Zhu X, Castellani RJ, Smith MA, Perry G (2007) Neuronal death and survival under oxidative stress in Alzheimer and Parkinson diseases. CNS & Neurological Disorders – Drug Targets 6:411-423.

O'Neill MJ, Bleakman D, Zimmerman DM, Nisenbaum ES (2004) AMPA receptor potentiators for the treatment of CNS disorders. Current Drug Targets. CNS and Neurological Disorders 3:181-194.

Ogawa N, Hirose Y, Ohara S, Ono T, Watanabe Y (1985) A simple quantitative bradykinesia test in MPTP-treated mice. Research Communications in Chemical Pathology and Pharmacology 50:435-441.

Oishi N, Hashikawa K, Yoshida H, Ishizu K, Ueda M, Kawashima H, Saji H, Fukuyama H (2007) Quantification of nicotinic acetylcholine receptors in Parkinson's disease with (123)I-5IA SPECT. Journal of the Neurological Sciences 256:52-60.

Ojo OO, Okubadejo NU, Ojini FI, Danesi MA (2012) Frequency of cognitive impairment and depression in Parkinson's disease: A preliminary case-control study. Nigerian Medical Journal 53:65-70.

Olsen RW, McCabe RT, Wamsley JK (1990) GABAA receptor subtypes: autoradiographic comparison of GABA, benzodiazepine, and convulsant binding sites in the rat central nervous system. Journal of Chemical Neuroanatomy 3:59-76.

Paisan-Ruiz C et al. (2004) Cloning of the gene containing mutations that cause PARK8-linked Parkinson's disease. Neuron 44:595-600.

Palomero-Gallagher N, Bidmon HJ, Zilles K (2003) AMPA, kainate, and NMDA receptor densities in the hippocampus of untreated male rats and females in estrus and diestrus. The Journal of Comparative Neurology 459:468-474.

Palomero-Gallagher N, Schleicher A, Bidmon HJ, Pannek HW, Hans V, Gorji A, Speckmann EJ, Zilles K (2012) Multireceptor analysis in human neocortex reveals complex alterations of receptor ligand binding in focal epilepsies. Epilepsia 53:1987-1997.

Palomero-Gallagher N, Bidmon HJ, Cremer M, Schleicher A, Kircheis G, Reifenberger G, Kostopoulos G, Haussinger D, Zilles K (2009) Neurotransmitter receptor imbalances in motor cortex and basal ganglia in hepatic encephalopathy. Cellular Physiology and Biochemistry 24:291-306.

Parks CL, Robinson PS, Sibille E, Shenk T, Toth M (1998) Increased anxiety of mice lacking the serotonin1A receptor. Proceedings of the National Academy of Sciences of the United States of America 95:10734-10739.

Picciotto MR, Higley MJ, Mineur YS (2012) Acetylcholine as a neuromodulator: cholinergic signaling shapes nervous system function and behavior. Neuron 76:116-129.

Piggott MA, Marshall EF, Thomas N, Lloyd S, Court JA, Jaros E, Burn D, Johnson M, Perry RH, McKeith IG, Ballard C, Perry EK (1999) Striatal dopaminergic markers in dementia with Lewy bodies, Alzheimer's and Parkinson's diseases: rostrocaudal distribution. Brain (Pt 8):1449-1468.

Planells-Cases R, Lerma J, Ferrer-Montiel A (2006) Pharmacological intervention at ionotropic glutamate receptor complexes. Current Pharmaceutical Design 12:3583-3596.

Polymeropoulos MH, Lavedan C, Leroy E, Ide SE, Dehejia A, Dutra A, Pike B, Root H, Rubenstein J, Boyer R, Stenroos ES, Chandrasekharappa S, Athanassiadou A, Papapetropoulos T, Johnson WG, Lazzarini AM, Duvoisin RC, Di Iorio G, Golbe LI, Nussbaum RL (1997) Mutation in the alpha-synuclein gene identified in families with Parkinson's disease. Science 276:2045-2047.

Ponsen MM, Stoffers D, Booij J, van Eck-Smit BL, Wolters E, Berendse HW (2004) Idiopathic hyposmia as a preclinical sign of Parkinson's disease. Annals of Neurology 56:173-181.

Porkka-Heiskanen T (1999) Adenosine in sleep and wakefulness. Annals of Medicine 31:125-129.

Porkka-Heiskanen T, Strecker RE, Thakkar M, Bjorkum AA, Greene RW, McCarley RW (1997) Adenosine: a mediator of the sleep-inducing effects of prolonged wakefulness. Science 276:1265-1268.

Quik M, Perez XA, Bordia T (2012) Nicotine as a potential neuroprotective agent for Parkinson's disease. Movement Disorders 27:947-957.

Quik M, Parameswaran N, McCallum SE, Bordia T, Bao S, McCormack A, Kim A, Tyndale RF, Langston JW, Di Monte DA (2006) Chronic oral nicotine treatment protects against striatal degeneration in MPTP-treated primates. Journal of Neurochemistry 98:1866-1875.

Ramboz S, Oosting R, Amara DA, Kung HF, Blier P, Mendelsohn M, Mann JJ, Brunner D, Hen R (1998) Serotonin receptor 1A knockout: an animal model of anxiety-related disorder. Proceedings of the National Academy of Sciences of the United States of America 95:14476-14481.

Rapport MM, Green AA, Page IH (1948) Serum vasoconstrictor, serotonin; isolation and characterization. The Journal of Biological Chemistry 176:1243-1251.

Raskin S, Durst R (2010) Bupropion as the treatment of choice in depression associated with Parkinson's disease and it's various treatments. Medical Hypotheses 75:544-546.

Richard IH et al. (2012) A randomized, double-blind, placebo-controlled trial of antidepressants in Parkinson disease. Neurology 78:1229-1236.

Rieger DK, Reichenberger E, McLean W, Sidow A, Olsen BR (2001) A double-deletion mutation in the Pitx3 gene causes arrested lens development in aphakia mice. Genomics 72:61-72.

Rinne JO, Myllykyla T, Lonnberg P, Marjamaki P (1991) A postmortem study of brain nicotinic receptors in Parkinson's and Alzheimer's disease. Brain Research 547:167-170.

Rinne JO, Laihinen A, Nagren K, Bergman J, Solin O, Haaparanta M, Ruotsalainen U, Rinne UK (1990a) PET demonstrates different behaviour of striatal dopamine D-1 and D-2 receptors in early Parkinson's disease. Journal of Neuroscience Research 27:494-499.

Rinne UK, Laihinen A, Rinne JO, Nagren K, Bergman J, Ruotsalainen U (1990b) Positron emission tomography demonstrates dopamine D2 receptor supersensitivity in the striatum of patients with early Parkinson's disease. Movement Disorders 5:55-59.

Ritz B, Ascherio A, Checkoway H, Marder KS, Nelson LM, Rocca WA, Ross GW, Strickland D, Van Den Eeden SK, Gorell J (2007) Pooled analysis of tobacco use and risk of Parkinson disease. Archives of Neurology 64:990-997.

Roberts E (1984) GABA-related phenomena, models of nervous system function, and seizures. Annals of Neurology 16:S77-89.

Rodriguez MC, Obeso JA, Olanow CW (1998) Subthalamic nucleus-mediated excitotoxicity in Parkinson's disease: a target for neuroprotection. Annals of Neurology 44:S175-188.

Ross GW, Petrovitch H, Abbott RD, Tanner CM, Popper J, Masaki K, Launer L, White LR (2008) Association of olfactory dysfunction with risk for future Parkinson's disease. Annals of Neurology 63:167-173.

Rudolph U, Mohler H (2006) GABA-based therapeutic approaches: GABAA receptor subtype functions. Current Opinion in Pharmacology 6:18-23.

Sanders SK, Shekhar A (1995) Regulation of anxiety by GABAA receptors in the rat amygdala. Pharmacology, Biochemistry, and Behavior 52:701-706.

Sato S, Chiba T, Nishiyama S, Kakiuchi T, Tsukada H, Hatano T, Fukuda T, Yasoshima Y, Kai N, Kobayashi K, Mizuno Y, Tanaka K, Hattori N (2006) Decline of striatal dopamine release in parkin-deficient mice shown by ex vivo autoradiography. Journal of Neuroscience Research 84:1350-1357.

Scatton B, Javoy-Agid F, Rouquier L, Dubois B, Agid Y (1983) Reduction of cortical dopamine, noradrenalinee, serotonin and their metabolites in Parkinson's disease. Brain Research 275:321-328.

Semina EV, Reiter RS, Murray JC (1997) Isolation of a new homeobox gene belonging to the Pitx/Rieg family: expression during lens development and mapping to the aphakia region on mouse chromosome 19. Human Molecular Genetics 6:2109-2116.

Shendelman S, Jonason A, Martinat C, Leete T, Abeliovich A (2004) DJ-1 is a redox-dependent molecular chaperone that inhibits alpha-synuclein aggregate formation. PLOS Biology 2:e362.

Shimura H, Hattori N, Kubo S, Mizuno Y, Asakawa S, Minoshima S, Shimizu N, Iwai K, Chiba T, Tanaka K, Suzuki T (2000) Familial Parkinson disease gene product, parkin, is a ubiquitin-protein ligase. Nature Genetics 25:302-305.

Smidt MP, Smits SM, Bouwmeester H, Hamers FP, van der Linden AJ, Hellemons AJ, Graw J, Burbach JP (2004) Early developmental failure of substantia nigra dopamine neurons in mice lacking the homeodomain gene Pitx3. Development 131:1145-1155.

Stahl SM, Pradko JF, Haight BR, Modell JG, Rockett CB, Learned-Coughlin S (2004) A Review of the Neuropharmacology of Bupropion, a Dual Norepinephrine and Dopamine Reuptake Inhibitor. Primary Care Companion to the Journal of Clinical Psychiatry 6:159-166.

Staropoli JF, McDermott C, Martinat C, Schulman B, Demireva E, Abeliovich A (2003) Parkin is a component of an SCF-like ubiquitin ligase complex and protects postmitotic neurons from kainate excitotoxicity. Neuron 37:735-749.

Sternberg DB, Isaacs KR, Gold PE, McGaugh JL (1985) Epinephrine facilitation of appetitive learning: attenuation with adrenergic receptor antagonists. Behavioral and Neural Biology 44:447-453.

Tanaka K, Suzuki T, Chiba T, Shimura H, Hattori N, Mizuno Y (2001) Parkin is linked to the ubiquitin pathway. Journal of Molecular Medicine 79:482-494.

Tang L, Zhao S, Wang M, Sheth A, Zhao Z, Chen L, Fan X, Chen L (2012) Meta-analysis of association between PITX3 gene polymorphism and Parkinson's disease. Journal of the Neurological Sciences 317:80-86.

Thomas B, Beal MF (2007) Parkinson's disease. Human Molecular Genetics 16 Spec No. 2:R183-194.

Thomas KJ, McCoy MK, Blackinton J, Beilina A, van der Brug M, Sandebring A, Miller D, Maric D, Cedazo-Minguez A, Cookson MR (2011) DJ-1 acts in parallel to the PINK1/parkin pathway to control mitochondrial function and autophagy. Human Molecular Genetics 20:40-50.

Tohgi H, Abe T, Takahashi S, Takahashi J, Nozaki Y, Ueno M, Kikuchi T (1993) Monoamine metabolism in the cerebrospinal fluid in Parkinson's disease: relationship to clinical symptoms and subsequent therapeutic outcomes. Journal of Neural Transmission: Parkinson's Disease and Dementia Section 5:17-26.

Ursin R (2002) Serotonin and sleep. Sleep Medicine Reviews 6:55-69.

Valente EM, Bentivoglio AR, Dixon PH, Ferraris A, Ialongo T, Frontali M, Albanese A, Wood NW (2001) Localization of a novel locus for autosomal recessive early-onset parkinsonism, PARK6, on human chromosome 1p35-p36. American Journal of Human Genetics 68:895-900.

Valente EM et al. (2002) PARK6-linked parkinsonism occurs in several European families. Annals of Neurology 51:14-18.

van den Munckhof P, Gilbert F, Chamberland M, Levesque D, Drouin J (2006) Striatal neuroadaptation and rescue of locomotor deficit by L-dopa in aphakia mice, a model of Parkinson's disease. Journal of Neurochemistry 96:160-170.

van den Munckhof P, Luk KC, Ste-Marie L, Montgomery J, Blanchet PJ, Sadikot AF, Drouin J (2003) Pitx3 is required for motor activity and for survival of a subset of midbrain dopaminergic neurons. Development 130:2535-2542.

Varani K, Vincenzi F, Tosi A, Gessi S, Casetta I, Granieri G, Fazio P, Leung E, MacLennan S, Granieri E, Borea PA (2010) A2A adenosine receptor overexpression and functionality, as well as TNF-alpha levels, correlate with motor symptoms in Parkinson's disease. FASEB Journal 24:587-598.

Varnum DS, Stevens LC (1968) Aphakia, a new mutation in the mouse. The Journal of Heredity 59:147-150.

Verbaan D, Boesveldt S, van Rooden SM, Visser M, Marinus J, Macedo MG, Fang Y, Heutink P, Berendse HW, van Hilten JJ (2008) Is olfactory impairment in Parkinson disease related to phenotypic or genotypic characteristics? Neurology 71:1877-1882.

Wang Y, Chandran JS, Cai H, Mattson MP (2008) DJ-1 is essential for long-term depression at hippocampal CA1 synapses. Neuromolecular Medicine 10:40-45.

Werber EA, Rabey JM (2001) The beneficial effect of cholinesterase inhibitors on patients suffering from Parkinson's disease and dementia. Journal of Neural Transmission 108:1319-1325.

Winn HR, Rubio GR, Berne RM (1981) The role of adenosine in the regulation of cerebral blood flow. Journal of Cerebral Blood Flow and Metabolism 1:239-244.

Wu J, Xiao H, Sun H, Zou L, Zhu LQ (2012) Role of dopamine receptors in ADHD: a systematic meta-analysis. Molecular Neurobiology 45:605-620.

Xia J, Zhang X, Staudinger J, Huganir RL (1999) Clustering of AMPA receptors by the synaptic PDZ domain-containing protein PICK1. Neuron 22:179-187.

Xiong H, Wang D, Chen L, Choo YS, Ma H, Tang C, Xia K, Jiang W, Ronai Z, Zhuang X, Zhang Z (2009) Parkin, PINK1, and DJ-1 form a ubiquitin E3 ligase complex promoting unfolded protein degradation. The Journal of Clinical Investigation 119:650-660.

Xu Y, Yan J, Zhou P, Li J, Gao H, Xia Y, Wang Q (2012) Neurotransmitter receptors and cognitive dysfunction in Alzheimer's disease and Parkinson's disease. Progress in Neurobiology 97:1-13.

Yu JT, Wang ND, Ma T, Jiang H, Guan J, Tan L (2011) Roles of beta-adrenergic receptors in Alzheimer's disease: implications for novel therapeutics. Brain Research Bulletin 84:111-117.

Zarow C, Lyness SA, Mortimer JA, Chui HC (2003) Neuronal loss is greater in the locus coeruleus than nucleus basalis and substantia nigra in Alzheimer and Parkinson diseases. Archives of Neurology 60:337-341.

Zhang L, Shimoji M, Thomas B, Moore DJ, Yu SW, Marupudi NI, Torp R, Torgner IA, Ottersen OP, Dawson TM, Dawson VL (2005) Mitochondrial localization of the Parkinson's disease related protein DJ-1: implications for pathogenesis. Human Molecular Genetics 14:2063-2073.

Zilles K, Schleicher A (1991) Quantitative receptor autoradiography and image analysis. Bulletin de l'Association des Anatomistes 75:117-121.

Zilles K, Schleicher A (1995) Correlative imaging of transmitter receptor distributions in human cortex. In: Autoradiography and Correlative Imaging (Stumpf WE. SH, ed), pp 277-307: Academic Press Inc.

Zilles K, Palomero-Gallagher N, Schleicher A (2004) Transmitter receptors and functional anatomy of the cerebral cortex. Journal of Anatomy 205:417-432.

Zilles K, Qu MS, Köhling R, Speckmann EJ (1999) Ionotropic glutamate and GABA receptors in human epileptic neocortical tissue: quantitative in vitro receptor autoradiography. Neuroscience 94:1051-1061.

Zilles K, Schleicher A, Palomero-Gallagher N, Amunts K (2002a) Quantitative Analysis of Cyto- and Receptor Architecture of the Human Brain. In: Brain Mapping: The Methods (Toga AW, Mazziotta JC, eds), pp 573-602: Elsevier Inc.

Zilles K, Palomero-Gallagher N, Grefkes C, Scheperjans F, Boy C, Amunts K, Schleicher A (2002b) Architectonics of the human cerebral cortex and transmitter receptor fingerprints: reconciling functional neuroanatomy and neurochemistry. European Neuropsychopharmacology 12:587-599.

Zimprich A et al. (2004) Mutations in LRRK2 cause autosomal-dominant parkinsonism with pleomorphic pathology. Neuron 44:601-607.

Appendix

Table A1: **AMPA** receptor densities (fmol/mg protein) and mean densities ± SD of controls and *Pitx3 aphakia* mice in various brain regions (Ligand: [^{3}H]-**AMPA**).

Animal	Group	OB	M	S	Pir	CPu	CA1	CA2/3	DG	V	SN	CB
1	Control	290	484	622	1271	684	1089	906	811	837	262	234
2	Control	445	694	676	1256	585	1910	1639	1305	747	314	352
3	Control	554	697	572	1216	669	1760	1129	1378	692	159	400
4	Control	566	843	789	1012	822	2281	1790	1608	828	452	376
5	Control	383	530	558	1127	441	1977	1587	1611	622	295	320
6	Control	443	434	460	921	341	960	771	799	514	244	289
	Mean	447	614	613	1134	590	1663	1304	1252	707	288	328
	SD	104	156	113	142	175	524	425	367	125	97	61
11	*Pitx3 aphakia*	378	608	592	1253	512	1975	1400	1432	497	246	345
12	*Pitx3 aphakia*	339	431	434	801	352	881	872	923	816	337	435
13	*Pitx3 aphakia*	461	839	765	1562	628	1669	1379	1226	1088	361	377
14	*Pitx3 aphakia*	316	425	387	816	355	764	612	506	725	131	296
15	*Pitx3 aphakia*	418	837	808	1667	682	2394	1668	1531	798	311	333
16	*Pitx3 aphakia*	389	500	401	1193	410	1763	1235	1301	785	258	243
17	*Pitx3 aphakia*	418	647	531	1267	480	1301	1149	1073	595	238	225
18	*Pitx3 aphakia*	276	490	384	779	339	2003	1174	1096	377	180	210
19	*Pitx3 aphakia*	344	460	421	997	412	806	692	682	493	193	182
20	*Pitx3 aphakia*	342	556	478	1006	471	990	803	721	366	199	245
21	*Pitx3 aphakia*	584	917	796	1586	639	2429	1880	1766	703	360	305
22	*Pitx3 aphakia*	485	679	654	1516	673	2281	1774	1566	802	383	350
	Mean	396	616	554	1204	496	1605	1220	1152	671	266	295
	SD	84	171	165	326	130	634	421	391	212	83	76

Table A2: **Kainate** receptor densities (fmol/mg protein) and mean densities ± SD of controls and *Pitx3 aphakia* mice in various brain regions (Ligand: [^{3}H]-**Kainate**).

Animal	Group	OB	M	S	Pir	CPu	CA1	CA2/3	DG	V	SN	CB
1	Control	2364	2231	2042	1549	2351	1130	1943	2032	2277	543	1124
2	Control	2388	2044	1773	1452	2309	1096	1850	1957	2017	646	1141
3	Control	2130	1814	1561	1355	2026	982	1621	1756	1925	645	991
4	Control	2865	2262	1983	1486	2445	1133	1879	2086	2162	550	1243
5	Control	2143	2430	2090	1735	2500	1095	1988	1978	2064	518	1094
6	Control	2289	1934	1516	1354	1895	1019	1769	1735	1894	651	1130
	Mean	2363	2119	1828	1488	2254	1076	1842	1924	2056	592	1121
	SD	269	229	249	142	241	62	132	145	145	61	81
11	*Pitx3 aphakia*	1941	2144	2052	1500	2559	1077	2031	1840	2370	560	1138
12	*Pitx3 aphakia*	1953	2670	2196	1985	2797	1025	2090	1954	2601	597	1142
13	*Pitx3 aphakia*	2093	2302	1975	1567	2534	1019	2077	1775	2690	628	1070
14	*Pitx3 aphakia*	1797	2211	1922	1581	2234	1089	2065	1818	2831	1554	1158
15	*Pitx3 aphakia*	2037	2015	1693	1445	2245	1113	1898	1837	2256	635	1171
16	*Pitx3 aphakia*	1855	2130	1813	1465	2400	1070	2119	1863	2855	520	1099
17	*Pitx3 aphakia*	2238	2335	1949	1642	2696	1020	1767	1734	2725	786	1265
18	*Pitx3 aphakia*	2350	2346	1896	1535	2464	1088	1801	1696	2111	727	1285
19	*Pitx3 aphakia*	2360	2455	2227	1819	2765	1062	1987	1956	2413	754	1403
20	*Pitx3 aphakia*	2102	2367	1940	1796	2523	1090	1970	1837	2424	629	1327
21	*Pitx3 aphakia*	2249	2126	1921	1427	2430	1000	1772	1707	2045	609	1408
22	*Pitx3 aphakia*	2051	2310	2073	1500	2510	1094	2016	1860		565	1362
	Mean	2086	2284	1972	1605	2513	1062	1966	1823	2484	714	1236
	SD	184	175	150	174	179	37	127	84	279	277	121

Table A3: **NMDA** receptor densities (fmol/mg protein) and mean densities ± SD of controls and *Pitx3 aphakia* mice in various brain regions (Ligand: [^{3}H]-**MK 801**).

Animal	Group	OB	M	S	Pir	CPu	CA1	CA2/3	DG	V	SN	CB
1	Control	1225	2181	2199	2384	1519	5109	2959	3893	2493	544	
2	Control	1342	2146	2284	2321	1521	4829	2906	3863	2520	615	
3	Control	1285	2240	2210	2429	1431	4585	2637	3522	2415	532	
4	Control	1287	2293	2174	2309	1458	4655	2789	3557	2454	547	
5	Control	1401	2165	2287	2529	1589	4421	2649	3499	2352	566	
6	Control	1449	2329	2264	2131	1443	4910	2978	3944	2489	590	
	Mean	1332	2225	2236	2350	1493	4751	2820	3713	2454	566	
	SD	83	74	48	134	60	247	152	207	62	32	
11	*Pitx3 aphakia*	1413	2308	2249	2281	1443	4838	2912	3798	2718	492	
12	*Pitx3 aphakia*	1278	2179	2072	2199	1453	4818	2847	3698	2657	496	
13	*Pitx3 aphakia*	1191	2295	2226	2288	1516	4563	2768	3752	2713	536	
14	*Pitx3 aphakia*	1224	2066	1913	2411	1465	4584	2718	3487	2765	574	
15	*Pitx3 aphakia*	1219	2166	2133	2404	1517	3977	2424	3183	2603	550	
16	*Pitx3 aphakia*	1228	2259	2193	2444	1573	4947	3042	3774	2522	501	
17	*Pitx3 aphakia*	1035	2430	2402	2351	1673	5041	3028	3929	2582	562	
18	*Pitx3 aphakia*	1284	2063	2007	1603	1224	4754	2907	3903	2527	438	
19	*Pitx3 aphakia*	1182	2202	2080	2248	1496	4551	2781	3504	2527	417	
20	*Pitx3 aphakia*	1129	2071	1990	2379	1423	5186	2807	3529	2529	407	
21	*Pitx3 aphakia*	1117	1875	1857	2145	1280	4582	2529	3274	2459	353	
22	*Pitx3 aphakia*	1069	2340	2273	2290	1566	5062	3008	3903	2560	353	
	Mean	1197	2188	2116	2254	1469	4742	2814	3644	2597	473	
	SD	103	152	160	224	123	323	191	248	96	78	

Table A4: **mGlu$_{2/3}$** receptor densities (fmol/mg protein) and mean densities ± SD of controls and *Pitx3 aphakia* mice in various brain regions (Ligand: [^{3}H]-**LY 341,495**).

Animal	Group	OB	M	S	Pir	CPu	CA1	CA2/3	DG	V	SN	CB
1	Control	3374	11500	12004	13065	9790	6056	3305	8992	14736	5571	2565
2	Control	2529	11372	11874	12427	9403	5119	3336	9602	13535	5097	1961
3	Control	2647	7697	8576	7643	3782	4143	2513	6803	12151	4353	2122
4	Control	3169	11826	12758	13222	10882	4379	3354	9142	12814	5260	1973
5	Control	2857	10299	11016	12818	10431	5193	3266	9078	11107	5750	1989
6	Control	2330	11459	11204	13586	9448	4488	3097	8515	11089	5465	2229
	Mean	2817	10692	11239	12127	8956	4896	3145	8689	12572	5249	2140
	SD	396	1556	1445	2231	2600	705	323	987	1428	495	233
11	*Pitx3 aphakia*	2479	9535	10131	13826	8507	4409	2850	7361	11447	5445	2568
12	*Pitx3 aphakia*	2468	10705	10924	12851	7905	4457	2972	7279	12521	5903	2470
13	*Pitx3 aphakia*	1926	12336	10854	9979	8972	3693	2026	7073	11808	8033	2933
14	*Pitx3 aphakia*	2311	12879	14326	9743	7915	4829	3227	9458	14437	4312	2487
15	*Pitx3 aphakia*	3294	9177	9148	12259	6960	4061	2816	6108	12137	4600	2990
16	*Pitx3 aphakia*	3331	10178	11371	10493	8208	5141	3272	8580	13524	5823	2330
17	*Pitx3 aphakia*	4174	12623	11986	12275	8962	5458	3680	9306	13900	6037	2659
18	*Pitx3 aphakia*	3003	10911	11857	11876	8174	5845	3932	9164	14482	7614	3215
19	*Pitx3 aphakia*	4403	11688	12108	13083	9940	4960	3399	8422	11832	7305	3225
20	*Pitx3 aphakia*	3197	11869	12077	11744	8520	4910	2991	7658	14480	5705	2460
21	*Pitx3 aphakia*	3082	10753	11551	11953	9621	5345	3421	7890	9688	5288	2906
22	*Pitx3 aphakia*	3167	11649	13928	12761	9267	4807	3730	8351	15497	5027	2731
	Mean	3070	11192	11688	11904	8579	4826	3193	8054	12979	5924	2748
	SD	722	1186	1436	1257	828	604	512	1013	1676	1171	303

Table A5: **$GABA_A$** receptor densities (fmol/mg protein) and mean densities ± SD of controls and *Pitx3 aphakia* mice in various brain regions (Ligand: [^{3}H]-**Muscimol** - agonist).

Animal	Group	OB	M	S	Pir	CPu	CA1	CA2/3	DG	V	SN	CB
1	Control	2330	1585	1776	1730	1125	2101	1062	2135	2153	1346	4114
2	Control	2378	1705	2021	2063	1582	1887	1095	2554	2275	1559	5661
3	Control	2409	1456	1680	1730	1326	1701	977	2625	2229	1588	5859
4	Control	1264	1657	2252	2011	1408	1368	844	2143	2168	1319	3859
5	Control	2394	1491	2256	1722	1221	1915	1019	2380	1815	1466	3595
6	Control	1785	1728	1862	1834	1400	1828	969	2074	2266	1254	4759
	Mean	2093	1604	1974	1848	1344	1800	994	2319	2151	1422	4641
	SD	471	112	244	153	159	248	88	236	172	136	951
11	*Pitx3 aphakia*	1751	1865	2673	2191	1368	1464	880	1835	2718	2107	6556
12	*Pitx3 aphakia*	2004	2286	2835	3151	1833	1934	1089	2695	2677	1588	6931
13	*Pitx3 aphakia*		2010	2518	2568	1412	1572	886	2426	2140	1241	8182
14	*Pitx3 aphakia*	2035	2891	3347	1919	1454	2153	1180	2440	2674	1949	6024
15	*Pitx3 aphakia*	1996	2215	2727	2518	1291	1897	1095	2590	2241	2381	7840
16	*Pitx3 aphakia*	1748	1852	2400	2113	1459	1963	1036	2521	2638	2196	5607
17	*Pitx3 aphakia*	1334	1806	2136	2043	1290	1718	962	2300	1864	1622	5453
18	*Pitx3 aphakia*	1644	1975	2180	1739	1284	1724	947	2273	3312	1308	6963
19	*Pitx3 aphakia*	1875	1989	2387	1910	1311	1845	1107	2587	2744	1310	6148
20	*Pitx3 aphakia*	1183	2119	2264	2448	1578	1797	1034	2560	2805	1847	7474
21	*Pitx3 aphakia*	2104	2099	2315	2135	1303	1763	952	2255	2679	1943	6433
22	*Pitx3 aphakia*	986	2052	2526	2516	1579	1796	999	2713	1760	1374	6511
	Mean	1696	2097	2526	2271	1430	1802	1014	2433	2521	1739	6677
	SD	375	289	337	388	166	181	93	243	439	386	845

Table A6: **$GABA_A$** receptor densities (fmol/mg protein) and mean densities ± SD of controls and *Pitx3 aphakia* mice in various brain regions (Ligand: [^{3}H]-**SR 95531** - antagonist).

Animal	Group	OB	M	S	Pir	CPu	CA1	CA2/3	DG	V	SN	CB
1	Control	1825	2203	2259	2945	1227	4082	2886	3122	1732	2018	2179
2	Control	1978	1813	1988	2348	1072	3486	2435	2634	1769	2586	2091
3	Control	2185	2421	2434	2250	1150	3890	2472	3044	2788	2511	2270
4	Control	1747	2664	2556	2623	1282	4741	3323	3453	2312	1796	2007
5	Control	1989	2285	2386	2305	1245	4301	2811	3290	2388	1477	1859
6	Control	2861	1983	1950	2289	1015	3842	2570	2766	2668	2100	2220
	Mean	2098	2228	2262	2460	1165	4057	2750	3052	2276	2081	2104
	SD	403	305	247	273	105	431	334	310	443	422	152
11	*Pitx3 aphakia*	934	1748	1794	1836	756	3861	2847	3505	2939	3439	2504
12	*Pitx3 aphakia*	2945	2308	2555	3176	1580	4885	4798	5732	3553	3681	3051
13	*Pitx3 aphakia*	1018	2953	2329	3561	1587	4364	4276	5503	2941	3736	2519
14	*Pitx3 aphakia*	2217	2875	2930	2309	1181	4685	3931	4255	3420	2310	2173
15	*Pitx3 aphakia*	1699	1850	2266	2471	1215	3325	3028	3812	2592	3145	2671
16	*Pitx3 aphakia*	2218	2416	2433	3377	1247	5242	4366	4934	3216	3485	1748
17	*Pitx3 aphakia*	2519	2585	2651	3204	1523	6009	5778	5813	3064	3144	2264
18	*Pitx3 aphakia*	3969	3001	3090	4044	1746	5691	4763	5906	3277	3864	2593
19	*Pitx3 aphakia*	4070	2662	2081	3356	1549	7274	7007	7906	3100	3312	2320
20	*Pitx3 aphakia*	2207	2253	2102	2324	914	3793	3352	4243	2491	2899	2758
21	*Pitx3 aphakia*	2075	2163	2229	2894	1212	3993	3743	4174	2196	2555	2901
22	*Pitx3 aphakia*	2535	2640	2057	2994	1300	5683	5033	6129	3354	2952	1667
	Mean	2367	2455	2376	2962	1317	4900	4410	5159	3012	3210	2431
	SD	969	408	377	626	293	1135	1185	1249	407	474	423

Table A7: **BZ** receptor densities (fmol/mg protein) and mean densities ± SD of controls and *Pitx3 aphakia* mice in various brain regions (Ligand: [^{3}H]-**Flumazenil**).

Animal	Group	OB	M	S	Pir	CPu	CA1	CA2/3	DG	V	SN	CB
1	Control	7982	6606	8174	6172	1670	8361	4538	6320	8325	10708	1964
2	Control	6984	5583	6385	4673	1375	7074	4214	5549	6518	6490	1943
3	Control	7241	5569	5896	4214	1367	6935	3895	4917	5699	6956	1725
4	Control	4787	5566	6917	4632	1404	7111	4550	6116	7166	8579	2352
5	Control	7041	5434	6861	4946	1526	7264	4114	5447	6482	5936	2249
6	Control	9586	7411	8721	5966	1842	9635	5418	6777	8172	8432	3120
	Mean	7270	6028	7159	5101	1531	7730	4455	5854	7060	7850	2225
	SD	1560	803	1078	788	191	1067	535	675	1032	1752	493
11	*Pitx3 aphakia*	8247	5851	7810	5949	1382	8969	5645	7466	7941	10457	3063
12	*Pitx3 aphakia*	10995	8190	10610	7514	2062	10781	7512	10230	10783	13010	3381
13	*Pitx3 aphakia*	9030	7368		8003	2023	11025	7624	10769	8964	10377	2444
14	*Pitx3 aphakia*	8825	7330	8454	6000	1657	8853	5429	7416	9399	11614	2803
15	*Pitx3 aphakia*	7966	7496	9311	6486	1859	8889	5520	8471	8271	12769	2822
16	*Pitx3 aphakia*	8347	5935	7838	6223	1572	7219	4538	7371	7156	10395	2655
17	*Pitx3 aphakia*	8101	6925	7799	7431	1904	7075	6074	8967	10141	13131	3160
18	*Pitx3 aphakia*	7897	6843	8091	6526	1823	8750	5833	7884	8369	11375	3092
19	*Pitx3 aphakia*	8544	8250	10441	9225	2325	10724	7289	10000	10614	15113	3433
20	*Pitx3 aphakia*	8367	8174	9403	8049	1934	9109	5701	8341	9426	15537	3198
21	*Pitx3 aphakia*	7332	5749	6838	6018	1537	7183	5071	6925	7316	10539	2836
22	*Pitx3 aphakia*	7600	8232	9652	8279	1968	9136	6576	9277		13097	3090
	Mean	8438	7195	8750	7142	1837	8976	6068	8593	8944	12284	2998
	SD	937	951	1211	1090	262	1367	985	1262	1252	1799	293

Table A8: **$GABA_B$** receptor densities (fmol/mg protein) and mean densities ± SD of controls and *Pitx3 aphakia* mice in various brain regions (Ligand: [^{3}H]-**CGP 54626**).

Animal	Group	OB	M	S	Pir	CPu	CA1	CA2/3	DG	V	SN	CB
1	Control	4149	10256	9407	10146	4264	10562	12996	12212	12137	4554	10543
2	Control	4890	11531	10472	12395	5250	10093	12946	11795	11066	5956	10602
3	Control	4598	10712	10465	11556	4879	9321	11012	10814	12984	6215	9216
4	Control	4282	9854	8961	11071	5145	10375	12833	12155	11168	5611	10633
5	Control	4150	10848	9316	11061	4868	10567	13456	11726	11482	4513	9983
6	Control	4172	9746	9096	9582	4219	8577	11601	10419	11288	5449	9282
	Mean	4373	10491	9620	10969	4771	9916	12474	11520	11687	5383	10043
	SD	305	675	676	1000	436	803	947	736	740	710	660
11	*Pitx3 aphakia*	4019	12234	10344	10915	4573	12180	14769	13287	15499	8154	11708
12	*Pitx3 aphakia*	5024	12689	11069	14379	5236	10678	13536	12508	13628	6752	8963
13	*Pitx3 aphakia*	3725	13515	11410	15174	5453	10796	12517	13334	15259	8541	9420
14	*Pitx3 aphakia*	3455	12152	7391	10750	4295	10863	14005	11709	13204	6139	9665
15	*Pitx3 aphakia*	4222	10718	9604	11718	4592	8949	11851	10329	14286	5724	8186
16	*Pitx3 aphakia*	3668	10669	9312	11954	4542	9271	11729	11001	11903	5562	8780
17	*Pitx3 aphakia*	4362	14479	13351	13623	5029	11285	15687	15097	16054	7606	12353
18	*Pitx3 aphakia*	4129	12799	12089	11588	4682	10392	12854	13542	15431	5409	11342
19	*Pitx3 aphakia*	4456	12737	13194	12301	4664	11015	14448	14340	15310	6756	11327
20	*Pitx3 aphakia*	4473	13468	12639	15414	5117	10756	13582	12312	15414	6318	11248
21	*Pitx3 aphakia*	4652	11469	11546	14818	4673	10443	13682	12716	17148	7134	13481
22	*Pitx3 aphakia*	5114	15852	13302	16814	6338	12665	15972	15091	17655	7308	12380
	Mean	4275	12732	11271	13287	4933	10774	13719	12939	15066	6784	10738
	SD	515	1491	1843	2008	555	1033	1361	1495	1615	1008	1682

Table A9: **M_1** receptor densities (fmol/mg protein) and mean densities ± SD of controls and *Pitx3 aphakia* mice in various brain regions (Ligand: [^{3}H]-**Pirenzepine**).

Animal	Group	OB	M	S	Pir	CPu	CA1	CA2/3	DG	V	SN	CB
1	Control	1863	3940	4034	5118	7495	7058	3912	7007	4826	389	
2	Control	2308	4881	4440	4978	8729	6795	3681	6905	2388	280	
3	Control	2911	4174	4622	5312	8810	7911	4736	7898	5754	543	
4	Control	1384	2631	2334	3407	5185	4908	2767	4840	2694	284	
5	Control	1459	2323	2514	3115	4410	7029	3643	7984	4805	318	
6	Control	2575	4616	4769	5443	8003	9112	4501	9041	5821	500	
	Mean	2084	3761	3785	4562	7105	7136	3873	7279	4381	386	
	SD	617	1052	1085	1025	1868	1386	700	1425	1494	113	
11	*Pitx3 aphakia*	2447	4500	4081	5328	7439	8055	4110	7501	6665	649	
12	*Pitx3 aphakia*	1566	2694	2701	3615	4512	6028	3145	5737	3740	373	
13	*Pitx3 aphakia*	930	2524	2552	3200	4064	5451	2857	5392	3275	313	
14	*Pitx3 aphakia*	1321	2724	2429	3282	4022	5556	2750	5078	3709	369	
15	*Pitx3 aphakia*	2459	4646	4709	5772	7934	9388	4907	8588	6043	617	
16	*Pitx3 aphakia*	2096	4560	3958	5068	6686	7391	3940	7325	5073	538	
17	*Pitx3 aphakia*	1133	2578	2239	2548	3770	4541	2339	4577	3568	374	
18	*Pitx3 aphakia*	2228	4761	4395	5143	7296	7317	3695	7017	5495	559	
19	*Pitx3 aphakia*	1380	2631	2508	3044	4181	4930	2563	4434	5490	668	
20	*Pitx3 aphakia*	1220	2429	2473	2926	4074	4177	2298	4330	3099	295	
21	*Pitx3 aphakia*	2229	4733	4565	5754	7974	8632	4474	8141	6626	479	
22	*Pitx3 aphakia*	2310	5699	5097	6711	8745	9755	5003	8680	6984	520	
	Mean	1777	3707	3476	4366	5891	6768	3507	6400	4980	480	
	SD	569	1200	1079	1403	1933	1917	980	1655	1440	132	

Table A10: **M_2** receptor densities (fmol/mg protein) and mean densities ± SD of controls and *Pitx3 aphakia* mice in various brain regions (Ligand: [^{3}H]-**Oxotremorine-M** - agonist).

Animal	Group	OB	M	S	Pir	CPu	CA1	CA2/3	DG	V	SN	CB
1	Control	2997	1100	1672	669	1773	510	538	364	1325	360	173
2	Control	3263	1034	1480	642	1773	556	590	360	1222	328	175
3	Control	2766	1105	1590	639	1979	576	587	370	1040	278	199
4	Control	2269	1293	1802	743	2266	610	649	404	1449	375	190
5	Control	3526	1245	1695	749	1934	657	681	433	1450	404	201
6	Control	2765	1299	1704	725	2134	705	729	480	1508	373	185
	Mean	2931	1179	1657	694	1976	602	629	402	1332	353	187
	SD	439	113	110	50	197	71	70	47	177	44	12
11	*Pitx3 aphakia*	2900	1096	1309	626	1398	619	623	396	1270	333	182
12	*Pitx3 aphakia*	3020	1203	1604	604	1636	645	716	419	1185	366	184
13	*Pitx3 aphakia*	2451	1139	1430	669	1762	635	649	415	1231	274	173
14	*Pitx3 aphakia*	2727	1172	1448	703	1800	661	614	421	1019	277	194
15	*Pitx3 aphakia*	2540	1078	1446	665	1490	608	592	419	1289	252	180
16	*Pitx3 aphakia*	3010	1209	1589	720	1793	628	718	482	1501	392	219
17	*Pitx3 aphakia*	2290	1077	1410	579	1380	491	556	371	1098	331	178
18	*Pitx3 aphakia*	2572	1006	1295	583	1352	508	543	366	1128	330	182
19	*Pitx3 aphakia*	2766	1203	1553	681	1636	667	782	489	1261	347	186
20	*Pitx3 aphakia*	2668	1107	1367	584	1617	527	553	382	1087	354	175
21	*Pitx3 aphakia*	3014	1132	1501	592	1533	588	667	432	1316	322	208
22	*Pitx3 aphakia*	2142	1278	1591	772	1815	698	720	492	1274	388	199
	Mean	2675	1142	1462	648	1601	606	644	424	1221	330	188
	SD	289	75	108	63	171	66	78	44	129	44	14

Table A11: **M_2** receptor densities (fmol/mg protein) and mean densities ± SD of controls and *Pitx3 aphakia* mice in various brain regions (Ligand: [^{3}H]-**AF-DX 384** - antagonist).

Animal	Group	OB	M	S	Pir	CPu	CA1	CA2/3	DG	V	SN	CB
1	Control	3408	1420	1927	865	4504	1011	965	705	1660	426	226
2	Control	3692	1651	2471	1155	5148	1073	954	749	2167	660	228
3	Control	3720	1538	2088	1213	5093	979	878	644	1784	614	232
4	Control	3058	1660	2402	1195	4757	962	934	566	1855	476	238
5	Control	3764	1752	2321	1187	5089	1251	1067	707	1980	460	225
6	Control	3126	1723	2450	1220	4941	1184	964	718	2257	448	197
	Mean	3461	1624	2276	1139	4922	1077	960	681	1951	514	224
	SD	313	124	220	136	249	117	62	66	229	98	14
11	*Pitx3 aphakia*	3394	1797	2449	1052	4841	1068	928	722	2243	628	283
12	*Pitx3 aphakia*	4019	1978	2761	1188	5197	1180	1076	819		395	281
13	*Pitx3 aphakia*	2858	2348	2382	1610	5119	1171	1040	764	2117	513	281
14	*Pitx3 aphakia*	3830	1914	2281	1114	5231	1245	974	784	2151	444	264
15	*Pitx3 aphakia*	3122	1775	2389	1089	4539	1205	962	739	2180	625	257
16	*Pitx3 aphakia*	3598	1774	2200	1239	4405	944	901	865	2449	547	262
17	*Pitx3 aphakia*	3291	1678	2190	1028	4360	1157	1032	732	2377	607	210
18	*Pitx3 aphakia*	3867	1941	2591	1245	5269	1178	1002	769		614	259
19	*Pitx3 aphakia*	3922	2173	2965	1383	5359	1266	1139	794	2297	617	241
20	*Pitx3 aphakia*	3342	1909	2364	1126	4908	1085	887	713	1741	466	227
21	*Pitx3 aphakia*	3690	1708	2360	1153	4808	1142	964	805	2017	526	241
22	*Pitx3 aphakia*	2683	1661	2210	1027	4531	1092	921	672	1778	440	208
	Mean	3468	1888	2428	1188	4881	1144	985	765	2135	535	251
	SD	429	206	237	169	357	87	75	53	234	84	26

Table A12: **M_3** receptor densities (fmol/mg protein) and mean densities ± SD of controls and *Pitx3 aphakia* mice in various brain regions (Ligand: [^{3}H]-**4-DAMP**).

Animal	Group	OB	M	S	Pir	CPu	CA1	CA2/3	DG	V	SN	CB
1	Control	2219	4397	4767	3906	8557	7449	4148	5790	5320	468	
2	Control	2435	4239	4745	3970	8826	7825	4465	6651	5041	590	
3	Control	2478	4403	4747	3889	9027	7271	4396	6177	5351	654	
4	Control	2368	4255	4493	4112	8700	6573	3968	5654	5545	636	
5	Control	2311	4216	4819	4190	7875	8032	5051	6976	5080	639	
6	Control	2489	4621	5024	4294	8115	7957	4610	6768	5677	621	
	Mean	2383	4355	4766	4060	8517	7518	4440	6336	5336	601	
	SD	105	154	170	164	439	549	378	545	250	69	
11	*Pitx3 aphakia*	2720	5710	5880	5183	9313	8961	4622	7228	6451	547	
12	*Pitx3 aphakia*	2361	5675	5161	4747	9169	9169	4690	6937	6932	759	
13	*Pitx3 aphakia*	1896	5728	5934	4794	9174	8623	4997	7021	5902	724	
14	*Pitx3 aphakia*	2122	5677	5675	4754	8316	7993	4261	6280	6033	650	
15	*Pitx3 aphakia*	2211	4621	5327	4297	9128	7725	3786	6166	5794	661	
16	*Pitx3 aphakia*	2085	5010	5402	4887	8824	7756	4439	6653	5784	728	
17	*Pitx3 aphakia*	2392	5196	5168	4221	8440	8238	4451	6889	6963	875	
18	*Pitx3 aphakia*	2690	5308	5608	4789	9408	7935	3957	6484	6255	791	
19	*Pitx3 aphakia*	2670	5534	5596	4717	8376	8195	4485	6596	6643	774	
20	*Pitx3 aphakia*	2399	4895	4930	4286	8459	7478	4145	6169	5352	621	
21	*Pitx3 aphakia*	2642	4786	5200	4682	8523	8047	4365	6396	6641	473	
22	*Pitx3 aphakia*	2363	4878	4854	4098	8456	8039	4268	6329	6428	762	
	Mean	2379	5252	5395	4621	8799	8180	4372	6596	6265	697	
	SD	267	407	350	322	412	504	326	354	500	112	

Table A13: **Nicotinic** receptor densities (fmol/mg protein) and mean densities ± SD of controls and *Pitx3 aphakia* mice in various brain regions (Ligand: [^{3}H]-**Epibatidine**).

Animal	Group	OB	M	S	Pir	CPu	CA1	CA2/3	DG	V	SN	CB
1	Control	224	435	423	225	590	206	179	246	440	334	
2	Control	231	498	419	206	576	237	204	288	512	353	
3	Control	252	455	410	230	585	230	185	285	441	393	
4	Control	260	441	386	248	520	249	183	280	466	316	
5	Control	238	422	394	231	528	228	201	254	462	268	
6	Control	249	451	384	225	549	225	197	286	413	313	
	Mean	242	450	403	227	558	229	192	273	456	329	
	SD	14	26	17	14	30	14	11	18	33	42	
11	*Pitx3 aphakia*	228	423	372	176	268	187	138	198	431	318	
12	*Pitx3 aphakia*	199	449	399	200	278	191	147	194	387	282	
13	*Pitx3 aphakia*	190	419	363	263	274	199	150	224	372	252	
14	*Pitx3 aphakia*	184	395	385	193	273	206	129	219	343	231	
15	*Pitx3 aphakia*	208	406	367	213	256	179	126	186	361	333	
16	*Pitx3 aphakia*	190	423	380	246	264	164	130	192		253	
17	*Pitx3 aphakia*	217	497	468	224	331	224	175	219	445	405	
18	*Pitx3 aphakia*	241	476	443	261	311	211	169	241	444	471	
19	*Pitx3 aphakia*	243	475	458	260	318	237	202	258	468	407	
20	*Pitx3 aphakia*	259	520	481	233	347	250	213	296	465	372	
21	*Pitx3 aphakia*	251	453	416	203	313	244	180	267	435	361	
22	*Pitx3 aphakia*	239	492	443	230	336	235	191	252	434	362	
	Mean	221	452	415	225	297	211	163	229	417	337	
	SD	26	40	43	29	32	28	30	34	43	73	

Table A14: **α_1** receptor densities (fmol/mg protein) and mean densities ± SD of controls and *Pitx3 aphakia* mice in various brain regions (Ligand: [^{3}H]-**Prazosin**).

Animal	Group	OB	M	S	Pir	CPu	CA1	CA2/3	DG	V	SN	CB
1	Control	770	1025	648	469	207	240	246	264	648	259	316
2	Control	829	1000	606	510	220	244	257	288	579	327	330
3	Control	833	1021	618	494	225	244	255	259	613	313	323
4	Control	819	1003	733	504	246	260	257	273	664	370	316
5	Control	915	990	606	532	208	241	243	238	593	277	325
6	Control	854	985	636	526	219	236	242	269	608	344	309
	Mean	837	1004	641	506	221	244	250	265	618	315	320
	SD	47	16	48	23	14	9	7	17	33	42	8
11	*Pitx3 aphakia*	982	1175	653	631	256	267	288	317	598	376	324
12	*Pitx3 aphakia*	991	1157	647	620	236	262	293	292	599	377	348
13	*Pitx3 aphakia*	908	1176	697	638	263	269	286	299	716	468	352
14	*Pitx3 aphakia*	900	1193	629	560	230	260	275	287	586	288	376
15	*Pitx3 aphakia*	951	991	712	569	250	275	290	290	607	369	354
16	*Pitx3 aphakia*	977	1012	627	624	237	283	278	314	611	459	363
17	*Pitx3 aphakia*	946	1054	606	569	214	228	262	272	536	325	318
18	*Pitx3 aphakia*	924	943	582	551	223	250	274	290	550	392	301
19	*Pitx3 aphakia*	940	1151	646	538	240	244	273	261	624	386	340
20	*Pitx3 aphakia*	929	1043	643	539	225	271	297	297	600	341	291
21	*Pitx3 aphakia*	989	987	635	526	227	248	266	287	512	321	324
22	*Pitx3 aphakia*	1026	1059	654	615	237	295	299	321	753	385	318
	Mean	955	1078	644	582	236	263	282	294	608	374	334
	SD	38	88	35	41	14	18	12	17	68	53	26

Table A15: **α_2** receptor densities (fmol/mg protein) and mean densities ± SD of controls and *Pitx3 aphakia* mice in various brain regions (Ligand: [^{3}H]-**UK14,304**).

Animal	Group	OB	M	S	Pir	CPu	CA1	CA2/3	DG	V	SN	CB
1	Control	254	230	231	510	130	289	198	260	294	200	197
2	Control	261	251	254	414	156	267	200	233	285	257	189
3	Control	236	231	216	373	134	279	180	219	245	189	152
4	Control	251	217	199	315	128	225	132	202	254	146	149
5	Control	228	246	258	419	136	298	165	241	249	214	174
6	Control	186	199	199	288	125	253	142	178	258	190	133
	Mean	236	229	226	386	135	269	169	222	264	199	166
	SD	27	19	26	80	11	27	29	29	20	36	25
11	*Pitx3 aphakia*	309	282	276	453	193	280	162	285	336	303	235
12	*Pitx3 aphakia*	283	316	296	450	211	307	241	326	424	360	234
13	*Pitx3 aphakia*	302	266	237	421	177	285	200	282	291	246	189
14	*Pitx3 aphakia*	286	273	234	399	160	258	219	276	340	230	186
15	*Pitx3 aphakia*	243	238	222	363	141	218	150	211	270	264	178
16	*Pitx3 aphakia*	262	282	243	400	160	270	199	282	278	266	203
17	*Pitx3 aphakia*	227	236	221	390	124	305	194	292	311	201	172
18	*Pitx3 aphakia*	287	250	251	442	148	268	172	251	282	187	179
19	*Pitx3 aphakia*	305	281	251	418	168	294	188	300	320	242	176
20	*Pitx3 aphakia*	208	216	205	344	127	211	154	219	230	186	138
21	*Pitx3 aphakia*	266	224	198	343	147	255	142	241	253	252	149
22	*Pitx3 aphakia*	306	256	235	434	160	234	169	248	245	270	163
	Mean	274	260	239	405	160	266	183	268	298	251	183
	SD	33	29	28	39	26	32	30	34	53	49	29

Table A16: **5-HT$_{1A}$** receptor densities (fmol/mg protein) and mean densities ± SD of controls and *Pitx3 aphakia* mice in various brain regions (Ligand: [^{3}H]-**8-OH-DPAT**).

Animal	Group	OB	M	S	Pir	CPu	CA1	CA2/3	DG	V	SN	CB
1	Control	80	244	209	151	54	785	124	180	186	43	
2	Control	78	218	190	149	48	721	135	173	148	57	
3	Control	84	187	177	161	48	776	139	164	172	54	
4	Control	71	207	170	158	45	750	126	152	143	43	
5	Control	77	197	171	144	44	771	135	178	144	46	
6	Control	82	159	131	96	44	720	122	184	131	48	
	Mean	79	202	175	143	47	754	130	172	154	49	
	SD	5	29	26	24	4	28	7	12	21	6	
11	*Pitx3 aphakia*	86	237	191	150	56	691	111	162	173	43	
12	*Pitx3 aphakia*	71	241	193	172	48	700	134	171	165	47	
13	*Pitx3 aphakia*	62	216	157	145	47	710	128	150	162	46	
14	*Pitx3 aphakia*	67	213	182	168	43	634	118	120	221	45	
15	*Pitx3 aphakia*	68	216	179	137	42	655	118	120	161	47	
16	*Pitx3 aphakia*	57	189	152	136	40	699	124	137	151	53	
17	*Pitx3 aphakia*	59	235	147	110	48	667	136	145	159	46	
18	*Pitx3 aphakia*	64	186	158	146	44	742	109	131	152	53	
19	*Pitx3 aphakia*	75	213	181	153	47	733	135	176	174	50	
20	*Pitx3 aphakia*	66	201	147	119	42	763	125	152	166	49	
21	*Pitx3 aphakia*	75	185	155	120	43	714	120	161	155	50	
22	*Pitx3 aphakia*	68	210	169	142	43	737	128	177	165	49	
	Mean	68	212	168	142	45	704	124	150	167	48	
	SD	8	19	17	19	4	38	9	20	18	3	

Table A17: **5-HT$_2$** receptor densities (fmol/mg protein) and mean densities ± SD of controls and *Pitx3 aphakia* mice in various brain regions (Ligand: [^{3}H]-**Ketanserin**).

Animal	Group	OB	M	S	Pir	CPu	CA1	CA2/3	DG	V	SN	CB
1	Control	342	797	735	658	1116	513	482	445	591	332	267
2	Control	388	801	728	721	1183	519	470	459	643	542	310
3	Control	378	805	769	869	1071	530	504	428	632	382	283
4	Control	338	804	797	777	1331	543	473	377	632	407	276
5	Control	348	776	750	686	1266	523	499	422	613	250	241
6	Control	347	722	680	699	988	489	453	392	543	338	232
	Mean	357	784	743	735	1159	520	480	421	609	375	268
	SD	21	32	40	77	127	18	19	31	37	98	29
11	*Pitx3 aphakia*	373	739	681	585	546	472	455	403	504	362	252
12	*Pitx3 aphakia*	399	827	742	617	652	567	555	485	657	432	302
13	*Pitx3 aphakia*	321	680	661	734	591	497	478	441	626	372	312
14	*Pitx3 aphakia*	365	720	799	731	593	476	468	432	638	498	316
15	*Pitx3 aphakia*	361	734	712	753	554	476	444	447	613	358	278
16	*Pitx3 aphakia*	412	721	707	765	707	572	572	513	653	382	321
17	*Pitx3 aphakia*	332	674	627	548	536	410	418	355	539	218	255
18	*Pitx3 aphakia*	344	630	621	633	627	495	440	448	513	295	290
19	*Pitx3 aphakia*	367	807	768	647	672	452	487	427	554	363	270
20	*Pitx3 aphakia*	317	777	673	658	632	489	470	408	566	408	279
21	*Pitx3 aphakia*	331	706	662	605	567	484	467	408	581	433	288
22	*Pitx3 aphakia*	337	786	738	651	626	518	533	473	676	453	278
	Mean	355	733	699	661	608	492	482	437	593	381	287
	SD	30	58	55	70	53	45	47	42	58	74	23

Table A18: **D$_1$** receptor densities (fmol/mg protein) and mean densities ± SD of controls and *Pitx3 aphakia* mice in various brain regions (Ligand: [^{3}H]-**SCH 23390**).

Animal	Group	OB	M	S	Pir	CPu	CA1	CA2/3	DG	V	SN	CB
1	Control					5061					1388	
2	Control					3543					1175	
3	Control					4266					1186	
4	Control					4567					1474	
5	Control					3863					0	
6	Control					4062					1454	
	Mean					4227					1113	
	SD					537					560	
11	*Pitx3 aphakia*					5050					1272	
12	*Pitx3 aphakia*					5303					1444	
13	*Pitx3 aphakia*					5014					1451	
14	*Pitx3 aphakia*					4032					1181	
15	*Pitx3 aphakia*					3836					1155	
16	*Pitx3 aphakia*					5379					1360	
17	*Pitx3 aphakia*					4631					1710	
18	*Pitx3 aphakia*					4124					1325	
19	*Pitx3 aphakia*					4979					1357	
20	*Pitx3 aphakia*					3617					1293	
21	*Pitx3 aphakia*					4131					1104	
22	*Pitx3 aphakia*					3839					890	
	Mean					4495					1295	
	SD					631					205	

Table A19: **D_2** receptor densities (fmol/mg protein) and mean densities ± SD of controls and *Pitx3 aphakia* mice in various brain regions (Ligand: [^{3}H]-**Raclopride**).

Animal	Group	OB	M	S	Pir	CPu	CA1	CA2/3	DG	V	SN	CB
1	Control					886						
2	Control					931						
3	Control					900						
4	Control					886						
5	Control					961						
6	Control					864						
	Mean					904						
	SD					35						
11	*Pitx3 aphakia*					1070						
12	*Pitx3 aphakia*					1000						
13	*Pitx3 aphakia*					952						
14	*Pitx3 aphakia*					963						
15	*Pitx3 aphakia*					925						
16	*Pitx3 aphakia*					1017						
17	*Pitx3 aphakia*					973						
18	*Pitx3 aphakia*					947						
19	*Pitx3 aphakia*					931						
20	*Pitx3 aphakia*					947						
21	*Pitx3 aphakia*					994						
22	*Pitx3 aphakia*					1004						
	Mean					977						
	SD					42						

Table A20: **D_2 / D_3** receptor densities (fmol/mg protein) and mean densities ± SD of controls and *Pitx3 aphakia* mice in various brain regions (Ligand: [^{3}H]-**Fallypride**).

Animal	Group	OB	M	S	Pir	CPu	CA1	CA2/3	DG	V	SN	CB
1	Control					2808						
2	Control					2253						
3	Control					2321						
4	Control					2571						
5	Control					2453						
6	Control					2678						
	Mean					2514						
	SD					212						
11	*Pitx3 aphakia*					2883						
12	*Pitx3 aphakia*					2717						
13	*Pitx3 aphakia*					2219						
14	*Pitx3 aphakia*					2442						
15	*Pitx3 aphakia*					2257						
16	*Pitx3 aphakia*					2083						
17	*Pitx3 aphakia*					2523						
18	*Pitx3 aphakia*					2509						
19	*Pitx3 aphakia*					2779						
20	*Pitx3 aphakia*					2304						
21	*Pitx3 aphakia*					2400						
22	*Pitx3 aphakia*					2638						
	Mean					2480						
	SD					243						

Table A21: **A_{2A}** receptor densities (fmol/mg protein) and mean densities ± SD of controls and *Pitx3 aphakia* mice in various brain regions (Ligand: [^{3}H]-**ZM 241 385**).

Animal	Group	OB	M	S	Pir	CPu	CA1	CA2/3	DG	V	SN	CB
1	Control					3006						
2	Control					3516						
3	Control					3846						
4	Control					3160						
5	Control					2837						
6	Control					3226						
	Mean					3265						
	SD					364						
11	*Pitx3 aphakia*					3876						
12	*Pitx3 aphakia*					2963						
13	*Pitx3 aphakia*					3140						
14	*Pitx3 aphakia*					3446						
15	*Pitx3 aphakia*					3030						
16	*Pitx3 aphakia*					4046						
17	*Pitx3 aphakia*					3783						
18	*Pitx3 aphakia*					3100						
19	*Pitx3 aphakia*					2810						
20	*Pitx3 aphakia*					3423						
21	*Pitx3 aphakia*					3661						
22	*Pitx3 aphakia*					3297						
	Mean					3381						
	SD					393						

Table A22: **AMPA** receptor densities (fmol/mg protein) and mean densities ± SD of controls, *Parkin* and *DJ-1* knockout mice in various brain regions (Ligand: [^{3}H]-**AMPA**).

Animal	Group	OB	M	S	Pir	CPu	CA1	CA2/3	DG	V	SN	CB
1	Control	683	1265	1160	1637	1079	3142	2339	2254	1074	383	900
2	Control	806	1515	1195	1866	1285	3442	2370	2194	1313	344	683
3	Control	568	1191	1096	1696	1073	3079	2285	1876	1111	396	396
4	Control	549	994	919	1328	876	2400	1828	1406	958	383	699
5	Control	444	861	891	1301	878	2865	2001	1685	915	291	558
6	Control	446	933	833	1301	726	2409	1673	1618	854	300	587
7	Control	555	877	855	1307	635	2922	1989	1792	938	302	540
8	Control	605	1064	950	1581	869	3351	2410	2172	956	320	695
9	Control	469	1178	1024	1658	863	3499	2389	2191	1003	341	723
10	Control	694	1053	954	1515	782	2342	1829	1504	960	407	537
	Mean	582	1093	988	1519	907	2945	2111	1869	1008	347	632
	SD	118	201	127	201	191	438	278	316	130	43	138
11	*Parkin* knockout	496	1090	896	1330	864	2618	1921	1656	863	365	358
12	*Parkin* knockout	411				874	3026	2159	1813	970	422	447
13	*Parkin* knockout	451	769	757	1392	743	1630	1511	1187	938	336	455
14	*Parkin* knockout	551	641	606	1051	643	1543	1241	1052	787	299	357
15	*Parkin* knockout	373	622	796	1213	670	1413	1493	1281	588	253	291
16	*Parkin* knockout	409				583	1380	1106	1043		267	262
17	*Parkin* knockout	632				554	1680	1411	1127		330	345
18	*Parkin* knockout	509	1004	978	1738	969	2567	2127	1872	1038	379	449
19	*Parkin* knockout	459	945	829	1305	694	1829	1581	1291	847	383	410
20	*Parkin* knockout	511	1003	912	1236	758	1704	1420	1185	961	344	355
	Mean	480	868	825	1324	735	1939	1597	1351	874	338	373
	SD	77	189	122	213	134	579	358	312	140	53	67
21	*DJ-1* knockout	489	902	850	1308	801	2730	1828	1596	1000	399	533
22	*DJ-1* knockout	558	1003	858	1426	799	3310	2319	2136	956	455	591
23	*DJ-1* knockout	522	1038	922	1420	927	2421	1649	1448	1214	424	510
24	*DJ-1* knockout	570	909	895	1434	926	2520	1915	1725	1023	496	545
25	*DJ-1* knockout	663	840	808	1801	722	2312	1802	1652	838	306	321
26	*DJ-1* knockout	426	903	844	1370	753	2285	1850	1484	1149	418	422
27	*DJ-1* knockout	480	1162	1016	1767	970	2397	1830	1606	1036	355	422
28	*DJ-1* knockout	530	1500	1411	2246	1329	3325	2792	2568	1147	399	540
29	*DJ-1* knockout	431	849	821	1166	673	2398	1943	1695	846	351	652
30	*DJ-1* knockout	453	1037	1050	1313	815	2200	1863	1570	1089	442	369
	Mean	512	1014	948	1525	872	2590	1979	1748	1030	405	491
	SD	73	198	182	321	187	409	333	345	126	56	104

Table A23: **Kainate** receptor densities (fmol/mg protein) and mean densities ± SD of controls, *Parkin* and *DJ-1* knockout mice in various brain regions (Ligand: [^{3}H]-**Kainate**).

Animal	Group	OB	M	S	Pir	CPu	CA1	CA2/3	DG	V	SN	CB
1	Control	1554	1999	1477	1036	2174	589	2193	1484	1789	284	558
2	Control	1250	1946	1569	1168	2318	605	2317	1596	1799	268	576
3	Control	1888	2299	1742	1448	2512	812	2673	1909	2321	424	745
4	Control	2336	2463	1827	1567	2833	871	2910	2067	2157	303	741
5	Control	1798	1892	1568	1207	2264	622	2193	1554	1815	326	652
6	Control	1572	2022	1621	1302	2302	674	2130	1610	1990	341	685
7	Control	1812	2115	1685	1196	2388	646	1966	1607	2014	346	688
8	Control	1794	2096	1692	1128	2352	622	1958	1568	1833	313	679
9	Control	1971	2213	1838	1415	2482	623	2075	1697	1931	219	578
10	Control	1943	2289	1818	1235	2451	589	2022	1619	2028	207	660
	Mean	1792	2133	1684	1270	2408	665	2244	1671	1968	303	656
	SD	290	180	124	163	182	97	314	180	173	64	66

11	*Parkin* knockout	1887	2193	1969	1475	2555	705	2558	1718	2487	256	664
12	*Parkin* knockout	1632				2433	698	2739	1662	1971	311	624
13	*Parkin* knockout	2286	2610	2041	1665	2987	823	2637	1930	2362	354	800
14	*Parkin* knockout	2226	2790	2124	1737	2787	839	2442	1920	2580	357	765
15	*Parkin* knockout	2054	2328	1893	1536	2473	749	2506	1769	2128	315	724
16	*Parkin* knockout	1810				2090	648	1989	1544		342	711
17	*Parkin* knockout	2169				2311	676	2100	1629		318	623
18	*Parkin* knockout	1957	2386	2026	1719	2454	753	2171	1726	2350	270	730
19	*Parkin* knockout	2085	2463	2032	1568	2513	605	2236	1683	2805	214	700
20	*Parkin* knockout	2103	2381	1992	1645	2402	674	2292	1787	2153	195	712
	Mean	2021	2450	2011	1621	2501	717	2367	1737	2354	293	705
	SD	201	196	71	97	246	74	247	121	270	57	57
21	*DJ-1* knockout	1793	2452	2087	1425	2473	681	2422	1690	2090	242	674
22	*DJ-1* knockout	1981	2076	1769	1397	2395	628	2088	1494	1988	276	682
23	*DJ-1* knockout	2289	2454	1901	1491	2561	700	2452	1747	2506	258	678
24	*DJ-1* knockout	1966	2688	2043	1448	2875	808	2893	1926	2131	364	704
25	*DJ-1* knockout	2090	2351	1889	1651	2370	692	2592	1702	2264	333	696
26	*DJ-1* knockout	2151	2558	1942	1540	2612	790	2635	1915	2704	360	774
27	*DJ-1* knockout	1933	2176	1779	1269	2303	632	2207	1630	2258	285	739
28	*DJ-1* knockout	1738	2350	1863	1278	2491	746	2476	1753	2157	317	684
29	*DJ-1* knockout	2040	2482	2101	1592	2490	686	2525	1905	2525	256	659
30	*DJ-1* knockout	2274	2497	1988	1541	2384	683	2179	1860	2311	263	736
	Mean	2025	2408	1936	1463	2495	705	2447	1762	2293	295	703
	SD	183	179	118	126	162	60	241	141	223	45	36

Table A24: **NMDA** receptor densities (fmol/mg protein) and mean densities ± SD of controls, *Parkin* and *DJ-1* knockout mice in various brain regions (Ligand: [^{3}H]-**MK 801**).

Animal	**Group**	**OB**	**M**	**S**	**Pir**	**CPu**	**CA1**	**CA2/3**	**DG**	**V**	**SN**	**CB**
1	Control	1449	1890	1822	1832	1318	3489	2244	2783	2048	631	
2	Control	1074	1838	1765	1832	1289	3298	2232	2727	1986	580	
3	Control	964	1737	1732	1564	1122	3361	2143	2722	2174	859	
4	Control	1159	1881	1814	1830	1260	3527	2388	2857	2154	792	
5	Control	1158	1865	1786	1771	1308	3412	2337	2781	2035	733	
6	Control	1154	1889	1880	1845	1317	3585	2356	2917	1992	725	
7	Control	1294	1985	2015	1922	1504	3462	2401	2881	2263	936	
8	Control	1259	1732	1781	1881	1392	3555	2449	2869	1967	736	
9	Control	1024	1733	1666	1939	1295	3397	2161	2665	1895	605	
10	Control	1104	1750	1750	1858	1414	3637	2353	2769	1939	525	
	Mean	1164	1830	1801	1827	1322	3472	2306	2797	2045	712	
	SD	133	83	90	99	96	101	99	77	111	122	
11	*Parkin* knockout	1349	1980	1809	2011	1378	3478	2329	2792	2124	671	
12	*Parkin* knockout	1169				1432	3532	2313	2917	2216	705	
13	*Parkin* knockout	1090	1907	2020	2090	1484	3859	2535	3074	2086	830	
14	*Parkin* knockout	1381	1899	1890	1953	1341	4011	2563	3069	2135	658	
15	*Parkin* knockout	1197	1864	1914	1812	1339	3617	2431	2971	2069	675	
16	*Parkin* knockout	1132				1400	3562	2433	2776		723	
17	*Parkin* knockout	1574				1604	4238	2718	3414		888	
18	*Parkin* knockout	1377	2069	1843	2318	1459	4040	2566	3114	2274	628	
19	*Parkin* knockout	1017	1674	1670	1874	1245	4020	2419	2890	1944	463	
20	*Parkin* knockout	1068	1847	1714	2047	1381	4017	2454	3024	2007	527	
	Mean	1235	1891	1837	2015	1406	3837	2476	3004	2107	677	
	SD	168	113	111	153	92	254	116	176	99	119	
21	*DJ-1* knockout	1280	1809	1822	1879	1357	3354	2291	2769	2093	679	
22	*DJ-1* knockout	1343	2113	1986	1864	1382	3569	2429	2903	2058	698	
23	*DJ-1* knockout	1200	2063	1856	1815	1345	3647	2297	2979	1998	681	
24	*DJ-1* knockout	1280	1961	1942	1808	1310	3485	2443	2936	2032	635	

25	*DJ-1* knockout	1236	2081	1917	1786	1303	3437	2290	2790	2052	775	
26	*DJ-1* knockout	1401	2034	1975	1902	1372	3447	2373	2819	2220	757	
27	*DJ-1* knockout	1252	1893	1784	1764	1424	3540	2352	2909	1987	743	
28	*DJ-1* knockout	1169	1925	1827	2010	1521	3604	2369	2952	2026	697	
29	*DJ-1* knockout	1058	1786	1658	2114	1254	3561	2242	2866	1946	556	
30	*DJ-1* knockout	1159	1776	1741	1823	1380	3822	2377	3072	1945	647	
	Mean	1238	1944	1851	1877	1365	3547	2346	2900	2036	687	
	SD	93	120	101	104	69	124	62	88	76	61	

Table A25: **$mGlu_{2/3}$** receptor densities (fmol/mg protein) and mean densities ± SD of controls, *Parkin* and *DJ-1* knockout mice in various brain regions (Ligand: [^{3}H]-**LY 341,495**).

Animal	**Group**	**OB**	**M**	**S**	**Pir**	**CPu**	**CA1**	**CA2/3**	**DG**	**V**	**SN**	**CB**
1	Control	2952	9207	10388	8219	7656	4821	3083	7613	10541	4291	2325
2	Control	2747	10354	11312	10734	9254	5475	3428	8136	12116	4660	2377
3	Control	2481	9777	10084	10162	7140	4733	2906	8157	10769	5056	2002
4	Control	2923	9865	11193	11764	7775	4392	2582	6641	13708	4630	1948
5	Control	2432	12058	12504	10656	9238	5257	3140	8164	13255	4068	1876
6	Control	2848	9750	10060	9658	8482	4597	2789	8142	12843	4345	2462
7	Control	2373	9547	9687	10059	8333	4559	2687	6844	9453	4137	1926
8	Control	2792	7602	7863	8018	5472	3627	2423	5363	8394	4207	2038
9	Control	2425	6427	6125	7525	4260	3322	2160	4545	7500	3246	1927
10	Control	2129	9063	10134	10325	6877	3990	2716	6185	10046	4086	2000
	Mean	2610	9365	9935	9712	7449	4477	2792	6979	10862	4273	2088
	SD	278	1516	1802	1363	1597	676	368	1299	2094	477	214
11	*Parkin* knockout	2941	10825	11000	10205	8242	4552	3080	7247	12558	4245	2365
12	*Parkin* knockout	3257				8593	4678	3098	7685	10806	4695	2704
13	*Parkin* knockout	1832	12950	12557	8728	10435	4781	2545	7426	10896	4086	1768
14	*Parkin* knockout	1904	8444	9590	9041	8586	4012	2386	6578	5371	4086	1588
15	*Parkin* knockout	2561	10128	10516	11130	9205	4630	2774	8571	12106	3898	1919
16	*Parkin* knockout	2433				9492	4867	2568	7642		4027	2295
17	*Parkin* knockout	2644				8840	3789	2241	7086		4210	2098
18	*Parkin* knockout	2801	9845	10139	13144	8242	3812	2407	5836	9715	3947	2415
19	*Parkin* knockout	2473	7622	6678	7871	6037	3118	2022	4856	7965	3273	1893
20	*Parkin* knockout	2383	9726	9390	8574	8038	4748	2716	7165	13305	3785	2470
	Mean	2523	9934	9981	9813	8571	4299	2584	7009	10340	4025	2151
	SD	434	1710	1798	1829	1141	582	345	1041	2621	363	354
21	*DJ-1* knockout	3190	11096	11562	9447	9233	5950	3621	7876	10460	5006	2587
22	*DJ-1* knockout	2965	10258	11301	9902	9058	5672	3644	7982	11718	4587	2660
23	*DJ-1* knockout	1896	8904	9489	9065	8042	5227	3039	7892	9997	4536	1881
24	*DJ-1* knockout	2342	9737	9945	9224	9607	4181	2591	7103	10967	4419	1669
25	*DJ-1* knockout	2505	11495	12729	11099	10038	5568	3199	8359	12518	4967	1897
26	*DJ-1* knockout	2437	11840	11913	9846	9827	4763	2925	8660	14013	4584	2031
27	*DJ-1* knockout	2958	9709	10028	7057	6662	4205	2853	5585	11015	4489	2503
28	*DJ-1* knockout	3175	9731	10894	9815	7892	3803	2650	5995	11344	4401	2266
29	*DJ-1* knockout	2188	5925	6281	5758	4267	4038	2342	4999	8337	3160	1857
30	*DJ-1* knockout	2656	11283	10073	9511	8428	5390	3043	7845	13418	4459	2294
	Mean	2631	9998	10422	9072	8306	4880	2991	7230	11379	4461	2164
	SD	435	1718	1775	1540	1755	778	421	1262	1661	504	346

Table A26: **$GABA_A$** receptor densities (fmol/mg protein) and mean densities ± SD of controls, *Parkin* and *DJ-1* knockout mice in various brain regions (Ligand: [^{3}H]-**Muscimol** - agonist).

Animal	Group	OB	M	S	Pir	CPu	CA1	CA2/3	DG	V	SN	CB
1	Control	588	1234	1481	986	866	955	612	1246	965	243	1976
2	Control	1064	1150	1374	809	867	976	712	1311	1438	281	2801
3	Control	1760	1566	1787	1405	1008	1585	849	1858	1962	741	3350
4	Control	2519	2063	2575	1656	1332	1779	901	2176	2808	1146	4300
5	Control	2688	2485	2848	2213	1481	1752	968	2203	2577	850	4716
6	Control	2696	2764	2958	2343	1730	1985	953	2171	2832	1021	4731
7	Control	1609	1808	2156	1574	1096	1571	830	1561	1398	500	2562
8	Control	807	1046	973	824	549	977	595	1037	1259	391	2100
9	Control	1577	1515	1721	1466	956	1340	880	1505	1521	433	2353
10	Control	2987	2228	2624	1906	1327	2073	1166	2286	2627	666	4321
	Mean	1829	1786	2050	1518	1121	1499	847	1735	1939	627	3321
	SD	856	587	683	539	347	420	173	461	712	310	1104
11	*Parkin* knockout	843	1023	989	767	714	919	571	1114	942	226	2282
12	*Parkin* knockout	2470				1423	1818	1050	2118	3073	1038	4339
13	*Parkin* knockout	782	1212	1400	1300	1122	1161	649	1469	1416	575	3014
14	*Parkin* knockout	1270	1321	1877	1805	1251	1436	792	1496	1729	315	3357
15	*Parkin* knockout	2361	2431	2702	2361	2084	1645	1080	2128	2933	929	5173
16	*Parkin* knockout	2109				970	1271	892	1574		341	2419
17	*Parkin* knockout	2795				1200	1611	868	1807		685	2984
18	*Parkin* knockout	2276	2326	2749	2363	1387	2055	1126	2310	3372	622	4349
19	*Parkin* knockout	951	1178	1377	1140	819	1002	795	1363	1314	413	2398
20	*Parkin* knockout	2768	3133	3592	2566	2270	2640	1292	2926	3565	1409	4990
	Mean	1863	1804	2098	1757	1324	1556	911	1830	2293	655	3531
	SD	812	818	941	702	505	524	225	542	1047	373	1097
21	*DJ-1* knockout	942	1052	1134	1011	702	1231	715	1505	1318	238	2941
22	*DJ-1* knockout	2661	2590	3037	2146	1738	1963	989	2020	2830	1163	4318
23	*DJ-1* knockout	2611	2102	2187	1841	1339	2283	1086	2111	2526	890	5051
24	*DJ-1* knockout	1923	2130	2568	2121	1515	1704	979	2074	2539	1119	4633
25	*DJ-1* knockout	3217	3049	3439	3411	1966	2225	1108	2319	3276	906	4129
26	*DJ-1* knockout	1114	1212	1372	994	753	1123	859	1364	1404	403	2449
27	*DJ-1* knockout	1868	2254	2161	1492	1323	2211	1052	2535	2882	1225	4937
28	*DJ-1* knockout	1093	1499	1685	1210	894	1158	872	1425	1458	428	1656
29	*DJ-1* knockout	857	1100	1394	1374	868	1155	770	1157	1276	396	2258
30	*DJ-1* knockout	3128	2275	2830	2314	1690	2506	1368	2584	3267	1423	4009
	Mean	1941	1926	2181	1791	1279	1756	980	1910	2278	819	3638
	SD	918	678	782	744	452	549	190	512	826	421	1213

Table A27: **$GABA_A$** receptor densities (fmol/mg protein) and mean densities ± SD of controls, *Parkin* and *DJ-1* knockout mice in various brain regions (Ligand: [^{3}H]-**SR 95531** - antagonist).

Animal	Group	OB	M	S	Pir	CPu	CA1	CA2/3	DG	V	SN	CB
1	Control	2465	2194	2706	2904	1225	3702	2726	3016	2639	2381	2307
2	Control	2219	2806	2757	2681	1274	3935	2817	2963	2450	2466	2073
3	Control	2110	2848	2701	2967	1473	4053	2980	3170	2420	2713	1929
4	Control	1778	3001	2650	3287	1654	4004	3102	3290	2995	2499	2117
5	Control	2998	2838	2743	3199	1470	4941	3661	3634	4052	3260	2220
6	Control	2880	3535	3928	3563	1726	5301	3729	4134	4453	4086	2270
7	Control	3115	4309	4075	3791	2196	6580	4668	4809	3271	2961	2563
8	Control	2673	3680	3465	3475	1910	5809	4353	4153	3465	2765	2171
9	Control	2166	3295	2926	3536	1810	4946	3664	3455	2787	1784	1292
10	Control	2275	3734	3378	3279	1690	5154	3958	3936	3087	2084	1691
	Mean	2468	3224	3133	3268	1643	4843	3566	3656	3162	2700	2063
	SD	435	608	540	341	295	927	655	595	672	643	356

11	*Parkin* knockout	2397	2197	2069	2034	937	3586	2585	2738	2855	2393	2197
12	*Parkin* knockout	1606				1183	4553	3940	4037	3075	2646	1932
13	*Parkin* knockout	2266	2820	2670	3616	1610	3670	2566	2981	2558	2615	2241
14	*Parkin* knockout	2702	3324	2881	4134	1739	4627	3789	3968	2665	2410	1884
15	*Parkin* knockout	2809	2817	3139	3146	1468	4045	3637	3708	4031	3405	2176
16	*Parkin* knockout	1793				1760	4411	3352	3318		2764	2470
17	*Parkin* knockout	2349				1312	5748	4243	4282		2621	2369
18	*Parkin* knockout	2530	3115	2871	3693	1318	5104	3648	3765	3397	2540	2471
19	*Parkin* knockout	1581	2318	2223	2739	1095	4060	2951	3088	2108	1638	1561
20	*Parkin* knockout	2114	2610	2706	2838	1264	5378	3757	3916	3300	2175	2432
	Mean	2215	2743	2651	3171	1369	4518	3447	3580	2999	2521	2173
	SD	435	405	380	706	273	718	572	516	590	448	299
21	*DJ-1* knockout	2341	2951	3009	3413	1630	5260	4123	3985	2813	2599	2142
22	*DJ-1* knockout	1794	2599	2316	2607	1266	4991	3770	3712	2568	2039	2205
23	*DJ-1* knockout	1889	4155	3826	5233	2396	5596	4383	4166	4431	3513	2051
24	*DJ-1* knockout	1532	3203	3621	3772	1957	4684	3737	3730	3192	2934	2386
25	*DJ-1* knockout	2920	3099	3120	2838	1695	6820	5220	5221	3713	3005	2053
26	*DJ-1* knockout	3112	4287	4093	4386	2330	6977	5188	5290	4329	3015	2575
27	*DJ-1* knockout	1916	3662	3232	3067	1689	4234	3067	3215	3483	2380	1695
28	*DJ-1* knockout	1826	2916	2699	2948	1409	3809	3088	3032	3055	2161	1944
29	*DJ-1* knockout	1965	2607	2552	3281	1475	4951	3550	3532	2771	1883	1333
30	*DJ-1* knockout	2197	3328	3387	3332	1562	6078	4270	4089	3438	2513	1827
	Mean	2149	3281	3186	3488	1741	5340	4040	3997	3379	2604	2021
	SD	509	589	567	794	377	1041	756	754	635	512	352

Table A28: **BZ** receptor densities (fmol/mg protein) and mean densities ± SD of controls, *Parkin* and *DJ-1* knockout mice in various brain regions (Ligand: [^{3}H]-**Flumazenil**).

Animal	**Group**	**OB**	**M**	**S**	**Pir**	**CPu**	**CA1**	**CA2/3**	**DG**	**V**	**SN**	**CB**
1	Control	5954	5904	6644	4851	1395	6339	3512	4896	6940	5469	1823
2	Control	6856	5934	6737	5631	1440	6560	3971	4931	7350	5850	1962
3	Control	5741	5486	5800	4343	1159	5868	3278	4400	6965	4974	1602
4	Control	5582	4999	5657	4610	1190	5560	2963	4017	6878	5386	1747
5	Control	5114	5053	5690	4871	1482	6848	3747	4983	6585	5639	1529
6	Control	6091	5634	6470	5287	1562	5903	3591	4405	6677	6270	1773
7	Control	5343	5256	6193	5061	1453	5962	3241	4158	6083	6691	1538
8	Control	5344	4439	5197	4303	1269	4469	2620	3290	5671	5222	1577
9	Control	4241	3662	4025	3067	1233	4506	2598	3454	3422	2848	1408
10	Control	4776	3867	4470	3612	1432	4285	2948	3505	4652	4436	1704
	Mean	5504	5023	5688	4564	1361	5630	3247	4204	6122	5278	1666
	SD	728	801	906	771	138	914	465	634	1231	1065	165
11	*Parkin* knockout	6206	4694	4837	3365	1002	6539	3615	4837	6552	6226	1679
12	*Parkin* knockout	5345				1101	5066	3090	4323	6741	5710	1745
13	*Parkin* knockout	5209	5556	6269	4858	1406	6857	3971	5106	6902	6883	1987
14	*Parkin* knockout	6234	6100	7369	5474	1486	7574	4099	5305	6016	7194	1783
15	*Parkin* knockout	5858	5426	6588	5109	1489	6225	3700	4582	6642	7194	1640
16	*Parkin* knockout	5018				1254	5636	3461	4114		6193	1759
17	*Parkin* knockout	5863				1038	6285	3643	4662		6355	1661
18	*Parkin* knockout	4542	4919	5663	5519	1270	5730	3443	4450	5575	5195	1365
19	*Parkin* knockout	4134	3881	4181	3151	1077	4451	2823	3400	5327	3944	1615
20	*Parkin* knockout	4924	4819	6135	4342	1632	6142	3658	4575	5723	4970	1643
	Mean	5333	5056	5863	4545	1276	6051	3550	4535	6185	5986	1688
	SD	705	715	1077	966	220	888	378	532	600	1047	157
21	*DJ-1* knockout	5281	5403	6330	5522	1398	6451	3735	4730	6702	4495	1889
22	*DJ-1* knockout	6274	5654	6566	5316	1370	6150	3690	4699	6840	5511	2082
23	*DJ-1* knockout	6155	5765	6893	5307	1358	6031	3048	4087	6490	5902	1790
24	*DJ-1* knockout	5066	5751	7089	5188	1450	6167	3757	4704	6548	5456	2148

25	*DJ-1* knockout	6345	6905	7463	5979	1581	6726	3755	5012	6996	6634	1860
26	*DJ-1* knockout	6563	6256	7481	5772	1637	6316	3939	5346	6979	6337	1972
27	*DJ-1* knockout	4656	4962	5750	4182	1277	5445	3083	4231	5299	5277	1239
28	*DJ-1* knockout	3798	4318	5019	4312	1289	5556	3339	4149	5764	5486	1373
29	*DJ-1* knockout	3874	3560	4465	3397	1310	4944	2936	3390	5498	4647	1566
30	*DJ-1* knockout	5534	5455	6260	4432	1706	5925	3532	4459	5655	5143	1795
	Mean	5355	5403	6332	4941	1438	5971	3481	4481	6277	5489	1772
	SD	1009	947	1005	820	153	527	355	549	653	672	295

Table A29: **$GABA_B$** receptor densities (fmol/mg protein) and mean densities ± SD of controls, *Parkin* and *DJ-1* knockout mice in various brain regions (Ligand: [^{3}H]-**CGP 54626**).

Animal	**Group**	**OB**	**M**	**S**	**Pir**	**CPu**	**CA1**	**CA2/3**	**DG**	**V**	**SN**	**CB**
1	Control	1661	6328	5057	5173	2875	4857	6656	5935	5961	3294	4904
2	Control	1883	5483	5255	5365	2758	4741	6152	5691	6510	3374	5428
3	Control	2016	6632	6021	5872	2724	5572	7427	6428	5449	3806	5290
4	Control	1906	6302	5846	5242	2889	5417	6800	6138	6226	3217	5058
5	Control	2388	6539	6055	6262	3275	5641	7377	6142	6726	4201	5703
6	Control	2398	6873	6647	7040	3805	6166	7578	6945	7360	4422	6391
7	Control	1922	6977	6111	6289	3513	5498	6922	6544	7001	3963	5587
8	Control	2176	6815	6049	5653	3111	5116	6637	6379	6389	3248	5720
9	Control	2114	6629	6049	6158	3064	5749	6680	6529	6917	3629	4620
10	Control	2262	7027	6150	5946	3457	6007	7340	6672	6915	3618	5198
	Mean	2073	6561	5924	5900	3147	5477	6957	6340	6545	3677	5390
	SD	239	453	456	573	359	463	456	369	563	417	498
11	*Parkin* knockout	2001	6032	5075	5269	2907	5343	7191	6310	6159	3413	5250
12	*Parkin* knockout	2147				3128	5310	7316	6374	6638	3619	5267
13	*Parkin* knockout	2033	5992	5875	7245	3165	6652	8577	7745	8038	4366	5948
14	*Parkin* knockout	2229	7077	5792	8254	3508	6856	8392	7856	8477	3888	5555
15	*Parkin* knockout	2537	7923	6850	6824	4303	7078	8975	8070	8647	5251	6789
16	*Parkin* knockout	2448				3995	7234	9350	8491		4496	5688
17	*Parkin* knockout	2300				3742	6605	8637	7812		4538	5122
18	*Parkin* knockout	2408	7879	6993	9339	3576	6586	8502	7575	8039	3922	5452
19	*Parkin* knockout	2476	6852	6313	7487	3545	6465	8395	7456	7507	4213	5253
20	*Parkin* knockout	2333	6843	6534	7722	3586	6693	8181	7508	8320	4647	6146
	Mean	2291	6942	6205	7449	3545	6482	8352	7520	7728	4235	5647
	SD	186	775	672	1257	414	652	666	689	898	543	519
21	*DJ-1* knockout	2306	6438	6045	7946	3283	5915	7197	6634	7266	3616	5628
22	*DJ-1* knockout	2343	7586	6797	7330	3547	6046	7462	6992	8217	4176	6000
23	*DJ-1* knockout	2362	6641	5331	7359	3160	6631	7631	7593	8879	3958	5466
24	*DJ-1* knockout	2325	7477	7005	7545	3858	6698	8532	7909	7751	4448	6283
25	*DJ-1* knockout	2724	7931	8362	8032	4583	6683	8405	7648	8159	5018	5776
26	*DJ-1* knockout	3224	7943	7731	8865	4666	7193	8497	7619	8789	5175	5901
27	*DJ-1* knockout	2393	7998	6992	7782	3798	6048	7772	7093	7851	4520	5609
28	*DJ-1* knockout	2329	7683	7367	7572	3904	6539	8415	7752	8387	4791	6408
29	*DJ-1* knockout	2308	7550	6866	7469	3801	6489	7508	7159	7908	4571	5269
30	*DJ-1* knockout	2726	8057	7039	8123	3816	6747	8064	7350	7344	4781	5416
	Mean	2504	7530	6953	7802	3841	6499	7948	7375	8055	4505	5776
	SD	301	562	834	466	483	392	495	399	542	480	373

Table A30: **M_1** receptor densities (fmol/mg protein) and mean densities ± SD of controls, *Parkin* and *DJ-1* knockout mice in various brain regions (Ligand: [^{3}H]-**Pirenzepine**).

Animal	Group	OB	M	S	Pir	CPu	CA1	CA2/3	DG	V	SN	CB
1	Control	853	1165	1162	1378	2259	2218	1311	2102	1659	204	
2	Control	704	1535	1504	1830	2771	2402	1439	2339	1641	255	
3	Control	735	1596	1569	1853	2726	2560	1529	2499	1963	281	
4	Control	852	1562	1553	1764	2855	2563	1551	2428	1641	247	
5	Control	979	1885	1919	2099	3785	3444	2005	3255	2443	366	
6	Control	537	1345	1388	1487	2570	2616	1495	2431	1634	278	
7	Control	693	1694	1625	1861	2987	2793	1753	2816	2115	323	
8	Control	670	1454	1402	1751	2789	2573	1478	2441	1713	259	
9	Control	471	1121	1001	1369	2239	2121	1233	2133	1343	157	
10	Control	506	1031	1008	1427	2206	2158	1239	2005	1232	147	
	Mean	700	1439	1413	1682	2719	2545	1503	2445	1738	252	
	SD	165	272	289	250	467	385	236	368	356	68	
11	*Parkin* knockout	951	1599	1583	2042	3193	2840	1819	2906	1808	311	
12	*Parkin* knockout	1064				3501	3139	1867	2942		284	
13	*Parkin* knockout	1205	2157	2143	2698	4156	3746	2125	3671	2640	360	
14	*Parkin* knockout	1389	2083	1932	2517	4053	3917	2391	3765	2712	356	
15	*Parkin* knockout	926	1630	1611	1652	3389	3448	1929	3280	2121	271	
16	*Parkin* knockout				1287	3713	3377	2030	3368		295	
17	*Parkin* knockout					3635	3328	1907	3282		289	
18	*Parkin* knockout	1144	1470	1352	1870	3320	3048	1838	3024	1429	199	
19	*Parkin* knockout	808	1147	1303	1057	2640	2475	1422	2403	1426	132	
20	*Parkin* knockout	716	1267	1137	1460	2439	2470	1375	2461	1608	127	
	Mean	1025	1622	1580	1823	3404	3179	1870	3110	1964	262	
	SD	220	382	358	577	549	487	301	455	543	83	
21	*DJ-1* knockout	814	1758	1654	1736	3117	2908	1725	2696	2163	295	
22	*DJ-1* knockout	1225	2073	1986	2443	3515	3395	2200	3357	2243	318	
23	*DJ-1* knockout	1308	2459	2152	2802	3867	4108	2535	3797	3138	336	
24	*DJ-1* knockout	1209	2143	2088	2424	3800	3956	2256	3797	2340	311	
25	*DJ-1* knockout	1179	1513	1467	1153	3414	3687	2078	3614	2059	340	
26	*DJ-1* knockout	938	1904	1873	1888	3553	3270	1891	3043	2065	336	
27	*DJ-1* knockout	862	1640	1699	1768	2893	2900	1821	2901	2036	286	
28	*DJ-1* knockout	939	1781	2007	2216	3520	3366	2078	3159	2154	269	
29	*DJ-1* knockout	585	1334	1332	1465	2494	2369	1430	2465	1828	162	
30	*DJ-1* knockout	735	1418	1296	1511	2570	2637	1528	2589	1668	238	
	Mean	979	1802	1755	1941	3274	3260	1954	3142	2170	289	
	SD	241	351	314	517	485	563	342	490	392	55	

Table A31: **M_2** receptor densities (fmol/mg protein) and mean densities ± SD of controls, *Parkin* and *DJ-1* knockout mice in various brain regions (Ligand: [^{3}H]-**Oxotremorine-M** - agonist).

Animal	Group	OB	M	S	Pir	CPu	CA1	CA2/3	DG	V	SN	CB
1	Control	2430	1340	1670	739	2561	745	797	565	1510	429	200
2	Control	2427	1475	1820	838	2942	696	716	508	1540	400	205
3	Control	2229	1228	1521	744	2441	663	671	494	1352	411	210
4	Control	2198	1307	1523	741	2702	731	695	527	1270	373	221
5	Control	2268	1287	1644	726	2356	699	700	535	1508	354	180
6	Control	2276	1377	1795	872	2753	773	807	607	1556	406	191
7	Control	1971	1052	1353	660	2012	615	629	510	1163	408	189
8	Control	2186	1067	1370	638	2061	669	683	505	1287	327	196
9	Control	2284	1144	1517	778	2408	698	697	601	1549	367	199
10	Control	2299	1134	1479	678	2342	699	726	561	1340	337	211
	Mean	2257	1241	1569	741	2458	699	712	541	1407	381	200
	SD	130	140	160	74	293	44	54	40	142	35	12

11	*Parkin* knockout	2708	1462	1801	841	2931	661	656	469	1769	433	226
12	*Parkin* knockout	2657				3342	744	732	594	1611	443	213
13	*Parkin* knockout	2673	1422	1679	859	3684	731	743	604	1624	519	247
14	*Parkin* knockout	2775	1526	1845	942	3475	713	757	554	1321	463	230
15	*Parkin* knockout	2769	1326	1647	911	2822	619	658	476	1427	492	207
16	*Parkin* knockout	2496				2738	723	735	546		473	202
17	*Parkin* knockout	2391				3235	624	636	483		457	211
18	*Parkin* knockout	2450	1200	1556	1076	3228	626	637	503	1285	368	228
19	*Parkin* knockout	2540	1188	1650	860	2851	647	649	496	1398	349	205
20	*Parkin* knockout	2805	1356	1755	857	3103	672	653	497	1372	382	209
	Mean	2626	1354	1705	907	3141	676	686	522	1476	438	218
	SD	147	128	100	83	309	48	49	49	171	56	14
21	*DJ-1* knockout	2280	1534	1749	951	2357	840	831	624	1530	365	220
22	*DJ-1* knockout	2530	1552	1883	802	2576	796	883	665	1532	406	235
23	*DJ-1* knockout	2823	1541	1908	933	2555	767	775	617	1441	433	246
24	*DJ-1* knockout	2364	1680	1971	925	3409	768	870	646	1568	502	257
25	*DJ-1* knockout	2632	1461	1786	799	2876	849	857	675	1652	444	203
26	*DJ-1* knockout	2328	1525	1835	908	2796	825	850	638	1739	439	205
27	*DJ-1* knockout	2392	1274	1594	795	2104	729	744	573	1484	379	242
28	*DJ-1* knockout	2271	1353	1802	828	2597	803	798	601	1595	453	228
29	*DJ-1* knockout	2486	1346	1619	912	2592	772	785	620	1350	384	221
30	*DJ-1* knockout	2606	1462	1823	859	2932	832	866	707	1607	493	242
	Mean	2471	1473	1797	871	2679	798	826	637	1550	430	230
	SD	178	120	119	61	354	39	47	38	110	47	18

Table A32: **M_2** receptor densities (fmol/mg protein) and mean densities ± SD of controls, *Parkin* and *DJ-1* knockout mice in various brain regions (Ligand: [^{3}H]-**AF-DX 384** - antagonist).

Animal	**Group**	**OB**	**M**	**S**	**Pir**	**CPu**	**CA1**	**CA2/3**	**DG**	**V**	**SN**	**CB**
1	Control	2798	1641	1956	998	4629	991	852	669	1312	544	245
2	Control	2834	1345	1802	772	4298	929	820	651	1647	437	239
3	Control	1904	1812	1909	1160	4026	860	719	610	1621	777	249
4	Control	2438	1639	1881	1204	4147	1242	1133	1028	1855	594	438
5	Control	2357	1612	1981	1180	4207	1255	1148	1049	1890	505	266
6	Control	2446	2103	2173	1054	4353	1297	1126	1025	2005	531	276
7	Control	2630	1727	2097	1417	4007	1213	1122	1008	1635	656	246
8	Control	2509	2001	2194	1456	4368	1342	1178	1072	1893	561	286
9	Control	2610	1778	2104	1351	4272	1339	1188	1057	2213	548	261
10	Control	2576	1669	2033	1325	4280	1159	1038	905	1949	533	240
	Mean	2510	1733	2013	1192	4259	1163	1032	908	1802	569	275
	SD	262	212	130	210	180	175	170	188	253	92	59
11	*Parkin* knockout	3312	2005	2605	1824	4742	1398	1264	1091	2481	757	308
12	*Parkin* knockout	3017				5283	1448	1219	1073	1686	586	375
13	*Parkin* knockout	1747	1956	2559	1267	4787	1262	1023	926	1601	722	269
14	*Parkin* knockout	2583	2355	2338	1676	4421	1475	1339	1237	1883	808	319
15	*Parkin* knockout	2419	1536	1918	1096	4512	1616	1380	1205		646	230
16	*Parkin* knockout	2245				3946	1030	873	797		479	227
17	*Parkin* knockout	2517				4639	1058	1029	908		463	1400
18	*Parkin* knockout	2637	1405	1657	965	4034	1117	856	768	1174	474	223
19	*Parkin* knockout	2573	1307	1614	973	3947	1073	841	770	1443	447	192
20	*Parkin* knockout	2322	1418	1668	914	4265	1074	899	755	1303	429	225
	Mean	2537	1712	2051	1245	4458	1255	1072	953	1653	581	377
	SD	423	395	439	366	428	214	210	186	436	143	364
21	*DJ-1* knockout	2199	1912	2325	1204	4688	1312	1080	947	2192	905	344
22	*DJ-1* knockout	3043	1961	2345	1417	4860	1555	1261	1090	2033	673	354
23	*DJ-1* knockout	2465	2166	2249	1685	3910	1335	1174	1025	1870	760	279
24	*DJ-1* knockout	2531	1644	1884	1182	3992	1348	1202	1055	1750	575	268

25	*DJ-1* knockout	2498	1501	1698	750	3984	1041	965	839	1610	505	229
26	*DJ-1* knockout	2111	1728	1964	1186	3999	1295	1087	976	1805	527	246
27	*DJ-1* knockout	2580	1889	2247	1375	4058	1220	1125	995	1892	619	303
28	*DJ-1* knockout	2305	1839	2243	1221	4296	1419	1225	1087	2109	597	378
29	*DJ-1* knockout	2568	1975	2133	1456	4266	1258	1086	945	1566	550	321
30	*DJ-1* knockout	2592	1691	1956	899	4259	1265	1071	1016	1826	630	284
	Mean	2489	1831	2105	1237	4231	1305	1127	997	1865	634	301
	SD	257	193	217	270	319	133	88	76	202	121	48

Table A33: **M_3** receptor densities (fmol/mg protein) and mean densities ± SD of controls, *Parkin* and *DJ-1* knockout mice in various brain regions (Ligand: [^{3}H]-**4-DAMP**).

Animal	**Group**	**OB**	**M**	**S**	**Pir**	**CPu**	**CA1**	**CA2/3**	**DG**	**V**	**SN**	**CB**
1	Control	2498	3467	3642	2896	8034	6353	3263	5295	4239	585	203
2	Control	1309	3705	3842	3319	8152	6081	3389	5374	3950	591	214
3	Control	1223	3130	3302	2944	4988	5068	2665	4201	4178	789	581
4	Control	2038	2836	2897	2648	4931	4272	2736	3628	3175	710	501
5	Control											
6	Control											
7	Control	1736	2929	3064	2705	4681	3754	2358	3130	3153	606	425
8	Control	1206	2065	2422	2133	3418	3374	2057	2760	2822	613	400
9	Control	1369	2309	2475	2292	3496	3610	2104	2963	2505	604	438
10	Control	1648	2369	2346	2354	3621	3786	2354	3152	2884	542	402
	Mean	1628	2851	2999	2661	5165	4537	2616	3813	3363	630	395
	SD	455	578	569	393	1916	1160	499	1039	667	80	130
11	*Parkin* knockout	2426	3204	3310	3356	5236	5551	3523	4825	3789	843	631
12	*Parkin* knockout	2013				5468	5136	3004	4692		822	643
13	*Parkin* knockout	1905	2470	2561	2815	4640	4593	2801	4303	3425	836	485
14	*Parkin* knockout	1895	2581	2522	2703	4950	4090	2649	3429	3295	754	517
15	*Parkin* knockout											
16	*Parkin* knockout											
17	*Parkin* knockout	1525				6828	4975	2697	4071		708	607
18	*Parkin* knockout	1214	2541	2459	2141	5958	4895	2601	4047	1949	505	146
19	*Parkin* knockout	1087	2902	3231	1894	6117	4768	2857	3993	3006	462	148
20	*Parkin* knockout	1528	3315	3409	2448	6386	5693	3136	4673	3579	491	166
	Mean	1699	2835	2915	2559	5698	4963	2908	4254	3174	678	418
	SD	444	362	445	520	750	514	307	466	656	165	225
21	*DJ-1* knockout	2028	3565	3717	3356	5809	5610	3810	4807	3907	1084	664
22	*DJ-1* knockout	2051	3135	3124	3079	4732	4167	2761	3325	3670	738	653
23	*DJ-1* knockout	2286	3651	3421	3710	5173	5426	3645	4623	3727	917	564
24	*DJ-1* knockout	2168	3002	3336	3848	5820	4713	3043	4186	3394	759	549
25	*DJ-1* knockout											
26	*DJ-1* knockout											
27	*DJ-1* knockout	1446	2134	2475	2307	3573	3367	2171	2819	2764	540	449
28	*DJ-1* knockout	1273	2098	2375	2267	3354	3676	2475	3169	2895	649	439
29	*DJ-1* knockout	1504	2448	2383	2146	3856	3017	1934	2756	2738	692	416
30	*DJ-1* knockout	1342	2566	2471	2044	3919	3427	2152	3135	2234	679	399
	Mean	1762	2825	2913	2845	4529	4176	2749	3603	3166	757	517
	SD	410	606	546	739	992	979	701	815	593	170	106

Table A34: **Nicotinic** receptor densities (fmol/mg protein) and mean densities ± SD of controls, *Parkin* and *DJ-1* knockout mice in various brain regions (Ligand: [^{3}H]-**Epibatidine**).

Animal	Group	OB	M	S	Pir	CPu	CA1	CA2/3	DG	V	SN	CB
1	Control	132	253	219	108	317	123	94	151	261	162	
2	Control	128	280	241	119	334	153	118	188	293	196	
3	Control	129	288	258	125	355	120	98	155	292	206	
4	Control	124	284	276	134	377	132	108	173	297	203	
5	Control	120	286	243	124	330	123	105	175	281	183	
6	Control	127	274	238	127	316	126	111	163	290	185	
7	Control	113	291	249	121	353	112	91	154	291	206	
8	Control	113	279	253	127	365	132	122	188	286	226	
9	Control	116	246	236	115	333	112	105	153	248	149	
10	Control	118	259	257	103	331	132	106	164	278	195	
	Mean	122	274	247	120	341	126	106	166	282	191	
	SD	7	15	15	9	19	11	9	13	15	21	
11	*Parkin* knockout	125	298	277	113	351	146	123	186	334	189	
12	*Parkin* knockout	120				359	145	116	178		176	
13	*Parkin* knockout	132	308	267	136	374	137	109	175	289	198	
14	*Parkin* knockout	130	302	291	140	364	130	121	184	315	207	
15	*Parkin* knockout	119	300	267	172	366	137	114	177	287	206	
16	*Parkin* knockout	139				369	142	131	175		198	
17	*Parkin* knockout	118				370	124	111	166		222	
18	*Parkin* knockout	126	292	252	152	364	123	107	163	316	179	
19	*Parkin* knockout	126	318	292	154	338	129	114	170	353	172	
20	*Parkin* knockout	120	310	289	145	375	125	106	167	316	209	
	Mean	125	304	276	145	363	134	115	174	316	196	
	SD	6	8	14	17	11	8	7	7	22	15	
21	*DJ-1* knockout	136	284	264	124	362	154	114	176	281	165	
22	*DJ-1* knockout	130	274	255	120	357	154	134	196	301	200	
23	*DJ-1* knockout	143	284	283	135	363	146	128	186	301	186	
24	*DJ-1* knockout	138	346	284	147	394	152	124	178	310	203	
25	*DJ-1* knockout	141	299	261	118	368	133	110	161	301	199	
26	*DJ-1* knockout	133	267	236	122	346	114	107	155	296	194	
27	*DJ-1* knockout	110	291	269	126	363	122	107	148	265	171	
28	*DJ-1* knockout	115	275	259	123	339	110	101	153	292	186	
29	*DJ-1* knockout	122	268	270	172	299	123	111	164	316	185	
30	*DJ-1* knockout	119	267	239	120	342	113	107	159	298	210	
	Mean	129	286	262	131	353	132	114	167	296	190	
	SD	11	23	15	16	23	17	10	15	14	13	

Table A35: **α_1** receptor densities (fmol/mg protein) and mean densities ± SD of controls, *Parkin* and *DJ-1* knockout mice in various brain regions (Ligand: [^{3}H]-**Prazosin**).

Animal	Group	OB	M	S	Pir	CPu	CA1	CA2/3	DG	V	SN	CB
1	Control	630	843	568	465	198	203	205	208	460	176	251
2	Control	532	613	467	462	158	178	188	186	413	182	237
3	Control	523	601	450	384	143	151	148	148	475	206	268
4	Control	603	690	567	525	223	279	258	257	556	248	297
5	Control	537	490	431	415	174	220	203	230	450	197	295
6	Control	633	729	640	629	279	303	290	311	590	294	326
7	Control	549	635	505	511	214	221	207	216	492	245	310
8	Control	328	394	335	313	145	176	175	195	345	201	214
9	Control	442	459	384	302	163	231	215	225	390	185	246
10	Control	479	489	414	397	195	250	230	252	422	191	244
	Mean	525	594	476	440	189	221	212	223	459	212	269
	SD	88	131	89	95	40	45	38	42	70	36	34

11	*Parkin* knockout	627	677	591	498	238	280	266	274	478	302	297
12	*Parkin* knockout	503				229	258	250	254	485	237	280
13	*Parkin* knockout	498	601	509	430	209	261	252	247	538	268	336
14	*Parkin* knockout	657	773	591	577	276	319	301	294	585	338	320
15	*Parkin* knockout	630	658	583	540	247	299	295	279	536	309	324
16	*Parkin* knockout	583				238	260	257	274		254	261
17	*Parkin* knockout	549				200	259	262	259		264	257
18	*Parkin* knockout	414	530	402	323	132	182	176	178	339	224	172
19	*Parkin* knockout	558	567	503	321	146	146	154	164	343	146	184
20	*Parkin* knockout	501	537	424	278	116	149	151	143	375	151	186
	Mean	552	620	515	424	203	241	236	237	460	249	262
	SD	71	81	73	110	51	58	53	51	89	60	59
21	*DJ-1* knockout	521	612	487	428	216	263	261	255	470	278	310
22	*DJ-1* knockout	567	604	478	425	220	276	266	275	515	282	296
23	*DJ-1* knockout	616	741	557	519	244	296	287	300	583	292	313
24	*DJ-1* knockout	545	635	464	396	203	243	231	234	503	219	281
25	*DJ-1* knockout	628	626	481	306	225	289	269	265	493	285	272
26	*DJ-1* knockout	590	625	517	471	250	274	259	268	465	234	300
27	*DJ-1* knockout	348	394	331	334	135	202	194	200	363	181	208
28	*DJ-1* knockout	395	431	353	318	149	165	156	160	354	184	224
29	*DJ-1* knockout	396	395	324	286	125	154	157	164	349	137	189
30	*DJ-1* knockout	385	382	298	260	119	170	172	169	317	164	205
	Mean	499	545	429	374	189	233	225	229	441	226	260
	SD	102	123	88	81	48	52	48	49	84	54	46

Table A36: **α_2** receptor densities (fmol/mg protein) and mean densities ± SD of controls, *Parkin* and *DJ-1* knockout mice in various brain regions (Ligand: [^{3}H]-**UK14,304**).

Animal	**Group**	**OB**	**M**	**S**	**Pir**	**CPu**	**CA1**	**CA2/3**	**DG**	**V**	**SN**	**CB**
1	Control	240	174	168	312	111	213	120	177	209	175	176
2	Control	170	194	194	352	125	208	125	169	193	187	168
3	Control	217	233	205	365	151	200	117	177	219	252	168
4	Control	172	215	186	375	167	238	142	193	195	198	167
5	Control	227	218	226	399	156	308	213	288	352	316	193
6	Control	202	278	224	452	190	251	156	216	341	247	183
7	Control	249	289	317	504	211	244	200	229	238	239	161
8	Control	199	223	226	397	145	198	125	185	195	182	172
9	Control	224	193	190	450	136	231	157	231	230	159	177
10	Control	173	205	177	398	125	182	99	166	194	148	142
	Mean	207	222	211	400	152	227	146	203	237	210	171
	SD	29	37	43	56	31	36	37	38	60	52	13
11	*Parkin* knockout	283	237	217	480	170	249	157	218	273	229	216
12	*Parkin* knockout	251				168	358	246	314	212	181	187
13	*Parkin* knockout	297	313	314	612	251	380	255	382	268	225	251
14	*Parkin* knockout	294	320	311	663	274	388	252	340	384	274	221
15	*Parkin* knockout	394	332	327	686	266	373	220	317	312	288	273
16	*Parkin* knockout	255				201	325	183	274		241	206
17	*Parkin* knockout	331				192	287	181	239		278	213
18	*Parkin* knockout	296	214	199	476	159	253	143	223	223	206	199
19	*Parkin* knockout	238	218	214	438	145	243	131	199	249	214	175
20	*Parkin* knockout	295	217	219	514	137	266	134	196	236	174	194
	Mean	294	264	257	553	196	312	190	270	269	231	214
	SD	45	54	57	99	51	59	49	65	56	40	30
21	*DJ-1* knockout	210	222	197	508	161	292	199	207	208	166	195
22	*DJ-1* knockout	246	250	211	417	169	344	202	300	251	243	233
23	*DJ-1* knockout	222	296	286	590	237	405	250	318	385	261	196
24	*DJ-1* knockout	281	287	242	478	203	304	171	216	295	257	234

25	*DJ-1* knockout	304	293	237	437	207	409	224	369	391	317	211
26	*DJ-1* knockout	319	302	259	501	238	350	232	282	352	303	230
27	*DJ-1* knockout	254	273	218	420	153	275	188	264	279	197	205
28	*DJ-1* knockout	260	234	217	445	188	239	161	215	265	245	231
29	*DJ-1* knockout	226	219	206	518	159	318	194	316	308	203	242
30	*DJ-1* knockout	286	268	235	519	170	266	179	240	316	256	229
	Mean	261	264	231	483	189	320	200	273	305	245	221
	SD	36	31	27	55	32	57	28	54	58	46	17

Table A37: **5-HT$_{1A}$** receptor densities (fmol/mg protein) and mean densities ± SD of controls, *Parkin* and *DJ-1* knockout mice in various brain regions (Ligand: [^{3}H]-**8-OH-DPAT**).

Animal	**Group**	**OB**	**M**	**S**	**Pir**	**CPu**	**CA1**	**CA2/3**	**DG**	**V**	**SN**	**CB**
1	Control	48	126	104	54	17	468	75	114	75	19	
2	Control	38	129	104	41	19	417	73	113	72	21	
3	Control	36	139	109	51	26	489	92	127	107	29	
4	Control	52	161	144	61	33	493	97	140	96	32	
5	Control	48	168	150	63	31	465	104	142	132	40	
6	Control	56	178	146	74	38	465	89	134	119	33	
7	Control	55	193	168	83	46	498	94	133	111	38	
8	Control											
9	Control	73	197	163	89	42	556	114	164	127	35	
10	Control	55	172	146	73	36	514	108	152	126	34	
	Mean	51	162	137	65	32	485	94	135	107	31	
	SD	10	25	23	15	9	36	13	16	21	7	
11	*Parkin* knockout	38	153	121	58	22	480	90	133	101	28	
12	*Parkin* knockout	42				20	487	87	137	101	21	
13	*Parkin* knockout	53	201	149	70	30	570	143	187	119	31	
14	*Parkin* knockout	57	183	144	115	34	589	144	189	135	33	
15	*Parkin* knockout	44	202	179	83	36	512	116	163	128	38	
16	*Parkin* knockout	46				30	500	103	144		35	
17	*Parkin* knockout	50				29	522	115	161		31	
18	*Parkin* knockout											
19	*Parkin* knockout	58	207	165	98	32	537	116	183	121	37	
20	*Parkin* knockout	53	181	141	96	30	586	130	178	123	35	
	Mean	49	188	150	87	29	531	116	164	118	32	
	SD	7	18	18	19	5	39	19	21	12	5	
21	*DJ-1* knockout	29	110	83	56	19	475	81	115	77	18	
22	*DJ-1* knockout	36	140	103	53	19	507	111	155	93	21	
23	*DJ-1* knockout	51	155	124	111	34	569	124	153	125	37	
24	*DJ-1* knockout	43	176	137	88	31	505	91	152	116	33	
25	*DJ-1* knockout	59	184	147	61	32	489	107	155	119	37	
26	*DJ-1* knockout	53	161	135	74	37	522	110	169	124	36	
27	*DJ-1* knockout											
28	*DJ-1* knockout											
29	*DJ-1* knockout	65	174	135	130	33	586	136	195	131	40	
30	*DJ-1* knockout	62	175	133	68	32	574	119	186	134	40	
	Mean	50	159	125	80	30	529	110	160	115	33	
	SD	12	23	20	26	6	40	16	23	18	8	

Table A38: **D_2** receptor densities (fmol/mg protein) and mean densities ± SD of controls, *Parkin* and *DJ-1* knockout mice in various brain regions (Ligand: [^{3}H]-**Raclopride**).

Animal	Group	OB	M	S	Pir	CPu	CA1	CA2/3	DG	V	SN	CB
1	Control					678						
2	Control					744						
3	Control					758						
4	Control					744						
5	Control					727						
6	Control					784						
7	Control					731						
8	Control					745						
9	Control					862						
10	Control					919						
	Mean					769						
	SD					67						
11	*Parkin* knockout					639						
12	*Parkin* knockout					625						
13	*Parkin* knockout					894						
14	*Parkin* knockout					861						
15	*Parkin* knockout					998						
16	*Parkin* knockout					873						
17	*Parkin* knockout					810						
18	*Parkin* knockout					816						
19	*Parkin* knockout					918						
20	*Parkin* knockout					876						
	Mean					831						
	SD					111						
21	*DJ-1* knockout					677						
22	*DJ-1* knockout					758						
23	*DJ-1* knockout					768						
24	*DJ-1* knockout					859						
25	*DJ-1* knockout					869						
26	*DJ-1* knockout					761						
27	*DJ-1* knockout					737						
28	*DJ-1* knockout					785						
29	*DJ-1* knockout					795						
30	*DJ-1* knockout					831						
	Mean					784						
	SD					55						

Table A39: **D_2 / D_3** receptor densities (fmol/mg protein) and mean densities ± SD of controls, *Parkin* and *DJ-1* knockout mice in various brain regions (Ligand: [^{3}H]-**Fallypride**).

Animal	Group	OB	M	S	Pir	CPu	CA1	CA2/3	DG	V	SN	CB
1	Control					1927						
2	Control					1949						
3	Control					1708						
4	Control					1769						
5	Control					1845						
6	Control					2076						
7	Control					1743						
8	Control					1830						
9	Control					1871						
10	Control					2087						
	Mean					1880						
	SD					131						

11	*Parkin* knockout					1991						
12	*Parkin* knockout					1952						
13	*Parkin* knockout					2140						
14	*Parkin* knockout					2016						
15	*Parkin* knockout					1996						
16	*Parkin* knockout					2100						
17	*Parkin* knockout					1815						
18	*Parkin* knockout					1771						
19	*Parkin* knockout					1968						
20	*Parkin* knockout					2145						
	Mean					1990						
	SD					125						
21	*DJ-1* knockout					2046						
22	*DJ-1* knockout					1874						
23	*DJ-1* knockout					1731						
24	*DJ-1* knockout					1836						
25	*DJ-1* knockout					1976						
26	*DJ-1* knockout					2171						
27	*DJ-1* knockout					1674						
28	*DJ-1* knockout					1900						
29	*DJ-1* knockout					2272						
30	*DJ-1* knockout					2269						
	Mean					1975						
	SD					212						

Table A40: **A_{2A}** receptor densities (fmol/mg protein) and mean densities ± SD of controls, *Parkin* and *DJ-1* knockout mice in various brain regions (Ligand: [^{3}H]-**ZM 241 385**).

Animal	**Group**	**OB**	**M**	**S**	**Pir**	**CPu**	**CA1**	**CA2/3**	**DG**	**V**	**SN**	**CB**
1	Control					2432						
2	Control					2398						
3	Control					2384						
4	Control					2285						
5	Control					2515						
6	Control					2410						
7	Control					2342						
8	Control					1976						
9	Control					2616						
10	Control					2419						
	Mean					2378						
	SD					168						
11	*Parkin* knockout					2328						
12	*Parkin* knockout					2284						
13	*Parkin* knockout					2642						
14	*Parkin* knockout					2492						
15	*Parkin* knockout					2349						
16	*Parkin* knockout					2372						
17	*Parkin* knockout					2464						
18	*Parkin* knockout					2478						
19	*Parkin* knockout					2791						
20	*Parkin* knockout					2665						
	Mean					2486						
	SD					166						
21	*DJ-1* knockout					2454						
22	*DJ-1* knockout					2340						
23	*DJ-1* knockout					2559						
24	*DJ-1* knockout					2708						

25	*DJ-1* knockout					2470						
26	*DJ-1* knockout					2501						
27	*DJ-1* knockout					2476						
28	*DJ-1* knockout					2830						
29	*DJ-1* knockout					2742						
30	*DJ-1* knockout					2847						
	Mean					2593						
	SD					175						

Table A41: **KA2** kainate receptor subunit mRNA levels (fmol x 10^{-3}/mg protein) and mean mRNA levels ± SD of controls, *Parkin* and *DJ-1* knockout mice in various brain regions.

Animal	Group	OB	M	S	Pir	CPu	CA1	CA2/3	DG
1	Control	113,48	75,82	65,75	76,40	71,87	68,92	107,48	120,71
2	Control	58,00	45,25	45,47	36,76	39,85	43,81	63,38	69,78
3	Control	55,82	42,17	36,78	40,57	35,73	38,67	61,06	65,10
4	Control	73,29	55,61	55,18	60,50	57,05	31,05	49,52	54,91
5	Control	68,13	57,84	53,31	52,59	53,88	43,67	68,49	66,54
6	Control	62,37	46,90	45,18	53,88	47,34	44,67	72,30	71,51
7	Control	94,60	52,59	54,40	53,95	49,85	51,53	82,46	84,62
8	Control	114,31	78,63	69,85	64,82	69,56	49,49	75,61	82,51
9	Control	67,02	45,75	44,17	47,55	40,14	37,19	57,77	59,35
10	Control	67,84	49,85	48,13	54,67	44,46	44,60	67,91	69,78
	Mean	77,49	55,04	51,82	54,17	50,97	45,36	70,60	74,48
	SD	21,93	12,66	10,12	11,46	12,28	10,18	15,96	18,62
11	*Parkin* knockout	49,64	53,23	51,65	50,36	52,37	46,28	86,09	76,73
12	*Parkin* knockout	80,93	56,62	51,80	56,90	54,31	53,23	81,00	94,53
13	*Parkin* knockout	96,69	68,70	72,73	77,62	77,98	49,93	80,28	88,20
14	*Parkin* knockout	84,26	53,23	52,30	57,91	55,90	38,92	62,66	66,97
15	*Parkin* knockout	110,21	74,31	60,36	73,81	70,28	44,60	73,16	69,20
16	*Parkin* knockout	102,37	46,47	47,34	65,01	51,22	48,27	75,32	86,69
17	*Parkin* knockout	132,94	79,20	62,30	81,51	74,67	37,50	56,83	64,83
18	*Parkin* knockout	87,48	60,64	60,43	80,14	67,05	39,12	71,94	84,71
19	*Parkin* knockout	84,89	47,48	40,72	52,25	44,60	31,11	56,02	67,98
20	*Parkin* knockout	101,43	60,14	53,16	71,15	59,49	47,34	81,51	85,89
	Mean	93,08	60,00	55,28	66,67	60,79	43,63	72,48	78,57
	SD	21,76	11,02	8,94	11,75	11,10	6,77	10,65	10,70
21	*DJ-1* knockout	110,71	63,95	59,64	62,30	54,89	41,90	76,34	71,67
22	*DJ-1* knockout	122,58	84,53	81,00	90,64	74,46	66,26	108,48	111,07
23	*DJ-1* knockout	86,69	56,62	54,31	52,44	46,62	57,69	91,94	100,07
24	*DJ-1* knockout	125,10	95,46	86,69	98,34	82,80	60,43	89,20	102,58
25	*DJ-1* knockout	68,82	55,75	47,84	52,96	49,21	62,08	98,20	108,34
26	*DJ-1* knockout	87,49	60,28	56,62	75,39	58,56	44,89	75,18	82,94
27	*DJ-1* knockout	67,62	70,07	72,59	84,46	63,16	38,67	69,78	75,72
28	*DJ-1* knockout	88,77	50,45	54,22	68,88	53,59	38,77	73,59	76,40
29	*DJ-1* knockout	84,38	49,93	52,23	59,35	49,13	48,27	78,41	84,17
30	*DJ-1* knockout	77,42	46,69	42,23	47,91	36,98	36,24	60,52	69,69
	Mean	91,96	63,37	60,74	69,27	56,94	49,52	82,16	88,26
	SD	20,66	15,85	14,56	17,39	13,57	11,13	14,48	15,75

Table A42: **$GABA_B$** receptor mRNA levels (fmol x 10^{-3}/mg protein) and mean mRNA levels ± SD of controls, *Parkin* and *DJ-1* knockout mice in various brain regions.

Animal	Group	OB	M	S	Pir	CPu	CA1	CA2/3	DG
1	Control	9,09	50,70	48,28	40,17	4,85	18,73	36,07	45,29
2	Control	1,55	41,66	43,15	29,17	4,29	19,94	43,52	46,51
3	Control	6,43	36,81	33,20	22,72	2,91	23,02	51,73	49,86
4	Control	6,15	38,03	37,47	25,82	4,75	14,73	32,53	39,52
5	Control	12,58	62,72	61,70	51,54	10,44	43,06	88,07	78,85
6	Control	14,80	61,42	50,79	43,06	11,37	20,41	43,43	43,15
7	Control	4,78	22,37	22,09	13,42	1,96	11,28	29,92	27,03
8	Control	7,55	49,02	48,93	36,93	6,80	24,23	45,11	47,72
9	Control	8,97	38,58	42,59	30,20	6,06	34,11	74,65	69,06
10	Control	5,13	51,26	45,95	38,68	5,22	21,72	47,81	46,32
	Mean	7,70	45,26	43,41	33,17	5,86	23,12	49,28	49,33
	SD	3,87	12,25	10,77	11,09	3,01	9,24	18,47	14,64
11	*Parkin* knockout	6,24	46,32	48,56	41,38	4,94	19,42	45,51	53,43
12	*Parkin* knockout	4,47	56,67	56,76	46,32	5,03	23,49	49,95	59,09
13	*Parkin* knockout	18,73	99,07	108,67	82,20	15,47	56,67	106,15	132,25
14	*Parkin* knockout	12,12	63,93	63,10	52,47	7,74	27,12	60,95	67,66
15	*Parkin* knockout	11,84	62,35	60,86	46,04	9,60	30,48	53,22	66,45
16	*Parkin* knockout	6,99	47,90	47,16	29,54	6,24	21,53	45,57	49,40
17	*Parkin* knockout	6,99	40,36	36,35	27,77	5,50	15,66	31,59	36,25
18	*Parkin* knockout	8,20	35,88	36,53	27,68	4,75	21,16	43,06	46,13
19	*Parkin* knockout	7,92	18,02	18,95	10,72	5,90	12,21	28,80	27,59
20	*Parkin* knockout	17,34	88,82	78,10	63,38	11,09	43,90	97,39	97,49
	Mean	10,08	55,93	55,50	42,75	7,63	27,16	56,22	63,57
	SD	4,81	24,24	24,96	20,42	3,48	13,58	25,86	30,84
21	*DJ-1* knockout	6,99	48,84	51,82	45,02	4,57	20,04	46,72	46,83
22	*DJ-1* knockout	7,36	53,78	59,37	47,35	7,22	35,60	75,58	77,26
23	*DJ-1* knockout	9,13	44,27	46,79	37,40	7,83	22,65	44,46	43,80
24	*DJ-1* knockout	11,65	71,48	73,16	65,80	12,68	28,61	55,92	64,40
25	*DJ-1* knockout	6,99	48,65	46,32	39,89	7,36	18,87	39,14	48,11
26	*DJ-1* knockout	15,47	61,33	57,50	48,74	7,92	27,87	50,98	64,77
27	*DJ-1* knockout	12,68	49,21	45,76	37,19	8,02	17,06	40,36	42,31
28	*DJ-1* knockout	19,20	78,38	79,41	63,93	12,40	26,93	61,88	57,88
29	*DJ-1* knockout	17,15	51,07	50,33	36,53	4,94	26,66	55,45	62,44
30	*DJ-1* knockout	4,19	22,83	22,37	13,79	0,65	12,70	31,69	33,44
	Mean	11,08	52,98	53,28	43,56	7,36	23,70	50,22	54,13
	SD	4,98	15,26	15,80	14,83	3,55	6,71	12,69	13,34

Danksagungen

Ich möchte meinen Betreuern danken. Herrn Prof. Zilles, für die Möglichkeit diese Arbeit an seinem Institut durchzuführen. Insbesondere danke ich ihm für das mir entgegengebrachte Vertrauen und den damit einhergehenden planerischen Freiraum. Außerdem für den konstruktiven Austausch, sowie für seine wertvollen fachlichen Anregungen. Herrn Prof. Wagner danke ich für die Bereitschaft diese Arbeit als Doktorvater zu betreuen. Ferner für das mir und meiner Arbeit entgegengebrachte Interesse und den unterstützenden fachlichen Austausch. Frau Prof. Amunts danke ich für die Möglichkeit meine Arbeit an ihrem Institut fortzuführen, sowie für die fachliche Beratung.

Bei der praktischen Durchführung dieser Arbeit ist mir von Seiten der Mitglieder meiner Arbeitsgruppe persönliches Engagement zuteil geworden, dem ich hier nicht angemessen gerecht werden kann. Insbesondere, weil diese Zeilen nicht essbar sind… Dennoch möchte ich sie namentlich nennen und mich herzlichst bedanken bei Sabrina Buller, Markus Cremer, Christian Schramm, Elena von Staden und Sabine Wilms.

Für die praktische und fachliche Hilfe bei der statistischen Auswertung bedanke ich mich bei Herrn Dr. Schleicher und Frau Dr. Palomero-Gallagher.

Ich danke meiner Familie, insbesondere meiner Mutter, für die Unterstützung in jeder nur denkbaren Form.

Ich danke Christian für die Unterstützung bei der Suche nach dem Namen des Spielers am ersten Mal. Für Veränderung und Gegensätze. Für so viel mehr.